GLUTAMATE RECEPTORS
IN THE
OLFACTORY SYSTEM

By

J. Mark Kinzie

A DISSERTATION

Presented to the Neuroscience Graduate Program

and

Oregon Health Sciences University

School of Medicine

in partial fulfillment of

the requirements for the degree of

Doctor of Philosophy

March 1999

School of Medicine

Oregon Health Sciences University

CERTIFICATE OF APPROVAL

This is to certify that the Ph.D. thesis of

John Mark Kinzie

has been approved

[redacted]

Thomas P. Segerson, M.D., Mentor

[redacted]

[redacted]

John P. Adelman, Ph.D., Member

[redacted]

Roger D. Cone, Ph.D., Member

[redacted]

Richard B. Simerly, Ph.D., Member

Associate Dean for Graduate Studies

TABLE OF CONTENTS

ABSTRACT

The detection of a specific odor within the environmental milieu and the discrimination between multiple odors depends on processing within the olfactory bulb, the brain region that receives all of the input from olfactory receptor neurons in the nasal cavity. Receptors for the neurotransmitter L-glutamate, by virtue of their localization within the olfactory system and their ability to relay (via ionotropic receptors) and modulate (via metabotropic receptors) neuronal activity, play important roles in this regard. In this thesis, I initially describe the cloning of the G protein-coupled metabotropic glutamate receptor subtype 7 and its characterization as a receptor sensitive to L-2-amino-4-phosphonobutyrate (L-AP4), a glutamate analog previously shown to activate a subclass of mGluRs in olfactory bulb mitral cells. The majority of this thesis examines the cellular and subcellular distribution of mGluR7 in the olfactory system. The anatomical distribution of mGluR7 mRNA expression as examined by *in situ* hybridization in the developing and adult rat central nervous systems, demonstrates that mGluR7 mRNA is among the most widely distributed of mGluRs in the rat nervous system. mGluR7 mRNA is expressed in most neuronal groups known to respond to L-AP4 including mitral cells of the olfactory bulb. Additionally, mGluR7 mRNA is abundantly expressed at all levels of the olfactory circuitry. Light and electron microscopic immunolocalization revealed that mGluR7 is expressed primarily in axon terminals, including those of mitral cells. However, mGlur7 is present postsynaptically at selected synapses, indicating that mGluR7 is not targeted exclusively to the axon. Olfactory information processing in mice deficient in mGluR1, a receptor subtype found abundantly within the olfactory bulb was also examined. Although the results are inconclusive, the work led to a collaborative project demonstrating that dendrodendritic inhibition in the olfactory bulb is driven by NMDA, not AMPA, receptors. The later findings suggest that olfactory information processing depends on long-lasting reciprocal and lateral inhibition.

INTRODUCTION

The olfactory system is remarkable in its ability to detect and discriminate thousands of airborne odorants. Olfaction begins when odorants enter the nasal cavity and stimulate olfactory receptor neurons within the olfactory epithelium. About two thousand olfactory receptors are expressed on olfactory receptor neurons within the olfactory epithelium, accounting for the tremendous range of chemical structures the olfactory system is able to detect. However, much of ability of the olfactory system to detect a specific odor within the environmental milieu and to discriminate between multiple odors occurs at the level of the olfactory bulb, the area that receives all of the output from the olfactory epithelium.

The work described in this dissertation involves the assignment of functional roles to receptors of the neurotransmitter glutamate using the olfactory bulb as a model system. The olfactory bulb is particularly well suited for this role because it can be activated in an intact animal by exposing it to odors. Additionally, the bulb is a highly laminated structure, containing sharply differentiated cell types and areas of distinct cell types. By localizing different glutamate receptors to specific regions of the bulb, a great deal of information can be inferred and tested about the role that the receptors play in the processing of olfactory information.

The classes of glutamate receptors

Glutamate transduces signals to neurons via many different receptors. Functionally, these receptors can be divided into two separate classes. One class comprises the ligand-gated ion channels, also termed ionotropic receptors. These receptors contain glutamate binding sites as well as ion channel domains and, thus, are able to respond to glutamate binding with rapid changes in membrane ion conductance (Nakanishi, 1992; Westbrook, 1994). The ionotropic receptors can further be divided into the AMPA/kainate class and the NMDA class. These two broad classes differ in their protein structures, but

their functional properties differ as well. Receptors of the AMPA class have quicker response times to glutamate binding and thus dominate fast excitatory synaptic responses. NMDA receptors, on the other hand, mediate slower responses (Bliss and Collingridge, 1993), but also have additional special features. Activation of the NMDA receptor is voltage-dependent; depolarization relieves the receptor channel of a blockage by magnesium. In addition, the NMDA receptor channel is calcium permeable (Mayer and Westbrook, 1987). The calcium entering the neuron through the NMDA receptor channel activates many enzymes such as protein kinase C and can cause the activation of immediate early genes such as *c-fos* (Ginty, 1997).

The second class, more recently characterized, is made up of G protein-coupled receptors. These receptors have been termed metabotropic glutamate receptors because they are involved in changing the metabolic activity of the neuron by triggering biochemical cascades (Eccles and McGeer, 1979). Upon binding of glutamate, the mGluRs activate G protein-coupled receptors which in turn can modulate, either positively or negatively, voltage gated ion channels, intracellular enzymes and the release of cytosolic calcium.

Discovery and Cloning of G protein-coupled glutamate receptors

The evidence that glutamate can bind to G protein-coupled receptors to activate second messengers in neurons is rather recent. In 1985, it was demonstrated that glutamate stimulates the production of inositol-1,4,5-trisphosphate (IP_3) in primary cultures of mouse striatal neurons (Sladeczek et al., 1985). The pharmacological profile of phosphatidyl inositol (PI) hydrolysis was not consistent with the activation of either the N-methyl-D-aspartate (NMDA) or the α-amino-3-hydroxy-5-methyl-4-isoxazole propionate (AMPA) ionotropic glutamate receptors, suggesting a distinct class of glutamate receptors (Schoepp et al., 1990). The first direct evidence of a glutamatergic receptor working through a G protein-linked second messenger system came from studies of mRNA-injected *Xenopus* (Sugiyama et al., 1987). Application of glutamate or quisqualate gave fluctuating

membrane current responses of delayed onset, a different response from the rapid onset smooth currents seen with glutamate-gated ion channels. The response was inhibited by pertussis toxin, indicative of either G_i or G_o protein involvement.

In 1991, the cDNA of a metabotropic G protein-coupled glutamate receptor (mGluR1α) was cloned from a rat cerebellar cDNA library by functional expression in *Xenopus* oocytes (Masu et al., 1991; Houamed et al., 1991). The cDNA of mGluR1α encodes a quisqualate-preferring 1190 amino acid membrane bound protein that in oocytes couples to a pertussis toxin sensitive G protein. *In situ* hybridization revealed highest expression in olfactory bulb mitral and tufted cells, cerebellar Purkinje cells and neurons of the hippocampus.

Since the cloning of mGluR1α, and the start of this thesis work in 1992, seven other mGluRs have been cloned based on homology. The mGluRs share some basic structural features with other cloned G protein-coupled receptors in that they contain seven regions of hydrophobic amino acids thought to be transmembrane a helical domains and proline/glutamine rich and glutamate/aspartate rich domains in the carboxy-terminus similar to those found in the cytoplasmic loops of adrenergic and muscarinic receptors. However, the structure of mGluRs is also very different from most other G protein-coupled receptors. For instance, the receptors lack amino acid sequence similarity with other known G protein-coupled receptors. Because of long amino- and carboxy-terminal domains, they are considerably larger than other G protein-coupled receptors. The third cytoplasmic loop of the mGluRs, known to be important in coupling of some receptors to G proteins (Lefkowitz et al., 1990), is unusually short for a G protein-coupled receptor (Masu et al., 1991). Since the cloning of the mGluRs, several structurally related receptors sensitive to calcium and GABA, have also been cloned (Brown et al., 1993; Ruat, et al. 1995; Kaupman, et al., 1997). Thus, all of these structurally related receptors make up a separate superfamily of G protein coupled receptors.

Three subfamilies of mGluRs

The seven mGluRs can be subdivided into three separate subfamilies based on their sequence similarity, pharmacology and coupling to second messengers (Table 1). One subfamily comprises the splice variants of mGluR1 and mGluR5. As with mGluR1α, the members in this subfamily couple to phospholipase C and increase IP_3 production and cytoplasmic calcium. The receptors have very similar agonist selectivity with quisqualate being the most potent agonist. However, in transfected Chinese hamster ovary (CHO) cells, mGluR1 is sensitive to inhibition by pertussis toxin, whereas mGluR5 is not (Abe et al., 1992).

The second subfamily contains receptors mGluR2 and mGluR3. Unlike the first subfamily, these receptors inhibit forskolin-stimulated cAMP production when transfected into CHO cells. L-glutamate and trans-1-aminocyclopentane-1,3-dicarboxylate (trans-ACPD) both are effective agonists. Although coupled to inhibition of adenylyl cyclase in CHO cells, these receptors may serve other functions in neurons such as the inhibition of neurotransmitter release. The other receptor in the subfamily, mGluR3, is interesting in that it is localized to glial cells.

The final subfamily is made up of receptors sensitive to the agonist L-2-amino-4-phosphonobutyrate (L-AP4). Like the second subfamily, activation of these receptors in transfected CHO and baby hamster kidney (BHK) cells inhibits forskolin-stimulated production of cAMP. mGluR6 mRNA expression is restricted to the inner nuclear layer of the retina where ON-bipolar cells are located (Nakajima et al., 1993). In these neurons, mGluR6 is thought to function by stimulating a cGMP phosphodiesterase thereby decreasing cGMP concentration and thus closing a cGMP-gated, cation-specific ion channel. mGluR4, mGluR7, and mGluR8 are more generally localized throughout the brain. L-AP4-sensitive receptors are believed to be presynaptically localized and to serve as autoreceptors which inhibit the release of neurotransmitter. One of the goals of this dissertation is to demonstrate that mGluR7 is localized presynaptically.

Table 1: The mGluR Subfamilies

Subfamily	Receptor	AAs	Result of stim. in BHK or CHO Cells	Pharmacology
I	mGluR1α	1199	Increase Ca^{2+} and IP_3	Quisqualate preferring
	mGluR1b	906		
	mGluR1c	897		
	mGluR5	1171		
II	mGluR2	872	Decrease cAMP	L-glutamate trans-ACPD
	mGluR3	879		
III	mGluR4	912	Decrease cAMP	L-AP4 preferring
	mGluR6	871		
	mGluR7	918		
	mGluR8	908		

Olfactory bulb mGluRs: location suggests function

One surprising finding that emerged from the cloning of metabotropic glutamate receptors (mGluRs) is the distinct representation of nearly all subtypes in olfactory bulb neurons (Kinzie et al., 1998). Given the highly organized and delineated structure of the olfactory bulb, a great deal can be surmised about mGluR function by determining cellular and subcellular distribution of the receptor subtypes.

On one level, olfactory input into cortical areas can be seen as rather direct (Figure 1). Odor molecules are detected by odorant receptor neurons each of which express just one of about two thousand olfactory receptor subtypes (Chess, et al.,1994). The axons of the olfactory receptor neurons extend through the cribriform plate and into the olfactory bulb where they synapse in structures termed glomeruli. Within glomeruli, the axons make glutamatergic synapses with primary dendrites of mitral and tufted cells. The mitral and tufted cells then direct the sensory information into the piriform cortex and other higher cortical areas. Receptor neurons expressing one type of odorant receptor project to at most a few olfactory bulb glomeruli (Ressler et al., 1994; Vassar et al., 1994). These observations support the notion that odor sensation is spatially encoded; that the information related to a particular odor is labeled according to the output neurons conveying the signal.

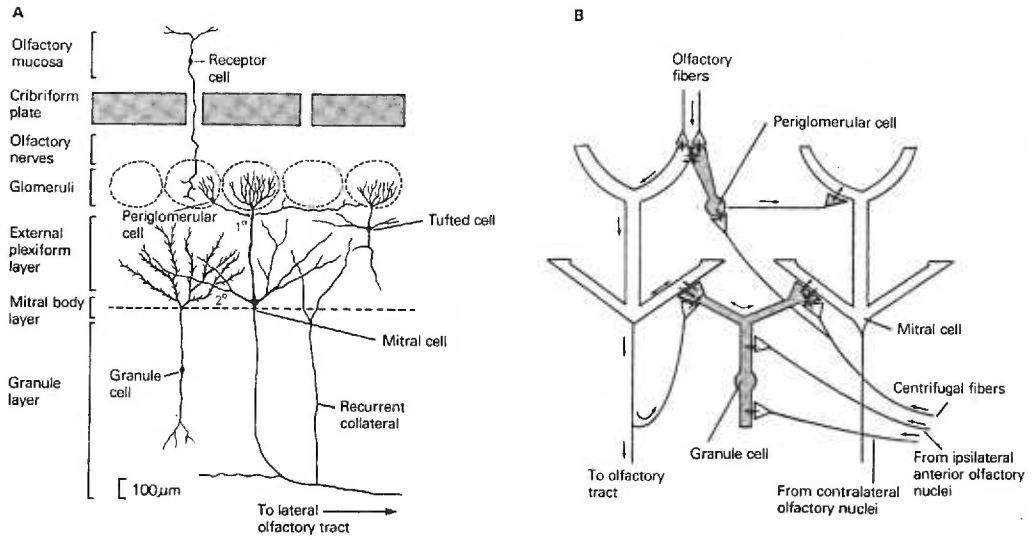

Figure 1: The mammalian olfactory bulb is organized in layers of cells. A, Neuronal elements. The mitral cell has primary (1°) and secondary (2°) dendrites and recurrent axon collaterals. There are also tufted cells, periglomerular cells and granule cells. The bulb is divided into five layers according to the distribution of these elements. B, Basic circuit diagram. The olfactory axons terminate in a layer of spherical structures of the neuropil termed glomeruli, where they synapse with the mitral cells, the tufted cells, and interneurons termed periglomerular cells. The dendrites of mitral cells and periglomerular cells are synaptically connected. Periglomerular cells distribute their axons to neighboring glomeruli. Secondary dendrites of the mitral cells make and receive synaptic contacts with the dendrites of granule cells. The output of the bulb is carried by axons of the mitral and tufted cells. (From Shepherd, 1972.)

The role of the olfactory bulb is not simply to direct the flow of olfactory information into olfactory cortical areas, however. A great deal of signal enhancement and processing goes on within the bulb. Experiments examining the topography of activation of glomeruli and mitral cells reveal rich patterns in response to odors such as propionic acid and isoamyl acetate (Slotnick, et al., 1987; Guthrie, et al., 1993; Sallaz, et al., 1993). Thus, it is an ensemble of activated glomeruli that must be transformed to enable an organism to associate odors with predators, food, potential mates, and prior experience. This transformation begins in the olfactory bulb where processing by neurons occurs at three distinct levels. The first site is within the glomeruli themselves where primary mitral/tufted cell dendrites synapse not only with olfactory receptor neuron axons but also with juxtaglomerular interneurons. The second site is the external plexiform layer where mitral cell secondary dendrites form reciprocal synapses with granule cells, another class of

interneurons. The third site is the mitral cell axon terminals in the olfactory cortex. Different mGluR subtypes are localized to all three of these sites and to different degrees have been implicated in processing and plasticity of olfactory sensation (Kinzie et al., 1995; Ohishi et al., 1995; Duvoisin et al., 1995).

mGluR2: An inhibitor of GABA release at dendrodenritic synapses

Perhaps the best studied example of how the location of an mGluR influences olfactory processing is the effect of mGluR2 at dendrodendritic synapses. Odorant signals exiting glomeruli encounter the external plexiform layer, a zone of extensive dendrodendritic contacts. These synapses are formed by secondary mitral cell dendrites oriented more laterally within this layer, and axonless interneurons, granule cells, whose cell bodies reside in the deeper granule cell layer. These are the most numerous synapses in the olfactory bulb (Shepherd, 1990) and are believed from physiologic and anatomical studies to be almost entirely reciprocal, with type I excitatory synapses from the mitral cell to the granule cells juxtaposed to type II inhibitory synapses oriented in the opposite direction. The dendrodendritic synapses provide for retrograde inhibition of excited mitral cells, as well as lateral inhibition (Jahr and Nicoll, 1982). Granule cells make inhibitory contacts directly with secondary dendrites of neighboring mitral cells. The importance of this lateral inhibitory network in olfactory learning and memory has been extensively studied. For example, in mice pheromones of the copulating male will not induce a block of pregnancy, however exposure to unfamiliar male pheromones will. Thus, there is a formation of an olfactory memory at the time of mating. This phenomenon has been termed the Bruce effect (Bruce, 1959). The mechanism of the memory induction stems from coincident centrifugal and olfactory inputs. The centrifugal input to dendrodendritic synapses encodes a pattern of inhibition of GABA release, allowing for favored patterns of mitral cell excitation coincident with odorant exposure leading to formation of an olfactory memory (Kaba and Keverne, 1988; Brennan et al., 1990).

The striking localization of mGluR2 to the dendrites of granule cells of the accessory olfactory bulb, the region involved in pheromone processing, was provocative evidence that these receptors are involved in the formation of an olfactory memory (Kaba et al., 1994). This was elegantly demonstrated in a pharmacological recapitulation of the Bruce effect. DCG-IV, a Group II-specific agonist, was infused into the accessory olfactory bulb of a female mouse during exposure to a male's urine. After mating with a second male, the odor of the first male did not interfere with implantation, indicating a memory for this pheromone ordinarily associated with mating. Physiologic studies suggest inhibition of GABA-induced IPSPs in accessory olfactory bulb mitral cells by DCG-IV (Hayashi et al., 1993), implying that retrograde inhibition is inhibited by local glutamate release whereas lateral inhibition of other mitral cells is presumably unaffected.

Evidence for an L-AP4 sensitive mGluR in mitral/tufted cells

In the 1980s when a G protein-coupled glutamate receptor coupled to PI production was reported, evidence was accumulating for another type of mGluR, one sensitive to the glutamate analog L-AP4. Koerner and Cotman reported that micromolar concentrations of L-AP4 inhibited extracellular excitatory postsynaptic potentials of the lateral perforant path (Koerner and Cotman, 1981). Other experiments demonstrated that L-AP4 failed to block excitation by applied L-glutamate, quisqualate or L-serine-O-sulfate which suggested that L-AP4 inhibited postsynaptic potentials by inhibiting neurotransmitter release. In 1992, mGluR4 was cloned and shown to be an L-AP4 sensitive receptor with mRNA expression in entorhinal cortex and other areas of the CNS known to contain L-AP4 sensitive receptors. However, no mRNA was found in the mitral and tufted cells of the olfactory bulb. Axons of these neurons form the lateral olfactory tract (LOT) and synapse on pyramidal neurons of the piriform cortex. This LOT-pyramidal neuron synapse was shown to contain L-AP4 sensitive receptors which when activated inhibit glutamate mediated excitatory postsynaptic potentials (Collins, 1982). This receptor was believed to

be presynaptically located and to inhibit neurotransmitter release (Anson and Collins, 1987). In addition, when cultured mitral cells were examined under whole-cell voltage-clamp methods, L-AP4 was found to inhibit high-threshold calcium currents (Trombley and Westbrook, 1992). The inhibition was irreversible in the presence of GTP-γ-S and was blocked by removing intracellular Mg^{2+} or by preincubation with pertussis toxin, therefore indicating the involvement of a G protein. Also, EPSPs evoked from monosynaptically coupled mitral cells in culture were reduced by the application of L-AP4 suggesting an mGluR was involved in the inhibition of neurotransmitter release.

Cloning of mGluR7

Because of the presumed existence of an L-AP4 sensitive receptor in mitral/tufted cells of the olfactory bulb, we screened a rat olfactory bulb library for novel cDNA clones, using probes derived from mGluR1 and mGluR4 (Saugstad et al., 1994). A full length cDNA clone encoding a metabotropic receptor (mGluR7) whose sequence was 69% identical to that of mGluR4 was isolated. Stimulation of mGluR7 with L-AP4 and glutamate (each at 1 mM) in stably transfected baby hamster kidney cells inhibited forskolin-stimulated cAMP formation, whereas ACPD (1 mM) and quisqualate (0.5 mM) were less effective. Inhibition of cAMP required high concentrations of agonist in the transfected cells, suggesting that inhibition of adenylate cyclase may not be the predominant transduction mechanism for this receptor in neurons. RNA blot analysis and *in situ* hybridization revealed that mGluR7 has an expression pattern in the central nervous system distinct from that of other L-AP4-sensitive mGluRs. Double-labeling with probes for mGluR1 and mGluR7 revealed that individual mitral/tufted neurons in the olfactory bulb expressed both mRNAs. The expression pattern and L-AP4 sensitivity of mGluR7 suggested that it mediates inhibition of transmitter release at selected glutamatergic synapses. The coexpression of multiple mGluR mRNAs in single neurons indicated that the cellular effects of mGluR activation are likely to result from the integrated action of

several receptor subtypes.

Unlike mGluR1, mGluR7 did not appear to couple to PI turnover in *Xenopus* oocytes. To test for mGluR7 involvement in the inhibition of adenylyl cyclase as had been shown for mGluR4, BHK cells were stably transfected with the mGluR7 cDNA and screened by RNA blot analysis and immunoblot analysis using a polyclonal antiserum prepared against a peptide representing amino acids 896-909. Confluent cells were assayed for cAMP production in the presence of isobutylmethylxanthine (1mM) after a 10-minute stimulation with forskolin (10 mM) in the presence or absence of mGluR agonists and antagonists. cAMP was measured by displacement of [^{3}H]cAMP. L-AP4 and L-glutamate were found to inhibit forskolin stimulated cAMP production with L-AP4 having a half-maximal inhibitory concentration of 0.5 mM and glutamate 1.3 mM (Figure 2). Though a high concentration of agonist was required for stimulation of the receptor, this may have be due to low levels of receptor expression or to low efficiency of coupling to adenylyl cyclase.

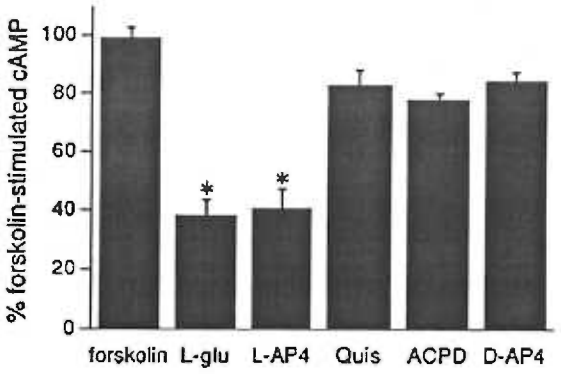

Figure 2: Inhibition of forskolin-stimulated cAMP production by mGluR7 in BHK cells. BHK cells transfected with mGluR7 were preincubated for 20 min with isobutylmethylzanthine (1 mM) and then incubated for 10 min with forskolin (10 μM), in the presence or absence of agonists or antagonists. Basal cAMP production was subtracted from the stimulated levels and the inhibition was plotted as a percentage of the forskolin-stimulated control. L-AP4 (1mM) and glutamate (L-glu; 1 mM) produced significant inhibition, whereas quisqualate (Quis; 0.5 mM) and ACPD (1 mM) produced small decreases that did not reach statistical significance. *, Significant ($p<0.05$) decreases in cAMP, compared with forskolin-treated controls.

The general pattern of RNA distribution for the mGluR7 was determined by RNA blot analysis and *in situ* hybridization. Hybridization of an mGluR7 cDNA probe to poly(A)+ selected RNA from several regions of adult rat brain revealed a single class of mRNA of approximately 4.4 kb. *In situ* hybridization indicated that mGluR7 is widely expressed throughout the central nervous system, unlike the the more constricted pattern for mGluR4, another L-AP4 sensitive receptor (Figure 2). The highest levels of mGluR7 expression were seen in the thalamus, neocortex and hypothalamus with moderate levels of expression in the hippocampus, olfactory bulb, brainstem and midbrain.

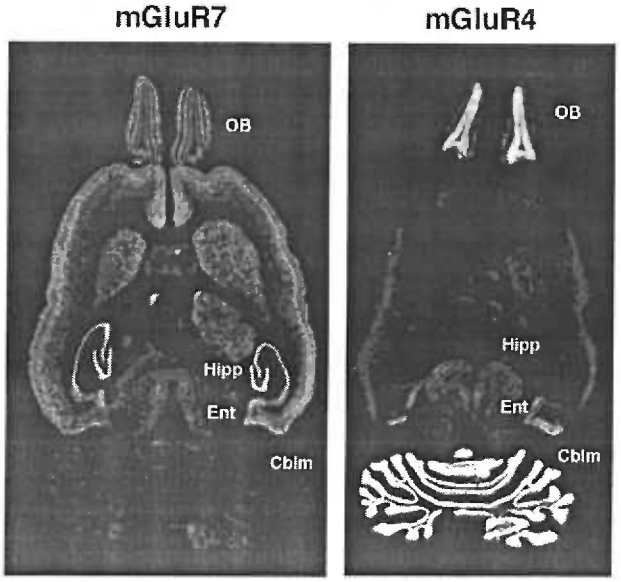

Figure 3: *In situ* hybridization of transverse sections labeled with a probe for mGluR7 mRNA, compared with a probe for mGluR4 mRNA, another member of the L-AP4-sensitive class of mGluRs. The distribution of mGluR7 was more widespread than that of mGluR4. OB, olfactory bulb; Hipp, hippocampus; ENT, entorhinal cortex; Cblm, cerebellum.

Distribution of mGluR7 mRNA in the developing and adult rat brain

My initial *in situ* hybridization work on mGluR7 suggested that the pattern of expression corresponded to that of the L-AP4 receptor. To further explore this hypothesis, I conducted a more thorough anatomic distribution study of mGluR7 in the developing and adult rat nervous systems. I found that mGluR7 mRNA is localized to neuronal groups known to respond to L-AP4 including mitral cells of the olfactory bulb, granule cells of the dentate gyrus and neurons of the entorhinal cortex and dorsal root ganglion. However, I also found that mGluR7 is widely expressed throughout the CNS, particularly in the

olfactory system. Nearly all neurons here express at least moderate levels of mGluR7 mRNA which suggests that the receptor could be performing a number of functions within the olfactory system. This work is discussed in chapter 1 and was published in *Neuroscience* (Kinzie et al., 1995).

Immunolocalization of mGluR7 in the rat olfactory bulb

The mRNA distribution study revealed that mGluR7 mRNA is expressed in mitral cells of the olfactory bulb suggesting that the receptor may be the L-AP4 sensitive autoreceptor found in mitral cell axons. Additionally, mGluR7 mRNA was found throughout the olfactory bulb. As discussed in chapter 2, in order to investigate the immunolocalization of mGluR7 in the olfactory system, I used a polyclonal antiserum specific for the carboxy terminus of the receptor. The principal area of immunoreactivity in the olfactory bulb was found in the cytoplasm mitral cell bodies. In the primary olfactory cortex, diffuse staining was present in layer Ia that was reduced following bulbectomy, consistent with mGluR7 being a presynaptic autoreceptor in mitral cell axons. However, in the olfactory bulb glomeruli immunoreactivity was present in axons and dendrites. The results indicate that mGluR7 is primarily presynaptic at olfactory bulb synapses, as would be predicted through physiological studies using L-AP4. The postsynaptic localization of mGluR7 at selected synapses, however, indicates that mGluR7 is not targeted exclusively to axonal compartments. This work has been published in the *Journal of Comparative Neurology* (Kinzie et al., 1997).

Modulation of *c-fos* induction in rat and mouse olfactory bulb

Although mGluR7 mRNA is abundantly expressed within the olfactory bulb, most of the translated protein is targeted outside of it. In order to explore the physiological role of an mGluR within the olfactory bulb, mGluR1 was examined. This subtype is coupled to phospholipase C and is highly expressed post-synaptically at mitral cell primary

dendrites. I hypothesized that upon activation of mGluR1, the release of intracellular calcium enhances the excitability of the mitral cell. As stated before, the mitral cell is unusual in that it contains dendrodendritic reciprocal synapses with interneurons called periglomerular cells. The result of increased dendritic calcium could be reflected in increased neurotransmitter release at the dendrodendritic synapses and therefore increased excitability of periglomerular cells. To test the hypothesis, I examined the induction of *c-fos* mRNA as a reporter of neuronal excitation. Exposure of mice to odors such as isoamyl acetate induce *c-fos* in specific regions of the olfactory bulb (Guthrie, et al., 1993). These patterns vary from odor to odor. I studied both wild-type and mGluR1 knockout mice to determine if they demonstrate different patterns of *c-fos* mRNA induction. Contrary to what I had hypothesized, the mGluR1 knock-out mice did not have detectibly different *c-fos* induction patterns. Additionally, the knockout mice appeared to react to odor and tyrosine hydoxylase expression in periglomerular cells does not differ from wild-type. Tyrosine hydroxylase expression is diminished with odor deprivation. Therefore, on the basis of my assays, the elimination of mGluR1 expression does not alter olfactory processing.

However, one positive finding that was made was that *c-fos* is induced in all mitral cells of rats injected with MK-801, a non-competitive NMDA antagonist. Granule cell responses are damped by MK-801, but can be overcome by exposing the rat to odor. The results corroborate electrophysiological studies in brain slices which demonstrated that NMDA receptor responses make up the majority of the excitatory synaptic response between mitral and granule cells. Additionally, feedback inhibition of mitral cells through the granule cell require the NMDA receptor. These experiments and their implications are discussed in chapter 3 and published in the *Journal of Neuroscience* (Schoppa, et al., 1998).

SUMMARY

The goal of this dissertation, therefore, is to examine the localization of one subtype of metabotropic glutamate receptor mGluR7, first by examining the CNS distribution of its mRNA and then by looking at receptor protein at the subcellular level. I will show that mGluR7 mRNA is widely distributed throughout the CNS including areas sensitive to the glutamate analog L-AP4. I will also show that mGluR7 mRNA is abundantly expressed in the olfactory system including olfactory bulb mitral cells. I will then focus on the cellular and subcellular distribution of mGluR7 in the olfactory system using immunohistochemical methods showing that the receptor is primarily presynaptic including mitral cell axons.

An additional goal of this dissertation is to demonstrate a functional role for an mGluR in olfactory information processing using mGluR1 null mutant mice. As will be discussed, attempts to elicit a functional difference in these mice versus wild-type were unsuccessful. However, these experiments led to a collaborative project that demonstrate that dendrodendritic inhibition in the olfactory bulb is driven by NMDA, not AMPA receptors. The findings suggest that olfactory information processing depends on long-lasting reciprocal and lateral inhibition.

DISTRIBUTION OF METABOTROPIC GLUTAMATE RECEPTOR 7 MESSENGER RNA IN THE DEVELOPING AND ADULT RAT BRAIN

J. Mark Kinzie, Julie A. Saugstad, Gary L. Westbrook and Thomas P. Segerson

Vollum Institute

Oregon Health Sciences University

Portland, Oregon 97201

Correspondence:

Thomas P. Segerson

Vollum Institute, L-474

Oregon Health Sciences University

3181 SW Sam Jackson Park Road

Portland, Oregon USA 97201

Phone (503) 494-5496

Fax (503) 494-4534

E-mail segerson@ohsu.edu

Abbreviations:

AP4	L-2-amino-4-phosphonobutyric acid
DTT	dithiothreitol
E	embryonic day
EDTA	ethylenediaminetetraacetic acid
LC	locus coeruleus
LOT	lateral olfactory tract
mRNA	messenger RNA
P	post-natal day
PO	primary olfactory cortex
SSC	standard saline citrate

Summary

The large number of metabotropic glutamate receptor subtypes suggest diverse roles in brain function, although specific distribution patterns can give clues to subtype-specific functions (Hayashi et al., 1993; Nakajima et al., 1993; Nomura et al., 1994; Ohishi et al., 1993). The metabotropic glutamate receptor mGluR7 is sensitive to the agonist L-2-amino-4-phosphonobutyric acid, a presynaptic inhibitor of neurotransmitter release. We examined the anatomic distribution of mGluR7 mRNA expression by *in situ* hybridization in the developing and adult rat central nervous systems. Our results demonstrate that mGluR7 messenger RNA is among the most widely distributed of mGluRs in both the developing and adult rat nervous system and that mGluR7 messenger RNA is expressed in most neuronal groups known to respond to L-2-amino-4-phosphonobutyric acid including mitral cells of the olfactory bulb, granule cells of the dentate gyrus and neurons of the entorhinal cortex and dorsal root ganglion. mGluR7 exhibits preferential expression in sensory afferent pathways and is highly represented in the periventricular zone of the hypothalamus, the latter implying a modulatory role for mGluR7 in neuroendocrine pathways. Most strikingly, the majority of neurons at all levels of olfactory circuitry are among the areas of highest mGluR7 mRNA content.

The anatomic distribution of mGluR7 messenger RNA suggests that mGluR7 activation may participate in the processing of hippocampal, sensory and olfactory information.

Key words: *In situ* hybridization, L-2-amino-4-phosphonobutyric acid, olfactory, hypothalamus, spinal cord, presynaptic.

Introduction

Receptors for the excitatory neurotransmitter glutamate either gate transmembrane flux of ions at the postsynaptic membrane or catalyze activation of guanyl nucleotide binding protein (G protein)-dependent signaling pathways that modulate synaptic function. This latter role for glutamate is subserved by the metabotropic class of glutamate receptors, (mGluRs). Although there is considerable recent information describing potential functions for mGluRs (Nakanishi, 1994; Schoepp and Conn, 1993; Westbrook, 1994), their elucidation continues to be hampered by a dearth of specific agonists and antagonists, in contrast to the former, or ionotropic, group of glutamate receptors. Many recent studies of mGluR function have been made possible by the identification of eight mGluR cDNAs that fall into three groups based on amino acid homology, signal transduction mechanism, and pharmacological profile. Group I includes the quisqualate-preferring mGluRs 1 and 5 that couple to hydrolysis of phosphotidylinositol and the release of intracellular calcium (Abe et al., 1992; Houamed et al., 1991; Masu et al., 1991; Saugstad et al., 1995). Group II includes the 1S,3R-aminocyclopentane-1,3-dicarboxylic acid preferring mGluRs 2 and 3 (Nakanishi, 1994; Tanabe et al., 1992; Tanabe et al., 1993), and group III includes the L-2-amino-4-phosphonobutyric acid (L-AP4) -preferring mGluRs 4, 6, 7 and 8 (Duvoisin et al., 1995; Okamoto et al., 1994; Saugstad et al., 1994; Tanabe et al., 1993). Groups II and III couple to the inhibition of forskolin-stimulated cyclic AMP production in heterologous cell lines. Within each group, however, pharmacologic agents cannot distinguish the effects of individual receptors. Therefore, molecular approaches will be indispensable for determining the function of individual mGluR molecules, both by defining their expression in CNS pathways and as tools for manipulating their expression.

Our laboratories, and that of Nakanishi, have identified one member of the L-AP4-preferring class of mGluRs (mGluR7) that is particularly widespread in its CNS distribution (Okamoto et al., 1994; Saugstad et al., 1994). Previous studies on CNS slice preparations and cultured neurons suggest that, with the exception of the ON bipolar cell in

retina, L-AP4 receptors act presynaptically to inhibit release of neurotransmitter (Mayer and Westbrook, 1987). The pathways most sensitive to inhibition by L-AP4 are the lateral perforant pathway from the pyramidal cells of entorhinal cortex to the granule cells of the dentate gyrus, and the lateral olfactory tract (LOT) from olfactory bulb mitral cells to superficial dendrites of pyramidal cells in the primary olfactory cortex (PO) (Anson and Collins, 1987; Collins, 1982; Hearn et al., 1986; Hori et al., 1982). Inhibitory presynaptic effects of L-AP4 are also observed in spinal cord afferents (Davies and Watkins, 1982; Evans et al., 1979) and in the mossy fiber pathway from dentate gyrus to CA3 hippocampal cells (Cotman et al., 1986; Lanthorn et al., 1984; Yamamoto et al., 1983). Preliminary studies of mGluR7 mRNA distribution in the CNS (Okamoto et al., 1994; Saugstad et al., 1994) suggest that its pattern of expression more closely approximates that of the presynaptic AP4 receptor described by physiological studies than other members of the class III subgroup. We examined this hypothesis by determining the anatomical expression of mGluR7 mRNA expression by *in situ* hybridization in the developing and adult rat CNS.

Experimental procedures

Male/Female Sprague-Dawley rats (Bantin and Kingman, Fremont, CA) at postnatal stages P0, P7, P14, P21 and adult were deeply anesthetized with pentobarbital and perfused transcardially with ice-cold saline, followed by ice-cold 4% paraformaldehyde in 0.1 M sodium borate (pH 9.5). The brains were removed quickly and post-fixed overnight at 4°C in 4% paraformaldehyde in borate buffer (pH 9.5) containing 10% sucrose. For embryonic day (E) 18 rat embryos, pregnant rats were perfused transcardially as above. The embryos were removed and fixed in 4% paraformaldehyde in borate buffer (pH 9.5) at 4°C, then post-fixed as above.

Cryostat microtome sections (25 μm) were mounted onto gelatin- and poly-L-lysine-coated glass slides and incubated for 15 min in 4% paraformaldehyde in 0.1 M phosphate-buffered saline, washed twice in 0.1 M phosphate-buffered saline, and treated for 30 min at 37°C in 10 μg/ml proteinase K in 100 mM Tris/50 mM EDTA (pH 8), followed by 0.0025% acetic anhydride in 0.1 M triethanolamine at room temperature. The sections were then washed in 2X SSC (1X SSC= 0.15 M NaCl, 0.015 M Na citrate), dehydrated in increasing concentrations of ethanol, and vacuum-dried at room temperature and stored at -80°C until use.

The probe for mGluR7 mRNA was generated using an *Xho* I fragment encoding amino acids 1-197, subcloned into pBluescript KS. An mGluR4 probe for use in control experiments was transcribed using an *Xho* I/*Pst* I fragment encoding amino acids 110-521, subcloned into pBluescript KS. Using linearized template DNA, ^{35}S -labeled antisense mGluR7 cRNA probe was transcribed as described (Saugstad et al., 1994), heated to 65°C for 5 min and diluted to 10^7 cpm/ml in hybridization buffer (66% formamide, 260 mM NaCl, 1.3X Denhardt's solution, 13 mM Tris (pH 8.0), 1.3 mM EDTA, 13% dextran sulfate). Hybridization mixture applied to the sections was covered with siliconized glass coverslips and sealed using DPX mountant. After incubating at 58°C for 20-24 hr, the slides were soaked in 4X SSC to remove coverslips, then rinsed in 4X SSC (4 times, 5

min each) prior to ribonuclease A treatment (20 μg/ml for 30 min at 37°C). The slides were then rinsed in decreasing concentrations of SSC containing 1 mM dithiothreitol (DTT) to a final stringency of 0.1X SSC, 1 mM DTT for 30 min at 65°C. After dehydrating the sections in increasing concentrations of ethanol, they were vacuum-dried and exposed to DuPont Cronex-4 X-ray film for 6 days. They were then dipped in NTB-2 liquid photographic emulsion (Kodak), exposed for 13 days, developed with D-19 developer and counter-stained with Thionin.

Melting temperature (T_m) control experiments of adult rat brain parasagittal sections were performed by hybridization with mGluR7 cRNA probe as described above with modification of wash temperature. Following hybridization and low stringency washes, individual sections were rinsed in 0.1X SSC, 1 mM DTT for 30 min at temperatures ranging between 65°C and 100°C, then treated thereafter as described above. The intensity of labeling of the sections washed at different temperatures was determined by densitometry of the autoradiograms as described below.

For competition experiments, sections were incubated overnight in either hybridization solution alone, hybridization solution containing 100-fold excess unlabeled mGluR7 probe or 100-fold excess unlabeled mGluR4 probe. Following rinses in 2X SSC, sections were incubated with hybridization mix containing the appropriate unlabeled probe and 10^7 cpm/ml ^{35}S -labeled mGluR7 probe. Subsequent treatments were performed as described above.

Film autoradiograms of hybridized sections were converted to digital images for anatomical analysis and semi-quantitative estimation of relative level of hybridization in various neuroanatomical structures. DuPont Cronex-4 X-ray film exposed to hybridized tissue sections was scanned by a Nikon LS3500 scanner at 118 pixel/cm resolution and the images analyzed using Image v1.55 software (NIH). Pixel density in each image was normalized to the density of layers II-IV of neocortex and examined in four bins of density

from highest to lowest. Accordingly, anatomical regions were assigned values of high, moderate, low and background hybridization. Emulsion autoradiographs of hybridized sections were analyzed by darkfield light microscopy.

Results

Probe specificity

The specificity of the probe for mGluR7 mRNA was established by several lines of evidence. First, an unlabeled mGluR7 antisense probe used in hundred-fold excess blocked hybridization by the labeled mGluR7 probe (Fig 1B). Second, an unlabeled mGluR4 cRNA control probe in 100-fold excess did not reduce hybridization of the labeled mGluR7 probe (Fig 1C). The mGluR4 probe was chosen because mGluR4 was the published receptor of most nucleotide sequence similarity to mGluR7 (69%) (Saugstad et al., 1994). Third, T_m analysis of the mGluR7 probe demonstrated that the probe was removed from all brain regions when hybridized sections were washed in the narrow temperature range of 90-99°C rather that being gradually removed over a wider temperature range, indicating that the mGluR7 probe hybridizes specifically to one species of mRNA. In addition, RNA blot analysis using the identical probe (Saugstad et al., 1994) recognizes a single species of mRNA at hybridizations of similar stringency. Furthermore, a preliminary pattern of mGluR7 mRNA expression by *in situ* hybridization employing an RNA probe generated from a distinct region of the mGluR7 cDNA (Okamoto et al., 1994) is consistent with the results of this study.

Overall Distribution Pattern in the Adult and Developing Rat Brain

Cells that express detectable levels of mGluR7 mRNA were widely distributed in each major division of the CNS, with high levels of expression in neocortex, olfactory bulb, olfactory cortex, thalamus, hypothalamus, and superior and inferior colliculi (Fig 1A). In contrast to the expression pattern reported for mGluR4 mRNA (Iversen et al., 1994; Tanabe et al., 1993; Testa et al., 1994), mGluR7 expression is low in cerebellum and high in dentate gyrus and hippocampus. The mGluR7 probe labeled only neurons, with no apparent hybridization in the corpus callosum or other fiber tracts. The densities of

hybridization signals over different regions of the CNS are presented in Table 1.

Parasagittal sections derived from whole embryos (E18) as well as brains of rats killed on P0, P7, P14, and P21 were examined for mGluR7 mRNA expression (Fig 2). At E18, mGluR7 mRNA labeling was prominent over neurons in the olfactory bulb, cortex, brainstem, spinal cord and dorsal root ganglia. In addition, high levels of mGluR7 mRNA expression were seen in the developing cerebellum, in contrast to the low levels observed in adult animals. Similarly, mGluR7 mRNA is abundant in the neocortex of early postnatal animals, with maximal labeling found in P0 neonates and decreases at later developmental stages. In the olfactory bulb, both mitral and granule cells appeared to express mGluR7 mRNA during the postnatal period, but labeling over granule cells decreased by adulthood. Interestingly, hybridization signals over cells in the glomerular layer of the olfactory bulb, representing either tufted cells or periglomerular cells, were not detectable until P7. This time course of expression in the glomerular layer may correspond to the migration of periglomerular cells into glomeruli (Valverde et al., 1992).

The most noticeable change in expression during development is in the cerebellum where Purkinje cells express mGluR7 mRNA at all postnatal stages, but labeling over cerebellar granule cells was detected only through P21 (cf. Fig 1A with Fig 2B, P21). In the adult mGluR7 mRNA expression all but disappears in granule cells, while mGluR7 mRNA expression in Purkinje cells is maintained.

A change in expression during development was also observed in the hippocampus. At birth, expression of mGluR7 mRNA in regions CA1-CA3 of the hippocampus is more prominent than in the dentate gyrus. At P7 and P14, labeling over regions CA1-CA3 and the dentate gyrus was of equal intensity, whereas in P21 and adult animals the dentate gyrus was more strongly labeled than CA1-CA3.

Olfactory bulb and anterior forebrain

mGluR7 mRNA is distributed widely throughout the olfactory bulb and anterior

forebrain in the adult rat (Fig 3, Table 1). In the main olfactory bulb, the most intense labeling was observed over the mitral and tufted cells (Fig 3B), with weaker hybridization seen over periglomerular and granule cells. In the accessory olfactory bulb, as in the main olfactory bulb, mitral cells were most intensely labeled. The anterior olfactory nuclei and tenia tecta showed moderate intensity of labeling. In the PO, we observed intense labeling with the mGluR7 probe over pyramidal neurons. Similarly intense hybridization was present over neurons in the olfactory tubercle and islands of Calleja, including the major island (Fig 3A), as well as over the nucleus of the lateral olfactory tract (Fig 3C). Areas of moderate hybridization included the dorsal part of the lateral septal nucleus and the triangular septal nucleus.

Middle forebrain, thalamus and basal ganglia

Numerous nuclei of the thalamus, hypothalamus and amygdala displayed high and moderate amounts of mGluR7 mRNA. In the thalamus, highest intensity labeling was observed over cells in the anterodorsal, paraventricular and centromedial nuclei (Fig 4A and 4D). Moderate levels were found in the rhomboid, reuniens, interanteromedial, gelatinosus and mediodorsal thalamic nuclei. In the hypothalamus, the highest intensity labeling was found over neurons in the ventromedial and dorsomedial nuclei (Fig 4A), the anterior hypothalamic area, the supraoptic nucleus (Fig 3C) and the arcuate nucleus. In the amygdala, cells in the lateral, anterior cortical, central, medial and basomedial nuclei contain the highest amounts of mGluR7 mRNA expression. The medial and lateral mammillary nuclei showed intense hybridization for mGluR7 mRNA (Fig 5B), whereas cells in the adjacent interpeduncular nucleus labeled with moderate intensity (Fig 5A).

In frontoparietal neocortex, hybridization for mGluR7 mRNA was absent in layer I, but was present at variable levels from layers II through V (Fig 4A). Layer IV appeared to have the highest intensity of labeling, perhaps due to higher cell density (Fig 4B and 4C). High power light microscopic examination of hybridizing cells in frontoparietal cortex

demonstrated accumulation of silver grains generally over cells with larger nuclei. Layers II and III exhibited somewhat lower intensity of hybridization than layer IV. The cingulate gyrus showed accentuated hybridization compared to adjacent regions of the frontoparietal cortex.

In the basal ganglia the caudate putamen and the nucleus accumbens have moderate levels of mGluR7 mRNA expression, whereas the globus pallidus contained virtually no labeling (Fig 4A). The labeling pattern over the caudate putamen was irregular (Fig 1A) suggesting hybridization over distinct clusters of neurons. This pattern may indicate segregation of striatal neurons into functional modules of mGluR7-expressing cells (Graybiel, 1990; Testa et al., 1994).

Posterior forebrain, hippocampus and midbrain

One of the areas most intensely labeled for mGluR7 mRNA was the granular layer of the dentate gyrus (Fig 1A). Scattered cells in the hilar region of dentate gyrus also were highly labeled. High intensity labeling was observed over the pyramidal layer of all regions of Ammon's horn. The subiculum and entorhinal cortex also exhibited high levels of mGluR7 mRNA compared to adjacent cortical regions, as did the retrosplenial cortex and the striate cortices 17 and 18. In the midbrain the central grey area, the medial geniculate nucleus, the superficial grey layer of the superior colliculus and the interpeduncular nucleus were the areas of greatest hybridization, though the level of mGluR7 mRNA in all these regions was moderate (Fig 5A).

Cerebellum and brainstem

In the cerebellum of adult rats, only Purkinje cells were labeled by the mGluR7 probe (Fig 6A), in contrast to prenatal and neonatal animals (Fig 2). However, mGluR7 mRNA was found at relatively low levels in adult Purkinje cells, although this may be due in part to low cell density in the adult Purkinje cell layer. In the brainstem, the locus

coeruleus (LC) was intensely labeled, both in immature and adult brain (Fig 6B), and light microscopic examination revealed dense accumulations of silver grains over the majority of cells in this nucleus. Pontine nuclei were moderately labeled, while weakly labeled areas included the dorsal and ventral parabrachial, spinal vestibular and inferior olivary nuclei, as well as the hypoglossal nucleus and nucleus of the solitary tract (not shown).

Spinal cord and dorsal root ganglia

In the spinal cord, Rexed lamina 1 and 2 were the most heavily labeled. However, scattered labeled cells were found throughout the gray matter of the spinal cord (Fig 7A). In dorsal root ganglion, scattered cells were found to be moderately labeled (Fig 7B). The distribution of labeled cells and the pattern of silver grain accumulation over the cytoplasm of these cells suggested that the mGluR7 probe labels a subpopulation of larger dorsal root ganglion neurons.

Discussion

The expression pattern of mGluR7 mRNA suggests that this receptor may be the most widely distributed of the identified mGluR subtypes in the CNS. Comparison of the anatomical distribution of mGluR7 mRNA with regional studies of L-AP4 neuropharmacology implies that mGluR7 mediates a component of L-AP4 activity . Moreover, the high correlation of mGluR7 mRNA expression with the known effects of L-AP4 on presynaptic neurotransmitter release in the LOT, perforant and spinal cord suggests a presynaptic function for mGluR7. mGluR7 may also play a role in normal CNS development as several neuronal areas, in particular the cerebellum, demonstrate transient expression of mGluR7 mRNA during development. Important roles for mGluR7 in sensory pathways, and especially olfaction, are implied by predominant expression of mGluR7 mRNA in sensory relay nuclei, and in nearly all olfactory cell groups.

Metabotropic glutamate receptor 7 distribution and L-AP4-sensitive presynaptic receptors

We examined in detail the distribution of mGluR7 mRNA in perikarya that give rise to axon terminals responsive to L-AP4. Physiologic studies suggest that axons of the LOT projecting from glutamatergic mitral and tufted cells in the olfactory bulb are sensitive to modulation by L-AP4 (Anson and Collins, 1987; Collins, 1982; Collins and Howlett, 1988; Trombley and Westbrook, 1992). Axons of mitral cells exit the olfactory bulb and travel along layers I and II of the PO sending projections *en passant* to superficial dendrites of pyramidal cells in layers II and III of the primary olfactory cortex. Because our studies show high levels of mGluR7 in mitral and tufted cells, in contrast to the lack of expression of mGluR4 and mGluR6 in these cells, it is possible that LOT L-AP4 receptors are encoded by mGluR7 mRNA. Recently, a fourth L-AP4-sensitive mGluR, mGluR8 (Duvoisin et al., 1995), has been characterized that is also expressed in mitral and tufted cells. Therefore, either mGluR7 or mGluR8 may represent L-AP4 receptors in LOT.

Alternatively, these receptors may be differentially targeted to separate pre- or post-synaptic sites.

In the hippocampus, the laternal perforant pathway and the medial perforant pathway, which originate with cell bodies in the entorhinal cortex and terminate on granule cells of dentate gyrus, is inhibited by L-AP4 (Ganong and Cotman, 1982; Harris and Cotman, 1983; Koerner and Cotman, 1981; White et al., 1977). Our studies demonstrate mGluR7 expression in the entorhinal cortex equivalent to or greater than expression seen in other cortical regions. Therefore, mGluR7 is an ideal candidate for the presynaptic L-AP4 receptor in the perforant pathway. However, mGluR4, another L-AP4-responsive mGluR, is also expressed in the entorhinal cortex (Saugstad et al., 1994; Tanabe et al., 1992). mGluR4 and mGluR7 may be targeted to identical or different regions of the same neuron or may be expressed in distinct populations of entorhinal pyramidal cells.

Granule cells of the dentate gyrus innervate CA3 cells from axons in the mossy fiber pathway. In the guinea pig, this pathway is also inhibited by L-AP4, consistent with a presynaptic action of L-AP4 inhibition on mossy fiber axon terminals (Cotman et al., 1986; Lanthorn et al., 1984; Yamamoto et al., 1983). mGluR7 mRNA is the only group III mGluR expressed at high levels in granule cells of the dentate gyrus, and thus would appear to mediate L-AP4 inhibition of CA3 activity. The function of L-AP4 in the mossy fiber pathway appears to be species-specific (Cotman et al., 1986; Lanthorn et al., 1984) or to inhibit only a subpopulation of granule cells of the dentate gyrus.

mGluR7 mRNA is expressed at moderate to high levels in dorsal root ganglion cells in both developing and adult rats and in neurons of the dorsal horn of the spinal cord. This pattern of mGluR7 mRNA expression parallels an expected pattern for a presynaptic inhibitory L-AP4 receptor in monosynaptic and multisynaptic spinal cord afferents (Evans, 1986).

mGluR7 mRNA in sensory pathways

mGluR7 appears to exhibit preferential expression in sensory afferent pathways. In addition to dorsal root ganglion and spinal cord dorsal horn, mGluR7 is expressed in the lateral and medial geniculate bodies, vestibular nuclei and trigeminal ganglion, as well as in numerous thalamic nuclei. The expression of mGluR7 in dorsal root ganglion neurons of one morphologic size and in lamina of spinal cord dorsal horn specific for pain and temperature sensation suggest that mGluR7 may have modality specificity in these sensory afferents (Mu et al., 1993).

Neuroendocrine pathways

Many hypothalamic nuclear groups express mGluR7 mRNA in a pattern suggestive of a role for mGluR7 in neuroendocrine function. Moderate levels of mGluR7 mRNA are detected in cells of most nuclei in the hypothalamic periventricular zone, the site of neurons that express hypophysiotrophic neuropeptides. mGluR7 mRNA is also present in neurons of the supraoptic nucleus, a nucleus that, together with the magnocellular part of the paraventricular nucleus, is a site of synthesis of the posterior pituitary hormones vasopressin and oxytocin. Therefore, the expression of mGluR7 in functionally related hypothalamic nuclei and their projections that are likely glutamatergic (van den Pol et al., 1990), suggests an important role for mGluR7 in neuroendocrine control of pituitary hormone secretion.

mGluR7 in the olfactory system

The pattern of mGluR7 mRNA expression is also striking in its representation in neurons involved in olfaction, both in the developing and adult animal. There is physiologic evidence, albeit controversial, for expression of L-AP4 receptors in primary olfactory cortex that may arise from intrinsic neurons of this region (Collins and Howlett, 1988; Hasselmo and Bower, 1991). In addition to distal projections from layers II and III, PO pyramidal neurons also give rise to association fibers that synapse superficially and

deeply on adjacent pyramidal cells of the PO. In rat olfactory cortex slices (Collins and Howlett, 1988), L-AP4 decreases the amplitude of the N'a'-wave recorded in PO after LOT stimulation, representing the activity of mitral cell axons on pyramidal cell dendrites. In these same studies, there is a decrease in the area of the N'b'-wave that may represent superficial synapses of association fibers of pyramidal cells. Therefore, L-AP4 receptors in PO neurons may be expressed intrinsically in the PO, where they could mediate plasticity of associative connections in the primary olfactory cortex, a potentially important phenomenon in the processing of olfactory information (Haberly and Bower, 1989).

In addition to afferent pathways from the olfactory bulb, projections to the olfactory bulb from other brain regions may also express mGluR7. The source of centrifugal adrenergic fibers to olfactory bulb granule cells is the LC (Shipley et al., 1985), which interestingly is the area showing the highest levels of mGluR7 mRNA. From this we postulate that terminals from LC projections to dendrodentritic synapses in olfactory bulb contain mGluR7. Adrenergic projections to the olfactory bulb are thought to be important in associative modulation of olfactory information. This is well characterized for the formation of olfactory memory in the accessory olfactory bulb (Kaba and Keverne, 1988), but is also thought to be important in the processing of olfactory signals in the main olfactory bulb (Leon, 1987). Presynaptic effects of mGluRs at these synapses in accessory olfactory bulb have been shown to mimic adrenergic effects in the formation of olfactory memory with high specificity (Kaba et al., 1994).

Conclusions

The expression of mGluR7 mRNA in most L-AP4-responsive neuronal groups implies that mGluR7 mediates, at least in part, the action of L-AP4 in these neurons, possibly by acting presynaptically. A predominant pattern of expression in sensory pathways and expression in hypothalamic neurons suggest roles for mGluR7 in sensory and neuroendocrine function. The striking pattern of expression in nearly all neurons involved in olfactory information processing is consistent with an important functional role in mGluR7 in the olfactory system, the oldest neocortical circuitry known to encode memory. However, more specific anatomical and physiological information about expression of mGluR proteins at synaptic sites is required to clearly define the functional roles of these receptors.

Acknowledgements: We thank R. Simerly for discussion and comments on the manuscript and R. Duvoisin for providing the mGluR8 manuscript before publication. This work was supported by NIH grants MH10314 (JMK), NS09200 (JAS), DC01783 (TPS), and the Klingenstein Foundation (GLW).

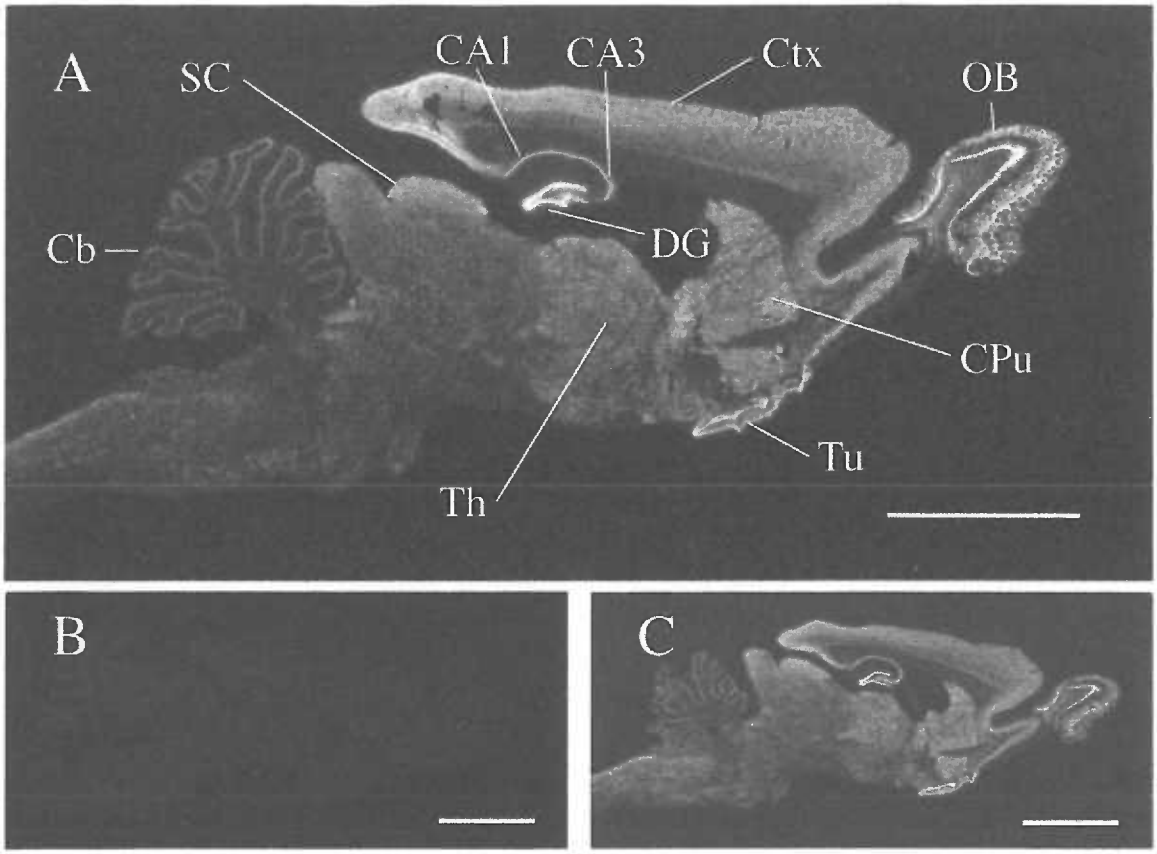

Figure 1. Distribution of mGluR7 mRNA in the adult rat brain. Autoradiograms of in situ hybridization with antisense mGluR7 cRNA probe are shown in the absence (A) and presence (B) of 100-fold excess unlabeled RNA probe and in the presence (C) of 100-fold excess unlabeled mGluR4 RNA probe. CA1, field CA1 of Ammon's horn; CA3, field CA3 of Ammon's horn; Cb, cerebellum; CPu, caudate putamen; Ctx, isocortex; DG, dentate gyrus; OB, olfactory bulb; SC, superior colliculus; Th, thalamus; Tu, olfactory tubercle. Scale bar, 5 mm.

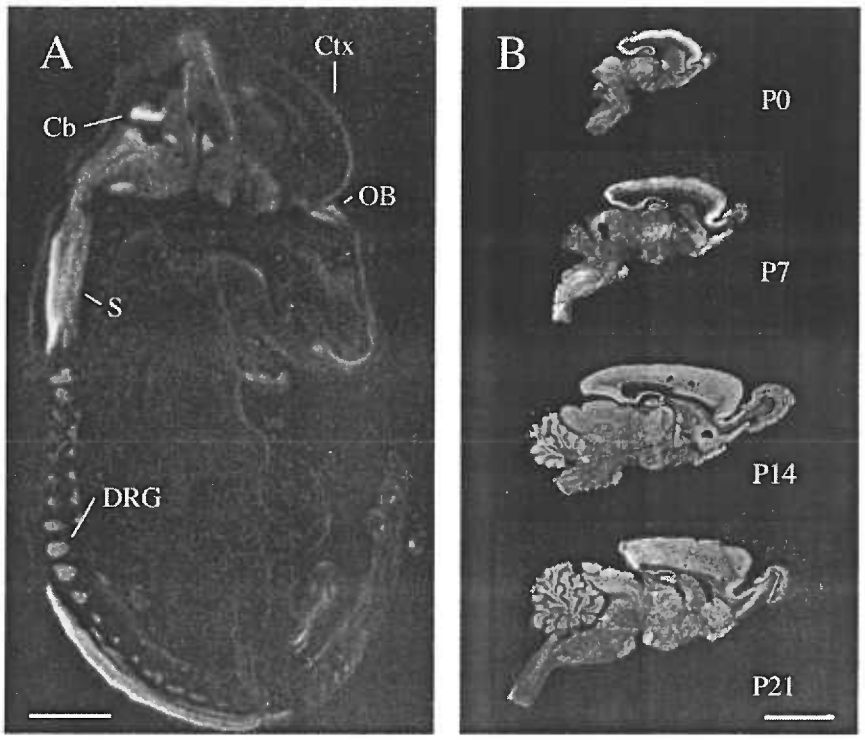

Figure 2. Developmental distribution of mGluR7 mRNA in rat. Autoradiograms of in situ hybridization with antisense mGluR7 cRNA probe in rat whole embryo E18 (A) and in brains of developmental stages P0, P7, P14 and P21 (B). Cb, cerebellum; Ctx, neocortex; DRG, dorsal root ganglion; OB, olfactory bulb; S, spinal cord. Scale bars, (A) 2 mm, (B) 5 mm.

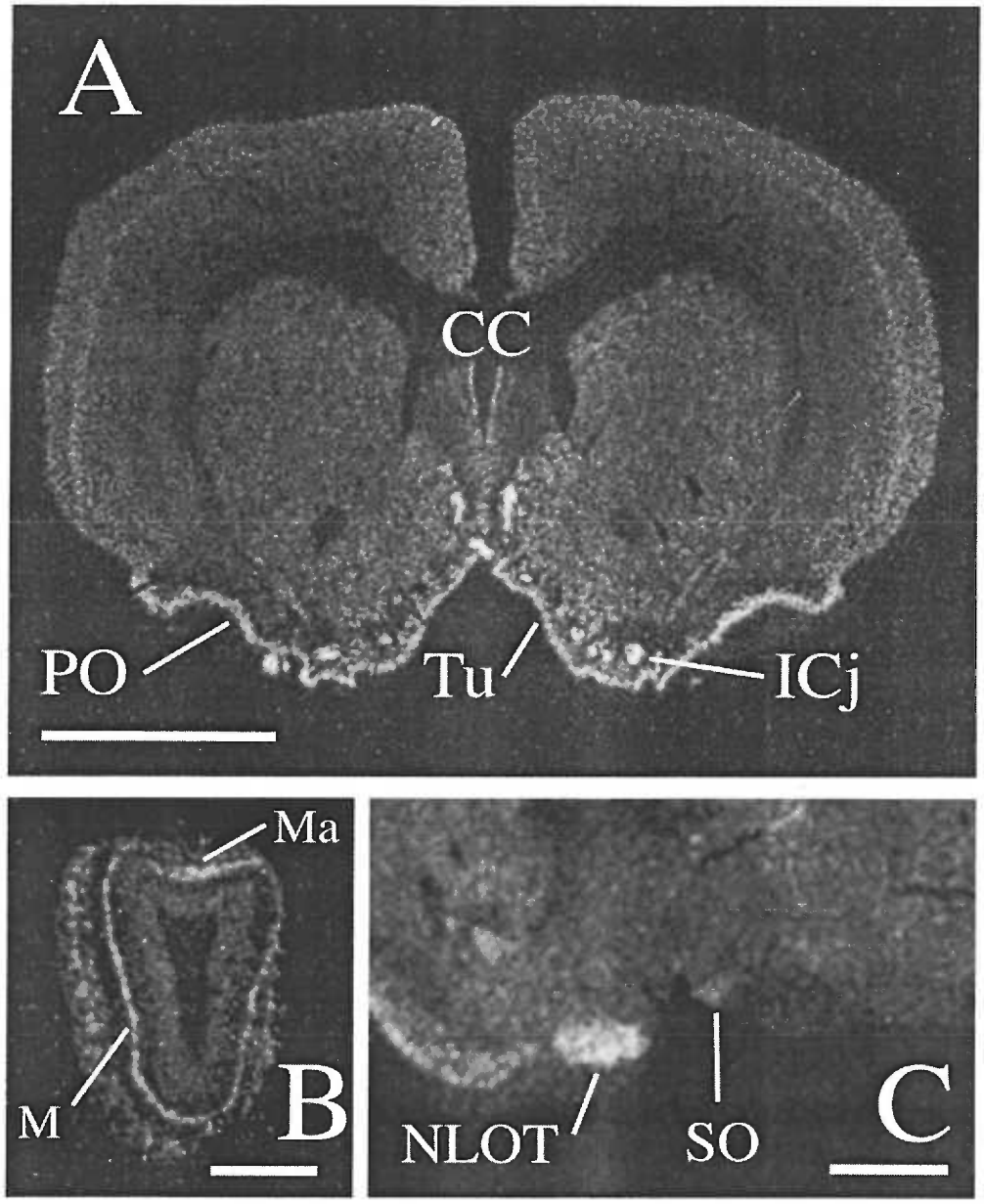

Figure 3. Localization of mGluR7 mRNA in the olfactory bulb and anterior forebrain. (A) In the anterior forebrain, pyramidal cells of the primary olfactory cortex (PO) and olfactory tubercle (Tu) show high levels of hybridization to mGluR7 probe, as do the islands of Calleja (ICj). (B) The mitral layers of the main olfactory bulb (M) and accessory olfactory bulb (Ma) are intensely labeled. In addition, the nucleus of the lateral olfactory tract (NLOT) and the supraoptic nucleus (SO) are also stongly labeled (C). Scale bars, (A) 3 mm, (B) and (C) 1 mm.

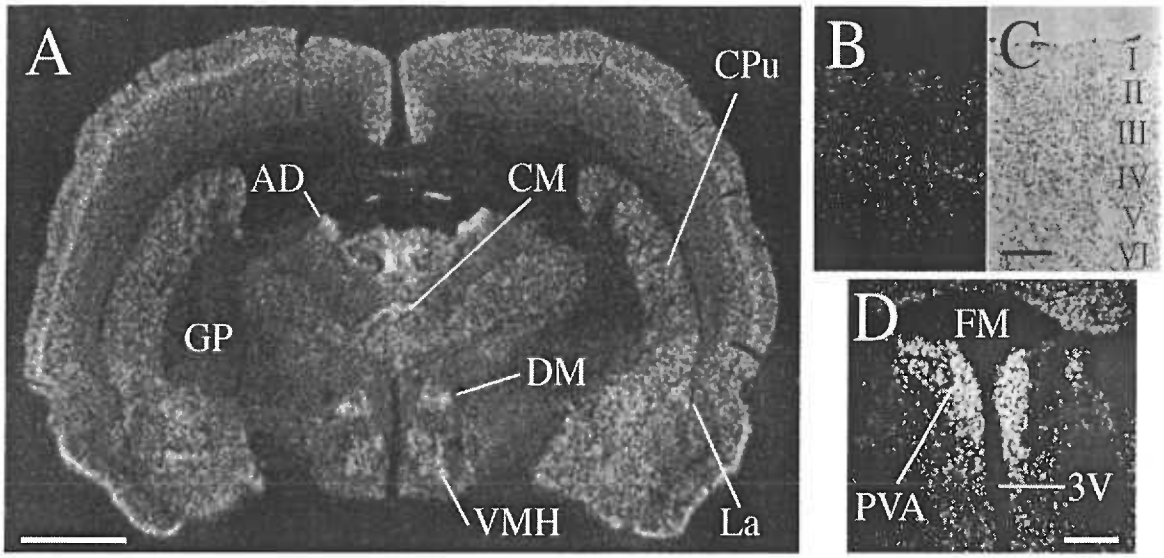

Figure 4. Localization of mGluR7 mRNA in the middle forebrain. Highly labeled regions of the middle forebrain (A) include the anterodorsal (AD) and centromedial (CM) thalamic nuclei, as well as the anterior subdivision of the paraventricular thalamic nucleus (PVA) (D). Moderate levels of hybridization were seen in the dorsomedial (DM) and ventromedial (VMH) hypothalamic nuclei, the lateral amygdaloid nucleus (La) and the caudate putamen (CPu). Only background levels of labeling was found in the globus pallidus (GP). Darkfield photomicrograph of the frontoparietal neocortex (B) demonstrates moderate levels of hybridization to mGluR7 probe over layers II, III, and IV. (C) Bright field photomicrograph of the identical section. 3V, third ventricle; FM, foramen of Monro. Scale bars, (A) 2 mm, (B) and (C) 250 mm, (D) 500 mm.

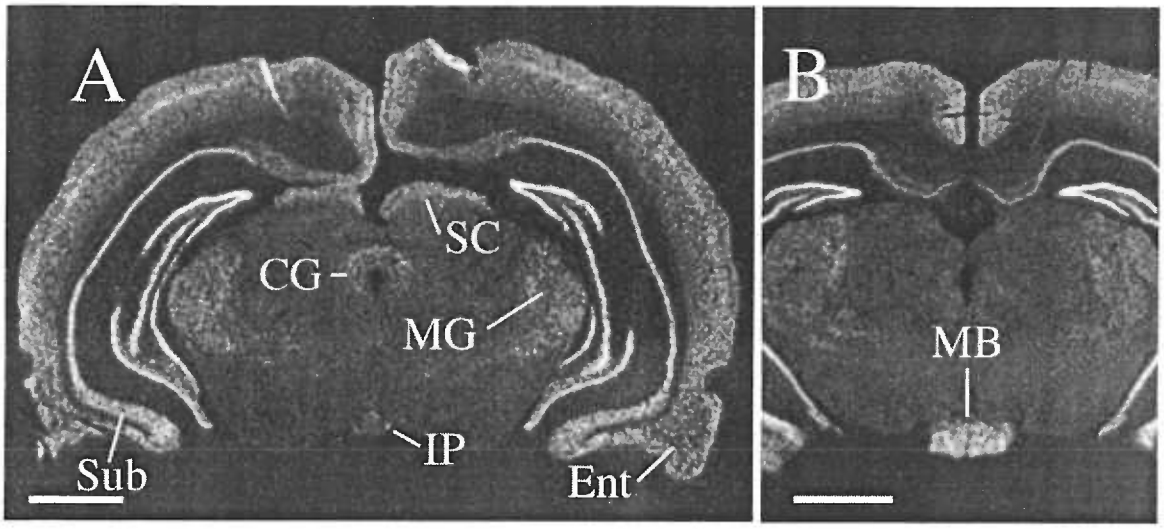

Figure 5. Localization of mGluR7 mRNA in the posterior forebrain and midbrain. Moderately intense hybridization is evident in the central gray (CG), superior colliculus (SC), subiculum (Sub), entorhinal cortex (Ent) and medial geniculate nucleus (MG), while low level labeling is seen in the interpeduncular nucleus (IP) (A). Strong hybridization is observed in the medial and lateral mammillary nuclei (MB) (B). Scale bars, (A) and (B), 2 mm.

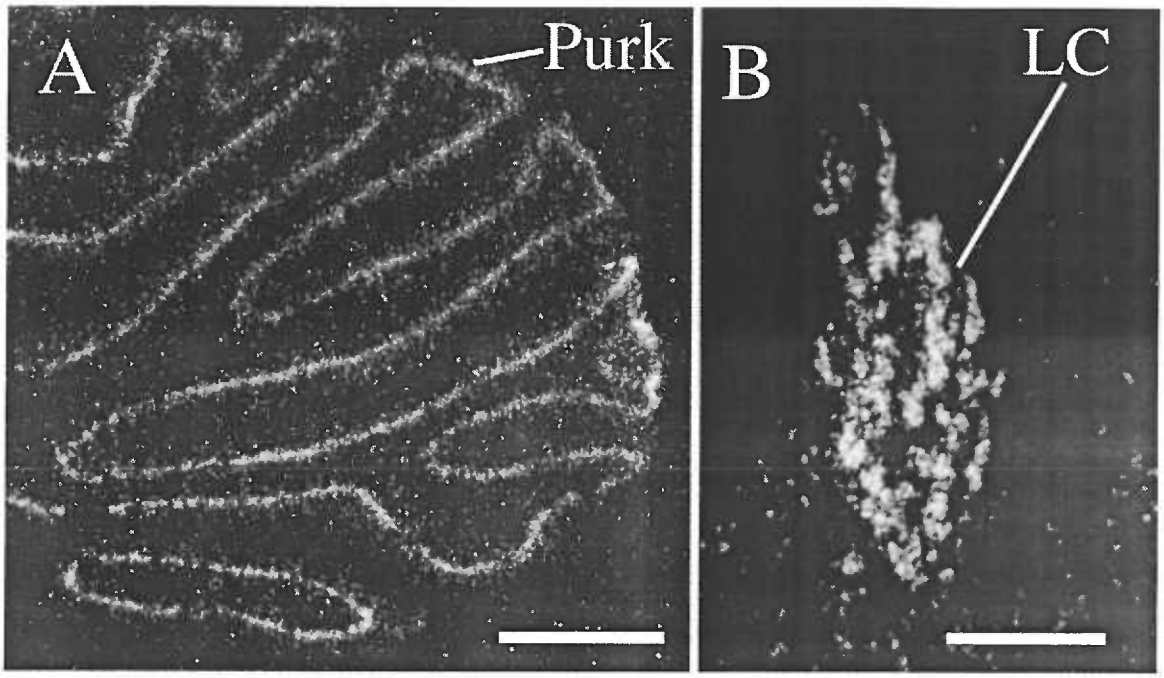

Figure 6. Localization of mGluR7 mRNA in the cerebellum and LC. (A) Low level hybridization is seen over the Purkinje cell layer of the cerebellar cortex (Purk) indicating the presence of mGluR7 mRNA in Purkinje cell bodies. (B) Neurons of the LC are intensely labeled. Scale bars, (A) 1mm, (B) 250 mm.

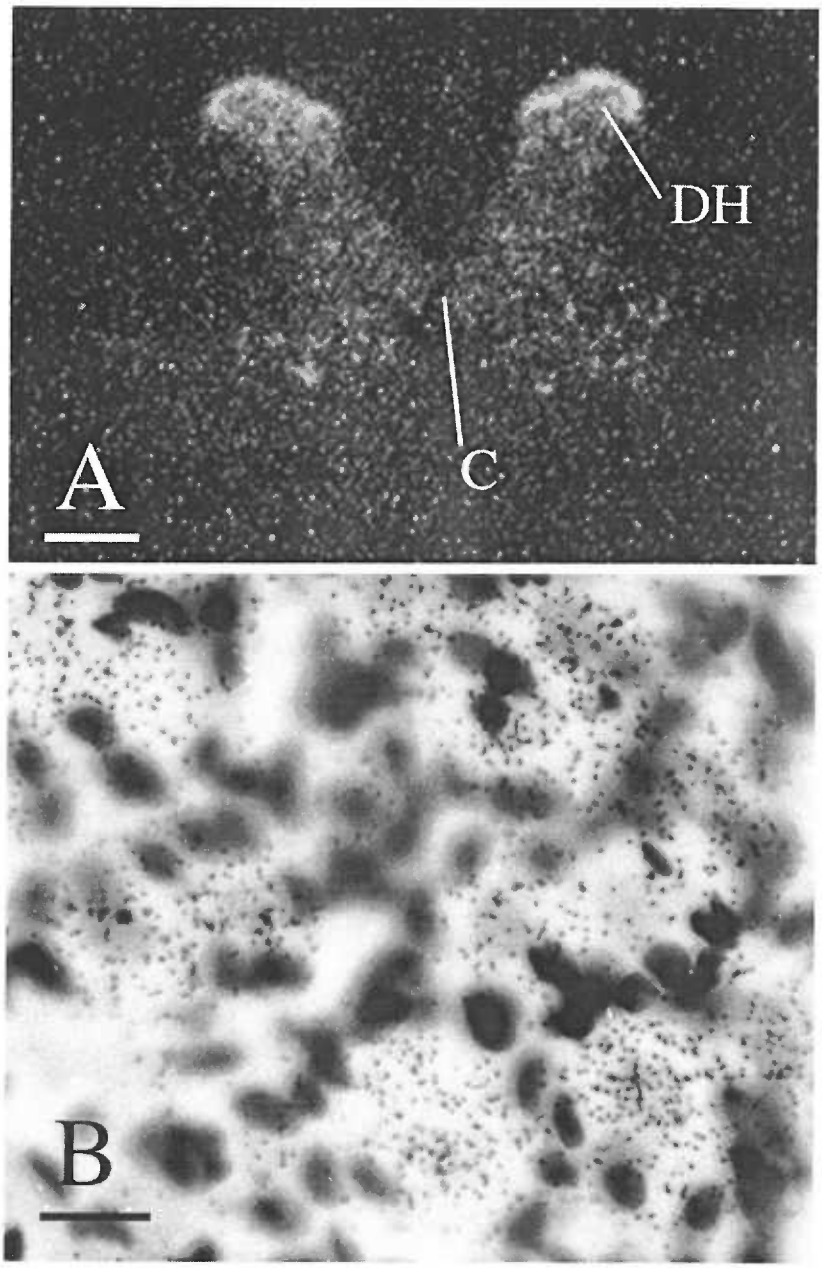

Figure 7. Localization of mGluR7 mRNA in the spinal cord and dorsal root ganglion. Autoradiograms of a representative section of upper thoracic spinal cord (A) demonstrate the presence of mGluR7 mRNA throughout the gray matter of spinal cord, with the highest intensity of labeling observed in Rexed layers I and II of the dorsal horn (DH). Brightfield micrograph of dorsal root ganglion (B) hybridized with mGluR7 cRNA probe shows silver grain accumulation over cytoplasm of cells whose nuclei stain weakly with thionin. C, central canal. Scale bars, (A) 1 mm, (B), 10 mm

IMMUNOLOCALIZATION OF METABOTROPIC GLUTAMATE RECEPTOR 7 IN THE RAT OLFACTORY BULB

J. Mark Kinzie[1,2], Michi M. Shinohara[1,2], Anthony N. van den Pol[4],

Gary L. Westbrook[1,3] and Thomas P. Segerson[1,2*]

Vollum Institute[1]

and

Departments of Medicine[2] and Neurology[3]

Oregon Health Sciences University

Portland, Oregon 97201

and

Section of Neurosurgery[4]

Yale University School of Medicine

New Haven, Connecticut 06510

Correspondence:

Thomas P. Segerson

Dept. of Medicine, Division of Endocrinology, L607

Oregon Health Sciences University

3181 SW Sam Jackson Park Road

Portland, Oregon USA 97201-3098

Phone (503) 494-5496

Fax (503) 494-4534

E-mail segerson@ohsu.edu

Abbreviations used in text:

AOB	Accessory olfactory bulb
AS-P	Astrocyte process
BHK	Baby hamster kidney - 21
CNS	Central nervous system
DAB	Diaminobenzidine
EPL	External plexiform layer
ER	Endoplasmic reticulum
GA	Golgi apparatus
GCL	Granule cell layer
GFAP	Glial fibrillary acidic protein
Ia	Layer Ia, piriform cortex
Ib	Layer Ib, piriform cortex
II	Layer II, piriform cortex
L-AP4	2-amino-4-phosphonobutyrate
LOT	Lateral olfactory tract
M	Mitochondrion
MAP	Microtubule-associate protein
MCL	Mitral cell layer
mGluR	metabotropic glutamate receptor
Mi	Mitral cell
mRNA	messenger ribonucleic acid
MOB	Main olfactory bulb
Nu	Nucleus
PBS	Phosphate-buffered saline
PMSF	phenyl methyl sulfonyl fluoride
PIR	Piriform cortex

ABSTRACT

Metabotropic glutamate receptors (mGluRs) constitute a large family of G protein-coupled receptors that are subdivided into three groups based on sequence similarity, pharmacological profiles and coupling to second messengers. Although mRNAs for seven of the eight mGluRs are expressed in the olfactory system, the localization and function of specific subtypes have not been fully characterized. Mitral cells of the olfactory bulb express mRNA for several mGluRs, including mGluR7, which has been suggested as a presynaptic glutamate autoreceptor. To investigate the immunolocalization of mGluR7 in the olfactory system, we used a polyclonal antiserum specific for the carboxy terminus of the receptor. Mitral cell somata and proximal dendrites were strongly labeled by the mGluR7 antibody. Electron microscopic analysis revealed that most of the mitral cell somatic staining was cytoplasmic. In olfactory bulb glomeruli, immunoreactivity was present in axons and dendrites. In the piriform cortex, diffuse staining was present in layer Ia that was markedly reduced following bulbectomy, consistent with expression of mGluR7 in mitral cell axon terminals. Electron microscopic analysis of this region confirmed the presence of mGluR7 in multiple axon terminals. Distinct labeled fibers in all levels of layer I appeared to originate from labeled piriform cortex pyramidal cells in layers II and III. Our results indicate that mGluR7 is primarily presynaptic at olfactory bulb synapses. However, the postsynaptic localization of mGluR7 at selected synapses indicates that mGluR7 is not targeted exclusively to axonal compartments.

Indexing terms: presynaptic; confocal; 2-amino-4-phosphonobutyrate; metabotropic glutamate receptor 7; mitral

INTRODUCTION

The olfactory system is designed to discriminate dilute concentrations of thousands of airborne odorant molecules. Afferent inputs from the olfactory epithelium reach the olfactory bulb and synapse on the apical dendrites of mitral and tufted cells within glomeruli. In the bulb, both centrifugal and intrinsic pathways are responsible for the spatial encoding and synaptic modulation of incoming sensory information. Many studies suggest that glutamate is the primary excitatory neurotransmitter at olfactory nerve terminals, at mitral cell output of dendrodendritic synapses, and at mitral cell axon terminals in olfactory cortex (Trombley and Shepherd, 1993). Recent evidence has emphasized that metabotropic glutamate receptors (mGluRs) may have a significant role in olfactory information processing at dendrodendritic reciprocal synapses in the bulb (Hayashi et al., 1993; Kaba and Nakanishi, 1995). Likewise, mGluR agonists can inhibit the output of the bulb by reducing transmitter release from mitral cell axons that project through the lateral olfactory tract (LOT) to olfactory cortical structures, including the piriform cortex. Immunolocalization of mGluRs is particularly important to an understanding of olfactory bulb function, given the predominance of dendrodendritic synaptic plasticity and juxtaposition of pre- and postsynaptic specializations.

Activation of mGluRs by glutamate modulates synaptic transmission through the inhibition or stimulation of ion channels and intracellular signal transduction (Abe et al., 1992; Westbrook, 1994; Pin and Duvoisin, 1995). Cloning of mGluR cDNAs has identified eight subtypes that fall into three groups based on amino acid homology, signal transduction mechanism, and pharmacological profile. Group I receptors (mGluR1, 5) are coupled to inositol phospholipid hydrolysis, whereas group II (mGluR2,3) and III (mGluR4,6,7,8) are negatively coupled to adenylate cyclase (Knopfel et al., 1995). In addition, alternative mRNA splicing of some mGluR subtypes gives rise to several distinct molecules that may vary in their distribution and signaling characteristics (Pin et al., 1992; Hampson et al., 1994; Minakami et al., 1994; Joly et al., 1995). Messenger RNAs coding

for seven of eight mGluR subtypes are expressed in the olfactory bulb (Abe et al., 1992; Shigemoto et al., 1992; Ohishi et al., 1993; Ohishi et al., 1993; Ohishi et al., 1995; Duvoisin et al., 1995; Kinzie et al., 1995). The only exception is mGluR6, which is restricted to retinal depolarizing bipolar cells, wherein it activates a postsynaptic phosphodiesterase (Nomura et al., 1994). However, the cellular pattern of expression of most mGluR proteins is only beginning to be explored. For example, whether particular subtypes are exclusively pre- or postsynaptic is unclear. In many brain regions, one splice variant of mGluR1, mGluR1α, has been localized to postsynaptic specializations of dendrites (Martin et al., 1992; Baude et al., 1993; Craig et al., 1993; Fotuhi et al., 1993). By contrast, mGluR1α immunoreactivity has been found at the presynaptic specialized membrane at dendrodendritic synapses in the external plexiform layer (EPL; van-den-Pol, 1995).

In this study, we focused on mGluR7, a group III mGluR that is expressed in mitral cells, tufted cells and groups of juxtaglomerular neurons in the (Kinzie et al., 1995; Ohishi et al., 1995). Group III receptors are selectively activated by 2-amino-4-phosphonobutyrate (L-AP4) which, in physiological experiments, causes inhibition of transmitter release from mitral cell axons (Anson and Collins, 1987; Trombley and Westbrook, 1992), suggesting that group III receptors including mGluR7 are presynaptically localized. We used a polyclonal rabbit antiserum against rat mGluR7 to determine the cellular and subcellular localization of mGluR7 in olfactory bulb neurons. Our data indicate that olfactory bulb mGluR7 is principally presynaptic, although dendritic mGluR7 immunoreactivity suggests that postsynaptic actions of mGluR7 should be reassessed.

Experimental procedures

Antisera

An antiserum to the carboxy-terminus of the rat mGluR7 (peptide sequence: KNSPAAKKKYVSNNLVI) was generously provided by Stefania Risso Bradley and P. Jeffrey Conn of Emory University (Bradley et al., 1996). An affinity purified antibody to rat mGluR1α was provided by Eileen Mulvihill and Betty Haldeman of Zymogenetics (Baude et al., 1993; Hampson et al., 1994). Monoclonal antibodies against glial fibrillary acidic protein (GFAP), microtubule-associated protein (MAP) 2A/B/C, MAP5 and a polyclonal goat antibody against calretinin were obtained from Chemicon International, Inc. (Temecula, CA).

Unilateral Bulbectomy

Two adult female Sprague-Dawley rats were deeply anesthetized with ketamine (40 mg/kg) and acepromazine (1 mg/kg) and positioned in a stereotaxic apparatus. The olfactory bulb on one side was exposed and removed by aspiration. Ablation was considered complete by exposure of the cribriform plate. The site of the lesion was filled with 1% agar and the wound was closed. After 7 days, rats were anesthetized, killed by decapitation and their brains processed for immunohistochemistry.

Immunoblot analysis of mGluR7

Baby hamster kidney-21 (BHK) cells stably expressing cDNAs encoding mGluRs 1α, 4 or 7 were used to determine antiserum specificity (Houamed et al., 1991; Thomsen et al., 1992; Saugstad et al., 1994). Wild type and mGluR-expressing BHK cells were grown to 75% confluency, rinsed with phosphate buffered saline (PBS: 137 mM NaCl, 2.7 mM KCl, 4.3 mM $Na_2HPO_4 \cdot 7H_20$, 1.4 mM KH_2PO_4, pH ≈ 7.3), and harvested with membrane harvesting buffer (10 mM sodium bicarbonate, pH 7.2, containing 1 mM

phenyl methyl sulfonyl fluoride (PMSF) and 1 μg/ml each leupeptin, pepstatin A, aprotinin; Sigma, St. Louis, MO). Membranes were centrifuged at X16,000*g* for 5 minutes, resuspended in the membrane-harvesting buffer, and stored at -80°C until use. Oocyte membranes were harvested by trituration in disruption buffer (7.5 mM sodium phosphate, dibasic, pH 7.4, 10 mM EDTA, 1 mM PMSF, and 1 μg/ml each leupeptin, pepstatin A, aprotinin) followed by centrifugation at X300*g* for 5 minutes. The supernatant was centrifuged at X16,000*g* for 30 minutes, and the membrane pellets were resuspended in disruption buffer containing 1% sodium dodecyl sulfate (SDS), denatured at 37°C for 30 minutes, and stored at -20°C until use.

For immunoblot of rat brain regions, brains were rapidly removed from 4 anesthetized rats and the olfactory bulb, hippocampus and cerebellum dissected and homogenized in 20 ml of 0.32 M sucrose, 10 mM Tris, 1 mM $MgCl_2$ (pH 7.0) containing protease inhibitors (1 μg/ml aprotinin, 1 μg/ml pepstatin and 1 mM PMSF). After centrifugation (X1000*g*, 10 minutes at 4°C) the supernatant was centrifuged at X30,000*g* for 20 minutes and the pellet resuspended in 2 mM HEPES, 2 mM EDTA (pH 7.5) with protease inhibitors. The crude synaptosomes were homogenized for 10 seconds and incubated on ice for 30 minutes. Lysed membranes were isolated by centrifugation (X20,000*g*, 20 minutes at 4°C), and quantified. Ten micrograms of protein were heated to 50°C for 10 minutes prior to gel fractionation.

Membrane protein aliquots were subjected to SDS-polyacrylamide electrophoresis (SDS-PAGE; 10% acrylamide) and transferred to nitrocellulose membranes (BioRad, Hercules, CA) by electrophoresis. The blots were blocked with 5% nonfat dry milk in Tris-buffered saline, pH 8.0, with 0.1% Tween-20 (TBST) at 4°C overnight. Blots were then incubated 4 hours at room temperature with anti-mGluR7 antiserum (1:8,000) containing sodium azide (0.025%) in TBST.

Membranes were rinsed and incubated for 45 minutes in TBST with horseradish peroxidase-conjugated goat anti-rabbit IgG (1:10,000; Amersham, Arlington Heights, IL)

at room temperature. Following several washes in TBST, immunoreactive proteins were visualized with enhanced chemiluminescence (Amersham), as recommended by the manufacturer.

Immunohistochemistry

Adult female Sprague-Dawley rats (n=18) were deeply anesthetized with pentobarbital and perfused transcardially with ice-cold saline, followed by ice-cold 4% paraformaldehyde in 0.1 M sodium borate (pH 9.5). The brains were removed quickly, blocked and post-fixed for 4 hours at 4°C in 4% paraformaldehyde in 100 mM borate buffer (pH 9.5). The brains were rinsed 6 times in PBS, followed by sectioning (75 μm) on a Vibratome 1000 Sectioning System (Lancer, St. Louis, MO).

For diaminobenzidine (DAB) immunohistochemistry, sections were rinsed in 14 mM NaCl, 2 mM K_2HPO_4 (KPBS) and blocked in 2% normal donkey serum, 0.02% nonfat dry milk in KPBS (1 hour at room temperature). The sections were then incubated in anti-mGluR7 serum (1:10,000) in 2% normal donkey serum, 0.02% nonfat dry milk in KPBS (3 days at 4°C). After rinsing in KPBS, sections were treated for endogenous peroxidase activity (1% H_20_2 in KPBS, 30 minutes at room temperature). Sections were then incubated in biotin-SP donkey anti-rabbit IgG at 1:200 (Jackson ImmunoResearch, West Grove, PA) for 4 hours, followed by incubation in avidin-biotin-peroxidase complex (Vector Laboratories, Burlingame, CA) for 2 hours. Sections were developed with a Ni- and Co- enhanced DAB/peroxide reaction (Pierce Chemical Co., Rockford, IL), mounted on gelatin-coated slides, dehydrated in graded alcohols, cleared in xylene, and then coverslipped with DPX.

For a control for specificity, some sections were incubated without primary antisera. In addition, some sections were incubated in antiserum that had been preincubated in peptide (10 μg/ml) corresponding to the C-terminal sequence of mGluR7 (KNSPAAKKKYVSNNLVI) from which the antiserum had been generated.

For fluorescent immunohistochemistry, two methods were used with equal efficacy. Some sections were cut on a freezing microtome (50 μm), rinsed, then permeabilized in 0.3% Triton X-100/KPBS, and blocked as above with the addition of 0.3% Triton X-100. The sections were then incubated in anti-mGluR7 (1:1,000) or anti-mGluR1α (1:500) sera overnight at 4°C. After rinsing sections in 0.3% Triton X-100/KPBS, sections were incubated in biotin-SP donkey anti-rabbit IgG at 1:200 (Jackson ImmunoResearch) for 4 hours, followed by Cy3/streptavidin at 1:200 (Jackson ImmunoResearch). Sections were mounted and coverslipped as above. Other sections were cut on a Vibratome (75 μm), rinsed in KPBS and blocked without permeabilization (three animals). The sections were then incubated in anti-mGluR7 (1:10,000) or anti-mGluR1α (1:500) sera for 3 days at 4°C. After rinsing sections in KPBS, sections were then incubated in Cy3 donkey anti-rabbit secondary (1:200; Jackson ImmunoResearch), rinsed and mounted. Slides were then imaged on a BioRad MRC1024 confocal imaging system a Nikon Diaphot 200 microscope. The scanned images were adjusted for brightness, contrast, and size in Photoshop 2.0.1 (Adobe Systems, Inc., Mountain View, CA) and labeled in Freehand 3.1 (Macromedia, San Francisco, CA) on a Macintosh 8100/80. Anatomical sites were identified using the *Brain Maps* atlas (Swanson, 1992).

Double-labeled fluorescent immunohistochemistry was performed as described above, using a mouse monoclonal primary antibody (anti-MAP2, anti-MAP5, anti-GFAP) coincubated with the anti-mGluR7 primary. Labeling by monoclonal antibodies was detected using a Cy5-labeled anti-mouse secondary (1:200) coincubated with the Cy3-labeled anti-rabbit secondary (1:200). Controls included the omission of one primary antiserum and incubation with two different fluorescent secondary antibodies. The slides were visualized with red (excitation λ: 568 nm/10 nm dichroic filter, emission λ: 605 nm/32 nm dichroic filter) and far red (excitation λ: 647 nm/10 nm dichroic filter, emission λ: 680 nm/32 nm dichroic filter) filter sets to insure that there was no cross-over detection of the respective emission spectra of the fluorescent labels.

Immuno-electron microscopy

Adult Sprague Dawley rats were heavily anesthetized with Nembutal (80 mg/kg) and perfused transcardially with physiological saline, followed by a fixative that contained 4% paraformaldehyde and 0.05% glutaraldehyde in a 0.1 M phosphate buffer. Fifty-micrometer-thick Vibratome sections were immersed in a graded series of sucrose concentratons up to 30% sucrose. Thick sections then were frozen twice in liquid nitrogen to lyse membranes and to increase penetration of immunoreagents. Sections of the olfactory bulb and forebrain caudal to the olfactory peduncle were incubated for 30 minutes in normal goat serum containing 0.1% lysine, 0.1% glycine, and 1% bovine serum albumin and were then placed in the anti-mGluR7 antiserum. After incubation in biotinylated goat anti-rabbit immunoglobulin and then in avidin-biotin-peroxidase complex (Vector Laboratories), sections were treated with DAB and hydrogen peroxide, osmicated for 30 minutes in 1% osmium tetroxide, and dehydrated through an ascending series of ethanol concentrations to 100%. To increase membrane contrast, the 70% ethanol contained 1% uranyl acetate. Some sections were also stained with 1% lead acetate, except where indicated. For controls, some sections were incubated without primary antibody, secondary antibody, or both. Ultrathin Epon sections were cut on a Reichert ultramicrotome (Reichert-Jung, Nussloch, Germany) and picked up on formvar-coated, carbon-stabilized single-slot grids. Sections were examined in a JEOL 1200 EXII transmission electron microscope (JEOL USA, Inc., Peabody, MA) at 60,000 accelerating volts. All animal procedures were approved by the Oregon Health Sciences University Animal Care Committee and were in conformance with NIH guidelines on the Care and Use of Animals in Research.

Results

Antibody specificity

To determine the specificity of the carboxy-terminal antipeptide antiserum for mGluR7, we performed immunoblots with this antibody of cell membranes obtained from dissected rat brain regions and from mGluR1α-, mGluR4- and mGluR7-expressing, and wild type BHK cells. Immunoblot of olfactory bulb and hippocampal membrane protein resolved a single band of approximately 130 kDa, whereas mGluR7-expressing BHK cell immunoblots demonstrated a doublet of similar mobility (Fig. 1A). This doublet is most likely due to alternate glycosylation of the mGluR7 protein (Bradley et al., 1996). In addition, the antisera recognized a single band in membranes prepared from *Xenopus* oocytes expressing mGluR7, but not mGluR8, demonstrating further that the antiserum was specific for mGluR7. Expression of mGluR7 and mGluR8 in oocytes was confirmed by coexpression with G-protein coupled inward rectifying potassium channel (Saugstad et al., 1997).

Preincubation of sections in peptide corresponding to the carboxy-terminal sequence of mGluR7 from which the antisera had been generated reduced DAB staining product to background levels (compare Fig. 1B and 1C). An antiserum purified by affinity for the immunizing peptide that recognizes a single protein species in immunoblots of olfactory bulb protein (Bradley et al., 1996) gave the same results as the antiserum used in these studies. Therefore, as the affinity purified antiserum was not available in sufficient quantity, crude antiserum for mGluR7 was used for the remainder of the experiments. No staining was observed when the antisera was omitted from the primary incubation . Each experimental result was confirmed by examination in multiple (two to six) animals.

mGluR7 immunoreactivity in the olfactory bulb

Sections of adult rat olfactory bulb and olfactory cortex were initially stained using the avidin-biotin complex method, followed by development with a Ni- and Co- enhanced DAB/peroxide reaction. At low-magnification light microscopy, somata of mitral cells and internal and intermediate tufted cells of the main olfactory bulb (MOB) were the most visibly stained, but granule cells were lightly and inconsistently stained (Fig. 1B). The EPL was not strongly stained, especially when compared to the staining pattern of mGluR1α (van-den-Pol, 1995). The most prominent staining was in dendritic processes of mitral cells that traversed the EPL in perpendicular orientation to the mitral cell layer. No staining was apparent in the olfactory nerve layer or in the LOT.

To trace labeled fibers coursing through the tissue planes, the remaining studies were analyzed with fluorescence using a BioRad MRC 1000 confocal microscope, which provides better contrast and resolution. The method has the added benefit of reducing artifact from diffusion of the reaction product. At lower magnification, the staining patterns were identical, with the most predominant staining seen in the cell bodies of mitral and internal tufted cells (Fig. 2A). The labeled dendrites of the mitral cells could be traced nearly to the glomerular layer. In addition, secondary dendrites projecting parallel to the mitral cell layer were labeled. Dendrites of internal and intermediate tufted cells, often more than one per cell, were also labeled. There was light, diffuse, punctate staining of the glomeruli, but small, stained, juxtaglomerular cell bodies, consistent with periglomerular cells, as well as larger, juxtaglomerular, stained cell bodies, suggestive of superficial tufted cells, could be discerned (Fig. 2B).

At higher magnification, mGluR7 immunoreactivity was present in the MOB mitral cell layer with a cytoplasmic staining pattern (Fig. 2C). The nucleus was not labeled. The staining intensity was greater in proximal dendrites, and was reduced more distally. Double-labeling experiments with MAP5, a cytoskeletal protein expressed in mitral cell bodies, axons, and dendrites, demonstrated colocalization with mGluR7 in mitral cell bodies and dendrites, but no mGluR7 immunoreactivity was seen in MAP5-labeled axons

. Within the inner plexiform layer, occasional punctate staining of fibers just deep and parallel to the mitral cell layer was observed (Fig. 2D). These fibers could be traced to nongranule cells in the granule cell layer and may represent short axon cells.

Staining of mitral and granule cell bodies was observed in the accessory olfactory bulb (AOB; Fig. 3), whereas the bright staining with immunofluorescence (Fig. 3B) was not seen if the tissue was preincubated with the immunizing peptide. Because the cell bodies of the mitral cells in this region are densely packed, process staining could not be evaluated. The granule cell layer of the AOB was also immunostained, but the lateral olfactory tract in this region was unlabeled. Glomeruli in this region were not distinctly discernible.

Immunoelectron microscopy of the olfactory bulb

The light microscopic finding of mGluR7 in mitral cell dendrites suggested that mGluR7 might be postsynaptic. This was not expected, because the group III mGluR agonist L-AP4 has no described postsynaptic effects except in retina. To investigate the ultrastructural localization of mGluR7, immuno-electron microscopic analysis of the olfactory bulb was performed using the anti-mGluR7 antiserum. Examination of mitral cells showed mGluR7 in the rough endoplasmic reticulum and the Golgi apparatus (Fig. 4). No staining was observed in nuclei, mitochondria or lysosomes. Small amounts of staining were found on the cell membrane, with no appreciable increase at synaptic junctions or at reciprocal dendrodendritic synapses in the EPL. In the granule cell layer, some cytoplasmic staining of narrow processes was seen, suggestive of astrocyte processes. Granule cells did not stain.

Within glomeruli, mGluR7 immunoreactivity was visible in several synaptic compartments. Immunoreactivity was present in presynaptic specializations that synapsed on other unlabeled presynaptic specializations (Fig. 5a). At axodendritic synapses, mGluR7 immunoreactivity could be found both pre- and post-synaptically (Fig. 5b and 5c,

respectively). The neuropil of the glomerular layer is composed of processes from a number of cell types (Shepherd, 1990). Immunoreactive profiles, therefore, could include dendrites of mitral, tufted, or periglomerular cells and axons of periglomerular cells or centrifugal fibers.

mGluR7 in the piriform cortex and anterior olfactory nucleus

Within the olfactory peduncle, there was minimal labeling of the LOT, although a minority of the fibers within the tract appeared moderately labeled (Fig. 6A). In the anterior olfactory nucleus (lateral part), there was diffuse staining of the molecular layer and many stained perikarya within the pyramidal layer (Fig. 6A). In the rostral piriform cortex, there was diffuse staining in the layer Ia but much less in layer Ib (Fig. 6A). Perikarya in layer II pyramidal neurons were immunoreactive. We observed a similar pattern in the piriform cortex caudal to the peduncle, with strong immunoreactivity in layer Ia, the region of synaptic contacts between mitral cell axons and dendrites of the piriform cortex pyramidal neurons (Fig. 6B). However, layer Ib, which contains synapses between recurrent collateral axons and dendrites of the piriform cortex pyramidal neurons, was not stained. Layer II contained many immunoreactive cell bodies, as did layer III. In addition, layer III contained many distinct fibers coursing through it in a parallel orientation to layer I. Longitudinal sections of the LOT failed to demonstrate strong fiber staining.

In layer Ia, in addition to diffuse staining, distinct arborizing fibers could be seen (Fig. 6C). These fibers appeared to originate in layer II neurons, process through to layer Ia, and branch out. Labeled fibers that appeared to originate in deeper layers and penetrate into superficial layers colabeled with MAP2 and mGluR1α suggesting that these fibers were dendrites. In contrast to mGluR7, antisera to mGluR1α did not demonstrate bright diffuse labeling of layer Ia.

Immunoreactivity following ablation of olfactory bulb

To investigate whether the diffuse staining in layer Ia represented mGluR7 localized to mitral cell axon terminals, we examined the contralateral and ipsilateral piriform cortex 1 week after unilateral bulbectomy (Fig. 7). Staining for GFAP demonstrated the expected reactive changes only in the ipsilateral piriform cortex, but the diffuse layer Ia staining for mGluR7 was not present. However, mGluR7 staining in layer Ia on the contralateral side was similar to that seen in nonbulbectomized rats. In contrast to mGluR7 immunoreactivity, the labeling of fibers and cell bodies in layers II and in some fibers of layer I of the piriform cortex by antisera to mGluR1α was unaltered by bulbectomy, as was the staining for MAP2, a cytoskeletal protein localized to dendrites. Staining for calretinin, a calcium-binding protein present in mitral cells (Wouterlood et al., 1985), was strong in the LOT and nearly as strong in layer Ia of the piriform cortex. After bulbectomy, there was a significant reduction in the ipsilateral staining of both regions, demonstrating that mitral cell axons and their terminals were reduced following bulbectomy.

Immunoelectron microscopy of piriform cortex

We also examined by ultrastructural analysis of peroxidase-stained tissue whether mGluR7-containing axon terminals were present in the layer of piriform cortex in which mGluR7 immunostaining was altered by bulbectomy. Some sections were counterstained with uranyl and lead to enhance contrast in nonimmunoreactive cells (Fig. 8A and 8B). Large numbers of immunoreactive axon terminals were found in the rostral piriform cortex (Fig. 8, A-D). This staining was particularly evident in tissue sections that were not further stained with heavy metals (Fig. 8C and 8D). The immunoreactive axons made asymmetrical Gray type I synaptic contacts, typical of excitatory axons. Presynaptic axons had small clear vesicles (Fig. 8A and 8D), and sometimes dense core vesicles were also evident (Fig. 8D). In many cases, multiple labeled axon terminals made contact with one dendrite (Fig 8C). In immunoreactive axons, the cytoplasmic side of the presynaptic membrane was consistently stained. The apparent labeling of synaptic vesicles is probably

due to diffusion and precipitation of the peroxidase reaction product near the antigen site. Consistent with this view, vesicles in immunoreactive axons that were further from the presynaptic membrane were often not labeled.

Discussion

Electrophysiological evidence has suggested that group III mGluRs generally have presynaptic actions. Because mGluR7 mRNA is expressed in mitral cells and L-AP4 inhibits release from mitral cell axons (Anson and Collins, 1987; Collins and Howlett, 1988; Hasselmo and Bower, 1991; Trombley and Westbrook, 1992), we expected that mGluR7 might be targeted to axon terminals of mitral cells. Our results are consistent with an axonal distribution of mGluR7 in mitral cell processes. However, the coincident dendritic localization of mGluR7 at postsynaptic sites in the glomerular layer suggests that mGluR7 may also have postsynaptic actions.

Distribution of mGluR7 mRNA and protein

The cellular distribution of mGluR7 immunoreactivity closely matched that expected from mRNA distribution patterns; however, the unexpected dendritic staining made us closely examine the specificity of the antiserum. Although most of our experiments were performed with a crude antiserum due to limited availability of affinity-purified antiserum, preadsorption of the antibody with the immunizing peptide in the absence of carrier protein abolished staining in olfactory bulb sections. The amino acid sequence of mGluR7 is most similar to other group III mGluRs (mGluR4 and mGluR8); thus, one might expect nonspecific cross-reactivity to be most apparent with these proteins. However, the C-terminal sequence used for the immunizing peptide is only 39% and 44% identical to the corresponding regions of mGluR4 and mGluR8, the other group III receptors expressed in the olfactory bulb. Consistent with these sequence differences, the antiserum recognized a single band in extracts from dissected rat brain regions and did not recognize mGluR4 expressed in BHK cells (see Results), or mGluR8 in Western blots from oocytes expressing functional mGluR8 receptors (unpublished observations). Because identified splice variants of mGluRs, including those of mGluR7 (van den Pol, unpublished), are divergent in their carboxy terminal sequences, an antibody raised to this part of the

mGluR7 molecule is unlikely to recognize other potential mGluR7 splice variants. Furthermore, antibody affinity-purified from this antiserum and well-characterized in hippocampal neurons (Bradley et al., 1996), gave an identical pattern of staining in our experiments. Thus we conclude that under the conditions of our experiments, the antiserum specifically recognized mGluR7.

The pattern of mGluR7 immunoreactivity in the olfactory bulb and piriform cortex closely parallels the distribution of mGluR7 mRNA as demonstrated by *in situ* hybridization (Kinzie et al., 1995; Ohishi et al., 1995). Strong immunoreactivity matched the high level of mRNA labeling in mitral cells, whereas mGluR7 immunoreactivity was difficult to detect in juxtaglomerular and granule cells that have low levels of mGluR7 mRNA. It is possible, however, that some of the EM synaptic labeling in glomeruli represent processes of periglomerular cells, other juxtaglomerular interneurons, or centrifugal input (Luskin and Price, 1983). One unexpected finding in our experiments was the more intense labeling of the granule cell layer in the AOB relative to the MOB. This difference was much less apparent by *in situ* hybridization (Kinzie et al., 1995; Ohishi et al., 1995).

We used bulbectomy to determine whether immunostaining of the piriform cortex represented mitral cell axon terminals that contained mGluR7. The marked reduction of staining in layer Ia of the piriform cortex after bulbectomy supports this idea. One caveat is that pyramidal cells in the piriform cortex can undergo transsynaptic degeneration as soon as 24 hours after bulbectomy (Heimer and Kalil, 1978; Friedman and Price, 1986; Westrum and Bakay, 1986). However, MAP2 and mGluR1α, which are expressed in piriform cortex pyramidal dendrites, were not affected at the time point examined. In addition to layer Ia, distinct labeled fibers in all levels of layer I could be visualized. These fibers appeared to originate from layers II and III of the piriform cortex and may be recurrent axons. Indeed, some electrophysiological evidence suggests that recurrent axons in layer Ib originating from neurons in layers II and III contain L-AP4 sensitive receptors

(Collins and Howlett, 1988). However, anatomical evidence suggests that these recurrent axons do not enter layer Ia (Price, 1973; Schwob and Price, 1984).

To confirm that our bulbectomy results reflect the presence of mGluR7 in mitral cell axon terminals, we examined mGluR7 immunoreactivity by EM in layer Ia of the piriform cortex. This analysis showed abundant staining of large axon terminals with small, clear vesicles, suggestive of olfactory bulb terminals. From these results, and those from our bulbectomy experiments, we conclude that mGluR7 is present at axon terminals of the LOT, where it functions as a presynaptic autoreceptor. However, we cannot discount the suggestion from our studies that mGluR7 may be in part dendritically targeted in piriform cortex pyramidal neurons.

Are mGluRs targeted to axons vs. somatodendritic compartments?

Early electrophysiological and immunohistochemical studies of mGluRs suggested that individual mGluR subtypes are localized either to somatodendritic or to axonal compartments. For example, mGluR1α immunoreactivity is found in postsynaptic membranes and is targeted to somatodendritic compartments in cultured hippocampal neurons (Martin et al., 1992; Craig et al., 1993; Shigemoto et al., 1992). Likewise, physiological activation of group I receptors increases excitability of dendrites. In contrast, the most obvious action of group II and III receptors is to inhibit transmitter release by a presynaptic mechanism (Schoepp and Conn, 1993; Saugstad et al., 1994). Thus, it was reasonable to suppose that group I receptors were targeted to dendrites whereas group II/III receptors were targeted to axons. However, there is increasing evidence that this dichotomy is incorrect. For example, presynaptic immunoreactivity has been seen for both the group I receptors mGluR1α and mGluR5 (Fotuhi et al., 1993; Romano et al., 1995). In mitral cells of the olfactory bulb, mGluR1α is found in dendrites, but this immunoreactivity is actually localized presynaptic to the mitral-granule cell dendrodendritic synapses (van den Pol, 1995).

Of the group III receptors, mGluR6 is the only subtype that appears to be exclusively postsynaptic (Nomura et al., 1994). However, this receptor is unusual in that it may be expressed in only a single cell type (retinal ON-bipolar cells) and has a specialized transduction pathway (Slaughter and Miller, 1985; Nawy and Jahr, 1990). The immunolocalization of the extra-retinal group III receptors (mGluR4,7,8) is just beginning to emerge. For mGluR4, prominent postsynaptic as well as presynaptic labeling has been demonstrated in hippocampal neurons (Bradley et al., 1996). However, current evidence suggests that mGluR7 and 8 (Kinoshita et al., 1996) are primarily axonal. For example, mGluR7 is localized predominantly to presynaptic axon terminals of asymmetrical synapses in the hippocampus (Bradley et al., 1996). Similarly, mGluR7 is localized to axon terminals in laminae I and II in the dorsal horn (Ohishi et al., 1995). The mGluR7 staining in mitral cell axon terminals in our experiments further supports a presynaptic localization. However, our results provide evidence that mGluR7 in the olfactory system is not exclusively axonal. Thus, it would appear that most, if not all, non-retinal group III mGluRs may be expressed in somatodendritic as well as axonal compartments.

Function of mGluRs in the olfactory system

The olfactory system may prove to be a unique system to examine the roles of individual mGluRs in synaptic transmission. The synaptic connections of the bulb are specialized to provide lateral inhibition that presumably mediates an essential component of olfactory discrimination. Therefore, the pathways that affect lateral inhibition at the dendrodendritic synapses could powerfully modulate incoming sensory information. This has been beautifully demonstrated by recent studies in the AOB. In these studies, activation of mGluR2 in granule cell dendrites at reciprocal synapses with mitral cell dendrites results in inhibition of γ-aminobutyric acid (GABA) release. Thus, mGluR2 activation at these synapses relieves the excited mitral cell from GABA-mediated feedback inhibition yet retaining the feed-forward inhibition of surrounding mitral cells (Hayashi et

al., 1993). This mechanism appears to be important for formation of olfactory memory during mating in mice (Kaba and Nakanishi, 1995). The function of the other six mGluRs in the olfactory system is less clear.

The somatodendritic staining of mGluR7 suggests that this receptor may be postsynaptically localized, although, in the case of mitral cells, this may represent targeting to presynaptic release sites of dendrodendritic synapses (van den Pol, 1995). Nonetheless, our EM results suggest that, in some neurons, dendritic mGluR7 is postsynaptically localized. It is not clear why a postsynaptic mGluR7-mediated response has not been detected previously. This discrepancy may result from postsynaptic targeting of mGluR7 in only a few neurons. Alternatively, a postsynaptic mGluR7 response might have been overlooked because of the low apparent agonist affinity of the receptor (Okamoto et al., 1994; Saugstad et al., 1994) or because the transducing signal for mGluR7 action at postsynaptic sites, such as a decrease in cyclic adenosine monophosphate (cAMP), is not easily detected by physiological techniques.

Another question raised by our results is why receptors that are as similar as mGluR7 and mGluR8 are coexpressed on mitral cell axons. Again, the approximate 500 fold less apparent affinity of mGluR7 for agonist compared to mGluR8 (Saugstad et al., 1997) may provide an explanation. This difference suggests that mGluR7 might only be activated near released quanta of glutamate. By contrast, mGluR8 could be activated at lower glutamate concentrations, for example, by spillover from adjacent synapses. Thus, mGluR7 and mGluR8 could operate in tandem to mediate homosynaptic and heterosynaptic inhibition, respectively.

Acknowledgments: We thank Stefania Risso-Bradley and P. Jeffrey Conn for providing the mGluR7 antibody, Betty Haldeman and Eileen Mulvihill for providing the mGluR1α antibody, Eva Shannon for assistance with confocal microscopy and Stephen Gancher for

assistance with olfactory bulbectomy. This work was supported by NIH: MH10314 (JMK), NIH: DC01783 (TPS), and NIH: NS10174 (ANvdP).

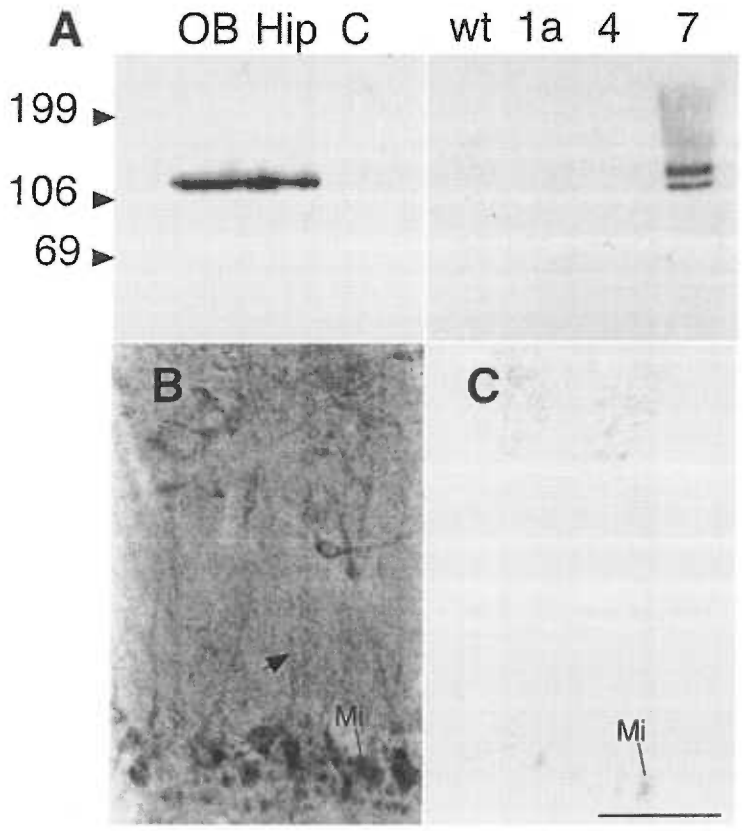

Fig.1. Specificity of metabotropic glutamate receptor 7 (mGluR7) antiserum. A: Immunoblot analysis was used with polyclonal antiserum directed against mGluR7 to determine reactivity in protein from membranes of dissected rat olfactory bulb (OB), hippocampus (Hip) and cerebellum (C) as well as from membranes obtained from wild-type BHK cells (wt) and BHK cells expressing mGluR1a (1a), mGluR4 (4) and mGluR7 (7). Molecular mobility standards are shown to the left in kDa. An immunoreactive doublet of about 130 kDa was observed in protein extracts from olfactory bulb and hippocampus, with no detection of mGluR7 in cerebellum. In cells lines, mGluR7 immunoblot detected a doublet of similar mobility only in extracts of cells expressing the mGluR7 cDNA. B: Diaminobenzidine (DAB) staining of main olfactory bulb for mGluR7. Mitral cell somata (Mi) and dendrites (arrow) are labeled in sections incubated with the antiserum used in these studies. C: Sections stained with the antiserum preincubated with 10 mg/ml immunizing peptide had much reduced staining, with a mitral cell body (Mi) barely visible. Bar: 50 mm.

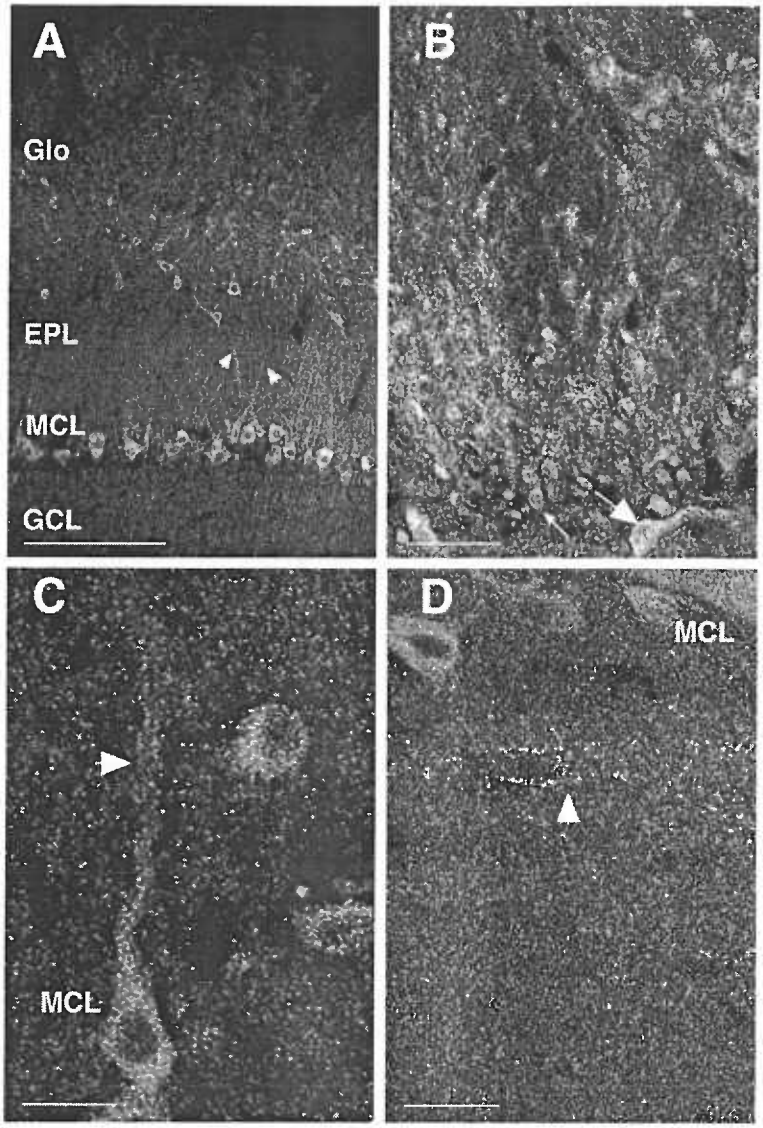

Fig.2. Confocal immunofluorescence analysis of mGluR7 in the rat olfactory bulb. A: Staining with the anti-mGluR7 antiserum reveals labeling of cell bodies and their proximal dendrites (arrows) in the mitral cell layer (MCL) and in the external plexiform layer (EPL). Smaller cells were labeled around the glomeruli (Glom). Cell bodies in the granule cell layer (GCL) were only slightly stained. Bar: 150 mm. B: Immunofluorescent labeling of a glomerulus, showing diffuse, punctate staining of neuropil. Groups of small juxtaglomerular cells (small arrow) and less numerous larger juxtaglomerular cells (large arrow) are also labeled. Bar, 150 μm. C: Higher magnification of the MCL of the main olfactory bulb reveals nuclear exclusion of staining and gradual decrease of labeling intensity in dendrites (arrow). Bar: 300 mm. D: Coursing parallel to the MCL, distinct labeled fibers could be visualized (arrow). Bar: 300 mm.

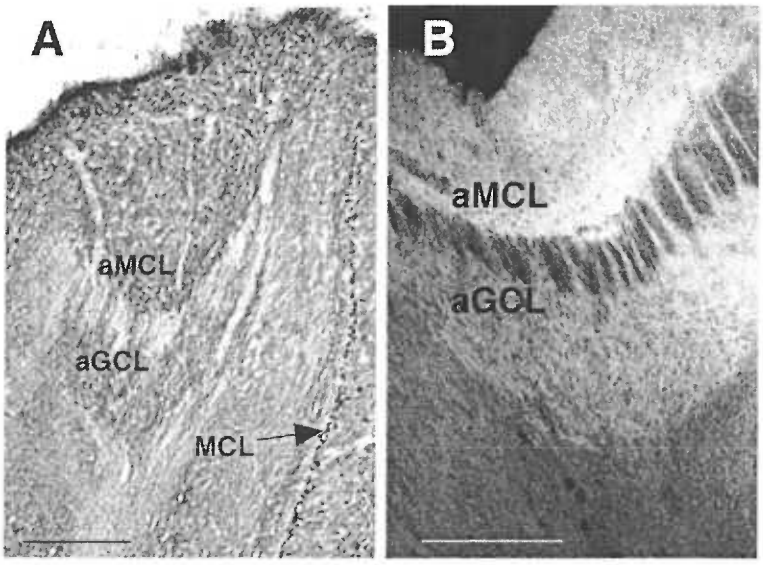

Figure 3. A. DAB-reacted immunostaining of accessory olfactory bulb for mGluR7, showing staining in the mitral cell layer (aMCL) and granule cell layer (aGCL), as well as more distinct staining in the adjacent mitral cell layer (MCL) of the main olfactory bulb. B. Immunofluorescence of the accessory olfactory bulb revealed bright staining of both the mitral (aMCL) and granule (aGCL) cell layers. Bars: 150 mm.

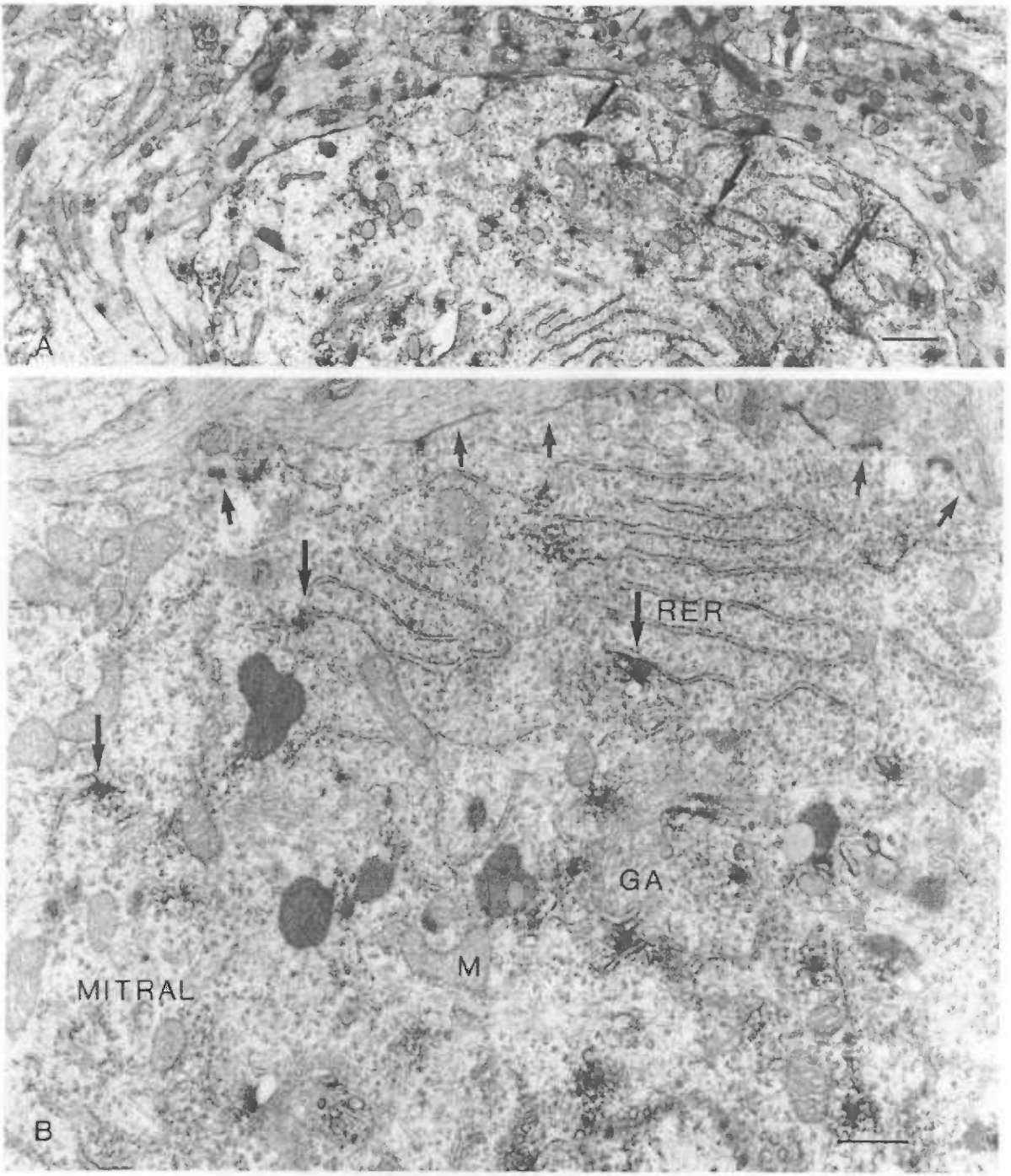

Fig.4. Mitral cells- perikarya. A: Low-magnification micrograph showing peroxidase labeling (arrows) in the cytoplasm of a mitral cell body. Labeling is associated with rough endoplasmic reticulum (RER). Little label is found on the plasma membrane. Bar: 1 mm. B: Higher magnification of another mitral cell, showing peroxidase (long arrows) on the rough endoplasmic reticulum (RER) and associated with the Golgi apparatus (GA). Mitochondria (M) and lysosomes show no label. Along the plasma membrane (small arrows), even at regions of synaptic contact, little labeling is found. Bar: 0.5 mm.

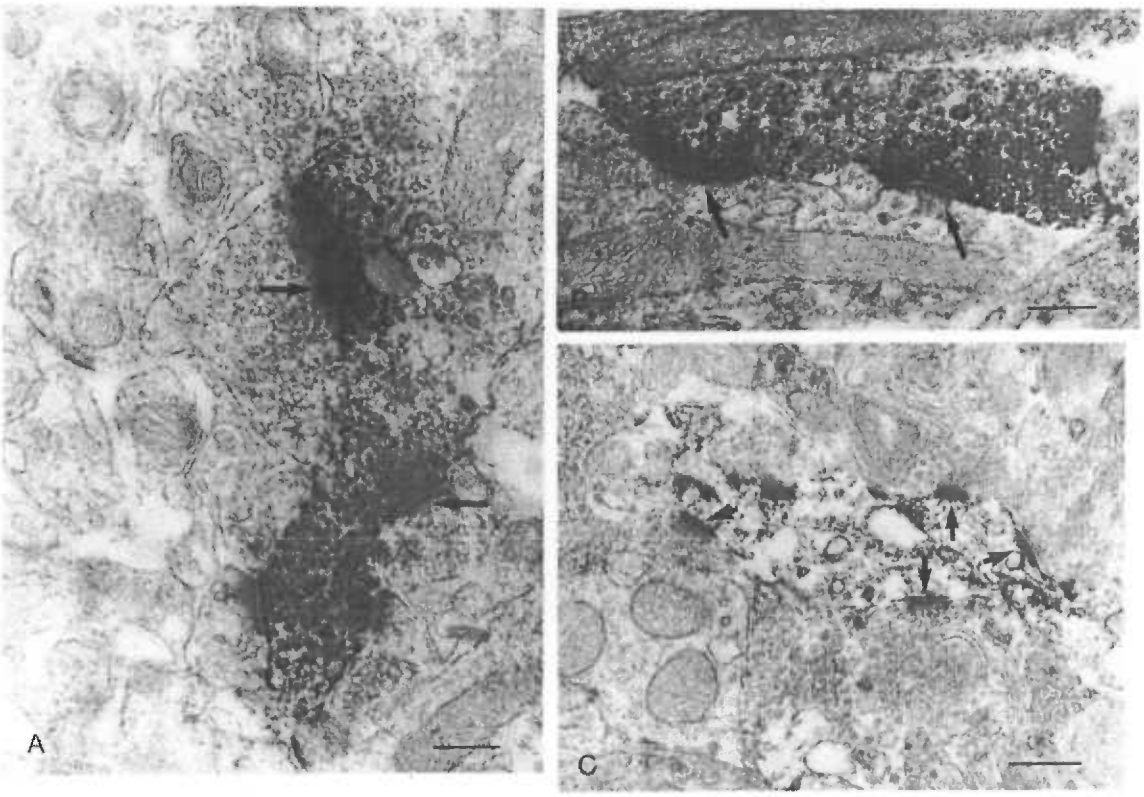

Fig.5. Neuropil labeling. A: A labeled presynaptic process in the glomerular layer contains a large number of synaptic vesicles, and is in synaptic contact (arrows) with other unlabeled processes that also contain synaptic vesicles. Bar: 0.3 mm. B: An immunoreactive, vesicle-rich process with the appearance of an axon makes synaptic contact (arrows) with unlabeled dendrites in the glomerular layer. Immunoreactivity is found in the presynaptic axon, and is particularly dense near the presynaptic membrane specialization. Bar: 0.25 mm. C. A dendrite in the glomerular layer shows peroxidase labeling, particularly associated with the postsynaptic specialization at contacts with multiple unlabeled, vesicle-containing processes (arrows). Bar: 0.3 mm.

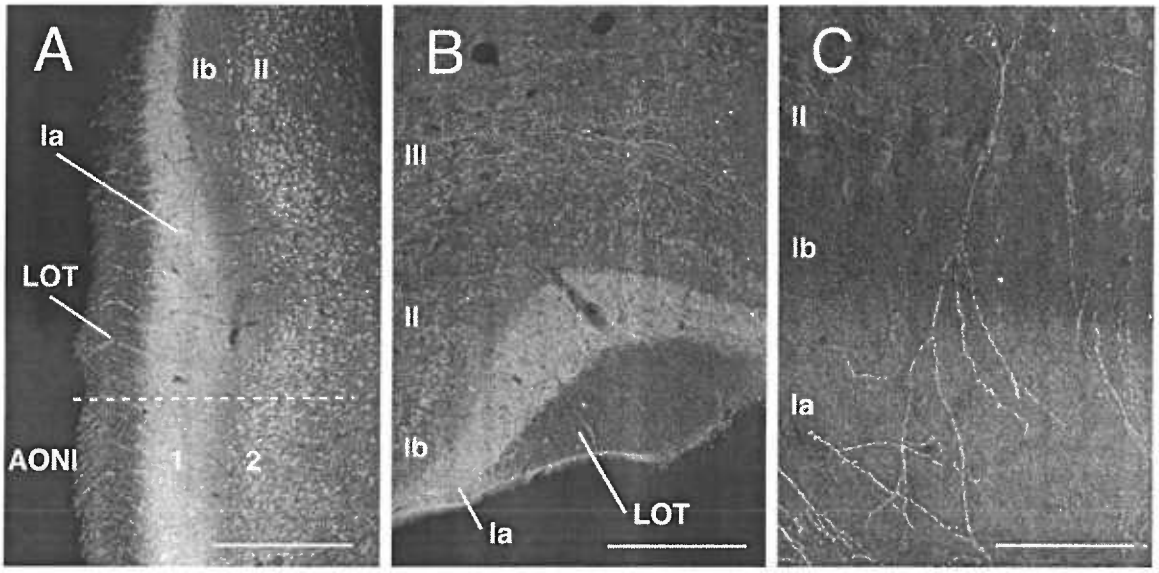

Fig.6. Confocal immunofluorescence analysis of mGluR7 in the olfactory peduncle and piriform cortex. A: Immunohistochemistry of the anterior olfactory nucleus, lateral part (AONl) and rostral piriform cortex at the level of the olfactory peduncle. The molecular layer of the anterior olfactory nucleus (1) is diffusely stained, while in the pyramidal layer (2), numerous immunoreactive cell bodies are present. There is staining of a few fibers traversing the lateral olfactory tract (LOT). In the rostral piriform cortex, there is intense, diffuse staining of layer Ia (Ia). Layer Ib (Ib) is not strongly stained. Somata in layer II (II) are clearly immunoreactive. Bar: 300 mm. B: Immunofluorescence in the piriform cortex more caudally also shows diffuse staining in layer Ia without labeling of the LOT. Cell bodies in layers II and III are immunoreactive as are fibers coursing through layer III. Bar: 300 mm. C: Higher magnification of layers I and II show distinct fibers that appear to originate in layer II branching out in layer Ia. Bar: 75 mm.

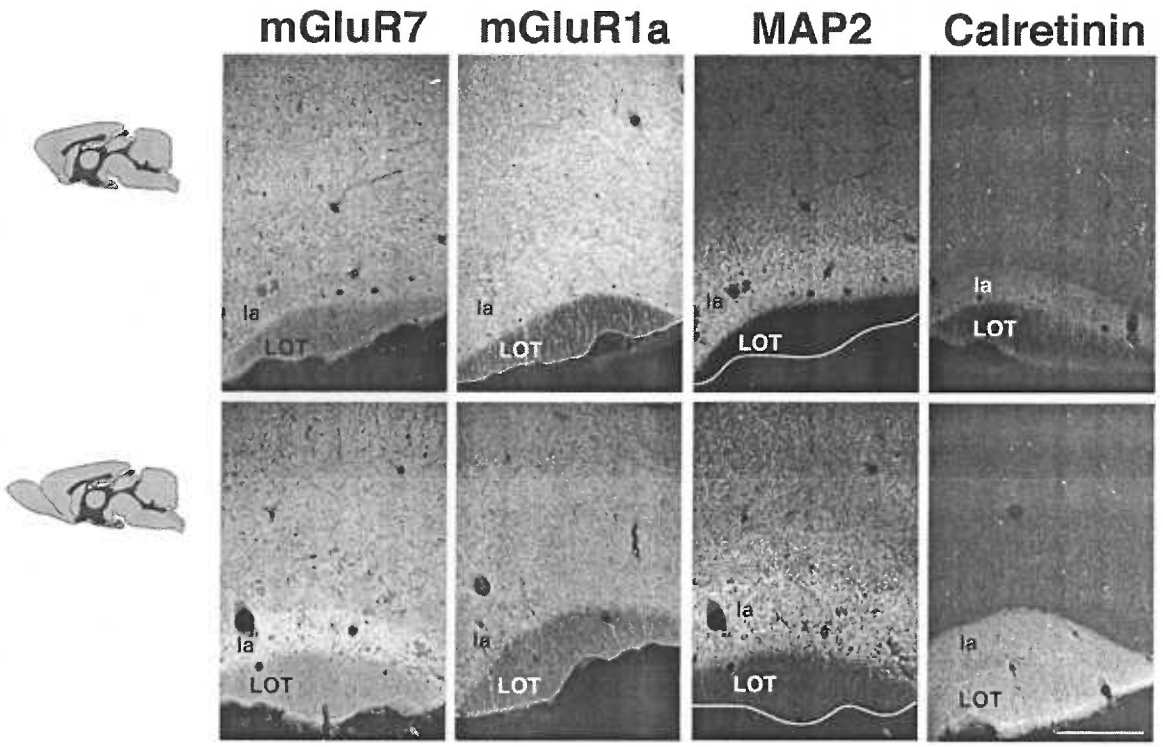

Fig.7. Confocal immunofluorescence following unilateral olfactory bulbectomy. Top row shows immunohistochemistry with mGluR7, mGluR1a, microtubule-associated protein (MAP)2 and calretinin antisera of coronal sections of the piriform cortex ipsilateral to the bulbectomy. Bottom row shows immunohistochemistry for the antisera in the piriform cortex of the contralateral side from the same rat brain section. Unlike mGluR1a and MAP2 staining, mGluR7 and calretinin staining is reduced in layer Ia in sections ipsilateral, but not contralateral to bulbectomy. Bar: 300 mm. Graphics from Swanson, 1992.

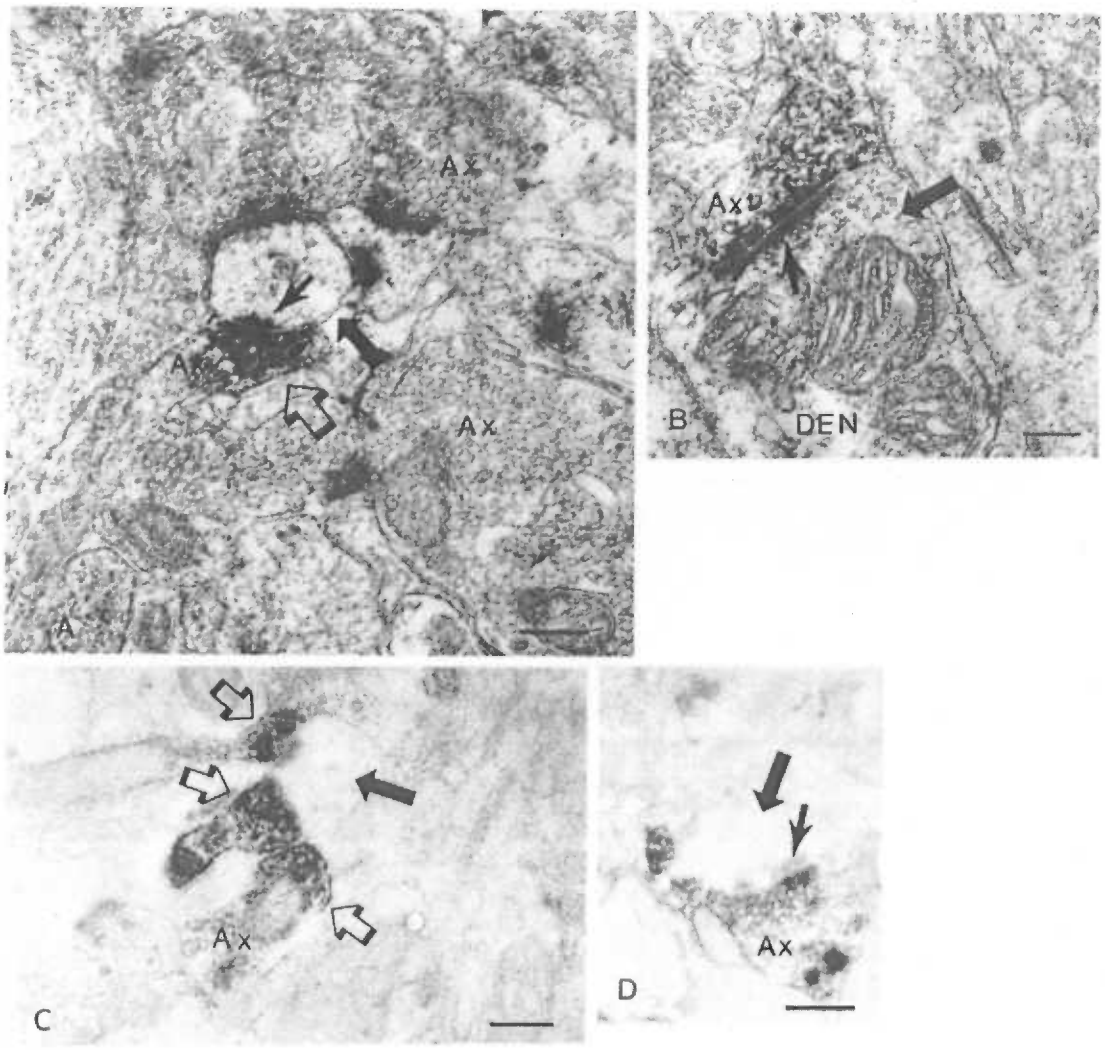

Figure 8. Electron microscopic immunohistochemistry for mGluR7 in layer Ia of rostral piriform cortex. A and B are counterstained with lead citrate and uranyl acetate. C and D received no lead staining, allowing for easier visualization of immunoreactive axons, but leaving non-immunoreactive profiles with low contrast. A, B: immunoreactive axons (Ax - hollow arrow) make asymmetrical synaptic contact (arrowheads) with a dendrite (filled arrow). C. Three immunoreactive axons (Ax - hollow arrows) contact a central dendrite (filled arrow). D. Single immunoreactive axon (Ax) makes synaptic contact with a dendrite (filled arrow). Postsynaptic density is indicated by arrowhead. Bars: A, 650 μm; B, 300 μm; C, 800 μm; D, 700 μm.

PROLOGUE TO CHAPTER 3:
PILOT STUDY OF *C-FOS* INDUCTION
IN mGluR1 KNOCKOUT MICE

J. Mark Kinzie, Yoshinori Sahara, Kathleen Spouffske,

Gary L. Westbrook and Thomas P. Segerson

Vollum Institute and Department of Medicine

Oregon Health Sciences University

Portland, Oregon 97201

INTRODUCTION

The olfactory bulb is particularly well-suited for the assignment of functional roles of neurotransmitter receptors. It can be activated in an intact animal by exposing the animal to odors and its synaptic and neuronal arrangement is clearly demarcated. The work with mGluR7 described in the last chapter demonstrated that, although there is a great deal of mGluR7 mRNA within the olfactory bulb, most of the translated protein is targeted outside of it. Therefore, to take advantage of the olfactory bulb to explore the physiological roles of metabotropic glutamate receptors, I chose a series of pilot experiments to explore the role of mGluR1 in olfactory information processing. As will be shown now, the experiments failed to demonstrate a clear role for mGluR1. However, these experiments did lead to further work on the role of NMDA receptors in olfactory processing which will be elaborated in the next chapter.

mGluR1 is widely distributed throughout the brain, especially in the olfactory bulb, hippocampus and cerebellum (Shigemoto et al., 1992). Functionally, mGluR1 has been shown to prolong excitation by increasing intracellular calcium or by affecting ion channel activity (Saugstad et al., 1995). In cerebellar Purkinje cells where mGluR1 is expressed at high levels, mGluR1 activation evokes a large inward current of several hundred pA, that is absent in mGluR1 knockout mice (Conquet et al., 1994). Additionally, mGluR1 mutant mice demonstrate deficient cerebellar LTD and impaired motor learning (Aiba et al., 1994).

Like mGluR7, mGluR1 is strongly expressed in olfactory bulb mitral cells (Shigemoto et al., 1992). However, unlike mGluR7, mGluR1 is targeted mainly to the dendrites. Within the olfactory bulb, the most striking immunohistochemical finding is the strong staining of glomeruli which is the result of mGluR1 localized to the terminals of the primary dendrites of mitral cells (van den Pol, 1995). This suggests that the receptor is well-positioned either to potentiate excitatory signals exiting the glomeruli or promote the spread of lateral inhibitory signals to neighboring glomeruli.

Because mGluR1 is so strongly and specifically expressed and because mGluR1 has a clear function in other brain regions, such as LTD in the cerebellum, I examined the role of mGluR1 in odor response in the olfactory bulb. In order to do this, I studied the pattern of *c-fos* mRNA induction in wild-type and mGluR1 knockout mice in response to odor induction. As will be elaborated in the next chapter, mRNA production of the immediate early gene *c-fos* is induced by the rise in intracellular calcium seen in neuronal excitation and thus has been widely used as an assay for studying the excitability of populations of neurons within many different brain regions, including the olfactory bulb (Guthrie et al., 1993; Guthrie and Gall, 1995; Sallaz and Jourdan, 1993).

The olfactory receptor neuron axons entering the olfactory bulb synapse with mitral cells and interneurons termed periglomerular cells. Mitral cells send their axons toward olfactory cortical areas. Periglomerular neurons have a complex array of synaptic arrangements. These cells receive direct excitatory input from olfactory receptor neurons, form reciprocal synapses with mitral cell dendrites and send out axons to make inhibitory synapses with mitral cell dendrites of neighboring glomeruli. mGluR1's position at the mitral cell dendrites can therefore be hypothesized to play either of two opposing roles. One view is that, by stimulating mGluR1 in mitral cell dendrites, calcium released by intracellular stores causes a sustained depolarization, making the mitral cells more excitable to odor stimulation. By removing mGluR1, as in mGluR1 mutant mice, then, mitral cells throughout the bulb would be less stimulated and, thus, *c-fos* expression would be diminished. On the other hand, stimulation of mGluR1 in the mitral cell dendrites could lead to greater stimulation of periglomerular cells through reciprocal synapses. The net result would be greater inhibition throughout the olfactory bulb. By removing mGluR1, mitral cells throughout would be more stimulated, but periglomerular cells would be less. As will be shown, neither of these scenarios could be discerned using the techniques available.

METHODS

Production of mGluR1 mutant and wild-type mice

Heterozygous mGluR1 mutant mice were a generous gift from Francois Conquet, Glaxo Institute for Molecular Biology, Geneva, Switzerland. Screening of mice bred from heterozygous mice was performed by PCR analysis of tail DNA using primers directed to the mGluR1 gene and the *lacZ*/neo^r expression unit inserted into the mGluR1 gene locus (Conquet *et al.*, 1994). Both wild-type and mutant mice were kept in the same room with a 12 hour light-dark cycle.

Anatomic studies

For basic anatomic and immunohistochemistry studies, mGluR1 mutant (20-25 g) and wild-type littermates (30-35 g) of the same age (3-4 weeks) were deeply anesthetized with pentobarbital and perfused transcardially with ice-cold saline, followed by ice-cold 4% paraformaldehyde in 0.1 M sodium borate (pH 9.5). The brains were removed quickly, blocked and post-fixed for 4 hours at 4°C in 4% paraformaldehyde in 100 mM borate buffer (pH 9.5). The brains were rinsed 6 times in PBS, followed by sectioning (75 μm) on a Vibratome 1000 Sectioning System (Lancer, St. Louis, MO). Some sections were stained with thionin and dehydrated in ethanol before mounting on gelatin-coated slides and coverslipped with DPX.

For sections immunostained tyrosine hydroxylase, sections were rinsed in 14 mM NaCl, 2 mM K_2HPO_4 (KPBS) and blocked in 2% normal donkey serum, 0.02% nonfat dry milk in KPBS (1 hour at room temperature) following sectioning. The sections were then incubated in monoclonal antibody to tyrosine hydroxylase (1:6400; Incstar, Stillwater, MN, USA) in 2% normal donkey serum, 0.02% nonfat dry milk in KPBS (3 days at 4°C). After rinsing in KPBS, sections were treated for endogenous peroxidase activity (1% H_20_2 in KPBS, 30 minutes at room temperature). Sections were then incubated in biotin-SP

donkey anti-mouse IgG at 1:40 (Jackson ImmunoResearch, West Grove, PA) for 4 hours, followed by incubation in avidin-biotin-peroxidase complex (Vector Laboratories, Burlingame, CA) for 2 hours. Sections were developed with a Ni- and Co- enhanced DAB/peroxide reaction (Pierce Chemical Co., Rockford, IL), mounted on gelatin-coated slides, dehydrated in graded alcohols, cleared in xylene, and then coverslipped with DPX.

In vivo analysis of *c-fos* mRNA activation

For odor experiments, mGluR1 mutant (20-25 g) and wild-type littermates (30-35 g) of the same age (3-4 weeks) were used. Mice were placed in a Buchner funnel (160 mm) covered by a glass funnel (155 mm) into which flowed 10 l/min. charcoal filtered, humidified air for 60 minutes. Filtered air, a 1:500 dilution (approximately 0.44 μM) or a 1:10 dilution (approximately 22 μM) of isoamyl acetate (IAA) saturated air was then supplied to the chamber for 5 minutes followed by 15 minutes of filtered air. Mice used in MK 801 experiments were injected with either 1 mg/kg MK 801 or saline and placed in odor delivery apparatus and given filtered, humidified air for 90 minutes prior to odor exposure (1:10 dilution of IAA). Mice used in double exposure experiments were either immediately exposed to a 1:10 dilution of IAA or filtered air, followed by 60 minutes of filtered air and 5 minutes of odor exposure to both groups.

Mice were deeply anesthetized with pentobarbital and perfused transcardially with 100 ml ice-cold saline containing followed by ice-cold 4% paraformaldehyde in 0.1 M sodium borate (pH 9.5). The brains were removed quickly and post-fixed overnight at 4°C in 4% paraformaldehyde in borate buffer (pH 9.5) containing 10% sucrose.

Coronal freezing microtome sections (25 μm) of the olfactory bulb were collected PBS, mounted onto Poly-Prep slides (Sigma) and incubated for 15 min in 4% paraformaldehyde in 0.1 M PBS, washed twice in 0.1 M PBS, and treated for 30 min at 37°C in 10 μg/ml proteinase K in 100 mM Tris/50 mM EDTA (pH 8), followed by 0.0025% acetic anhydride in 0.1 M triethanolamine at room temperature. The sections

were then washed in 2X SSC (1X SSC= 0.15 M NaCl, 0.015 M $Na_3C_6H_5O_7$), dehydrated in increasing concentrations of ethanol, and vacuum-dried at room temperature.

The probe for *c-fos* mRNA was generated using a 1.3 kb EcoRI/SacI fragment of *c-fos* subcloned into pGEM3z (from Dr. Phillip Stork, Vollum Instititute). Using linearized template DNA, ^{35}S -labeled antisense *c-fos* cRNA probe was transcribed as described[33], heated to 65°C for 5 min and diluted to 10^7 cpm/ml in hybridization buffer (66% formamide, 260 mM NaCl, 1.3X Denhardt's solution, 13 mM Tris (pH 8.0), 1.3 mM EDTA, 13% dextran sulfate). Hybridization mixture applied to the sections was covered with glass coverslips and sealed using DPX mountant. After incubating at 58°C for 20-24 hr, the slides were soaked in 4X SSC to remove coverslips, then rinsed in 4X SSC (4 times, 5 min each) prior to ribonuclease A treatment (20 μg/ml for 30 min at 37°C). The slides were then rinsed in decreasing concentrations of SSC containing 1 mM DTT to a final stringency of 0.1X SSC, 1 mM DTT for 30 min at 65°C. After dehydrating the sections in increasing concentrations of ethanol, they were vacuum-dried and exposed to DuPont Cronex-4 X-ray film for 3 days. The autoradiograms of hybridized sections were converted to digital images for the generating figures by a Nikon LS3500 scanner at 1670 dot per cm resolution and the images were manipulated using Photoshop (Adobe).

RESULTS

General appearance of mutant mice

The mGluR1 mutant mice appear healthy, are capable of caring for themselves, and are able to eat solid food. But, between the second and third week, the mutant mice can be easily identified on the basis of their motor coordination deficit and impaired balance. Muscle strength in the mice appeared intact. However, the mice were under-weight compared to the littermates, taking 3-4 weeks to each 20 g rather than the typical 2 weeks. When subjected to intense odor stimulation, wild-type mice tend to react with increased movement and sniffing behavior. mGluR1 mice also reacted with increased movement, albeit uncoordinated. Therefore, it appeared that the mice were able to smell.

Anatomic studies

Histological analysis of the olfactory bulb did not reveal any gross anatomical abnormalities in mGluR1 mutant mice compared to wild-type (Figure 1, top panels). Microscopic analysis of thionin-stained olfactory bulb sections revealed the same apparent densities of juxtaglomerular, mitral and granule cells. Areas of relatively low-cell densities such as the external and internal plexiform layers also appeared to have the same relative thickness. Additionally, both wild-type and mutant mice appeared to have comparable numbers of glomeruli.

Tyrosine hydroxylase, an enzyme involved in catecholamine biosynthesis, is abundant in the juxtaglomerular neurons of olfactory bulb and is rapidly down-regulated to near background levels in odor-deprived mice (Cho et al., 1996). If deficiency in the mGluR1 in mutant mice causes decreased olfaction in mice or decreased neuronal stimulation at the level of the olfactory glomerulus, it can be assumed that the degree of anti-tyrosine hydroxylase immunostaining would diminish as in odor-deprived mice. However, the degree of immunostaining in mGluR1 mutant mice was qualitatively similar

to wild-type mice. This coincides with the behavioral observation that the mGluR1 mutant mice are able to respond to odor and indicates that the olfactory system of the mice is at least grossly intact.

Odor response studies

As reasoned in the introduction, mGluR1 could be functioning to modulate synaptic transmission at the level of the glomerulus. Such an action could be reflected in modulation of periglomerular and mitral cells activity. Because granule cells receive the majority of their synaptic input from mitral cells, they too could be modulated by mGluR1 activity. In order to study the patterns of stimulation in response to odor, *c-fos* induction patterns were compared in wild-type and mGluR1 mutant mice. Figure 2 demonstrates representative results. The top panels shows coronal olfactory bulb sections of mice exposed to filtered air (labeled Ambient). Baseline levels of *c-fos* induction were low in both groups of mice and no discernable difference was detected in the patterns of *c-fos* activation. The middle panels show 1:500 dilution of IAA. In this representation, the number of glomeruli surrounded by periglomerular cells positive for *c-fos* induction is about the same in both sections. No differences were detected in mitral cell number or intensity. Within the granule cell layer, mGluR1 mutants appeared to have greater abundance of *c-fos* hybridization than wild-type. However, this finding was inconsistent compared to other sections of this mouse and other mGluR1 mutant mice subjected to the same IAA concentration. Finally, a higher concentration of IAA (1:10 dilution), both groups of mice have apparently maximal stimulation of olfactory bulb neurons, with seemingly all periglomerular, mitral and granule cells positive for *c-fos* induction.

NMDA receptor antagonist studies

While the above results were discouraging in not demonstrating a functional change in mGluR1 mutant mice, many reasons could account for this. For example, because

glutamate neurotransmission relies predominantly on NMDA and AMPA receptors, the functional effect of mGluR1's absence at the synapse might not be seen by the parameters of the *c-fos* assay. Therefore, the experiments were repeated in the presence of MK-801, a noncompetitive NMDA antagonist, in order to perturb the olfactory system in hopes of demonstrating a function for mGluR1.

In olfactory bulbs of mice injected with the non-competitive NMDA antagonist MK-801 (1 mg/kg, i.p.) but not exposed to odor the prominent feature seen by *in situ* hybridization for *c-fos* mRNA is the presence of a ring of increased mRNA expression representing the cell bodies of the mitral cells (Figure 3, upper left). Although olfactory bulbs of mutant mice appear to have in increased mRNA expression in granule cells compared to the wild-type, other sections failed to corroborate this finding.

Whereas mitral cells are predominant cells with *c-fos* mRNA expression in mice not exposed to odor, the general finding in mice injected with MK-801 and exposed to IAA is uniform *c-fos* mRNA induction. A ring of induction representing the mitral cell layer can be seen as seen with the MK-801/no odor condition. Additionally, there is uniform juxtaglomerular activation and the entire granule cell layer expresses *c-fos* mRNA. Comparison of wild-type and mutant sections revealed no discernable difference.

Double odor exposure experiments

As a final attempt to visualize a functional difference in the odor response of wild-type and mGluR1 mutant mice, a double odor exposure experiment was conducted. Many studies have demonstrated that mGluR1 responses can be potentiated. For example, Batchelor and Garthwaite (1997) have demonstrated that, in cerebellar Purkinje cells, a single activation of the climbing-fibre input markedly potentiated mGluR-mediated excitation at parallel-fibre synapses. The potentiation was the result from a transient rise in cytosolic Ca2+ that promoted excitation through mGluRs. I reasoned that a similar type of potentiation may exist in the olfactory bulb, that is, the effects of mGluR1 activation may

be more pronounced following prior stimulation of olfactory pathways. In order to test this hypthesis wild-type and mGluR1 mutant mice were exposed to odor for five minutes, ambient air for 60 minutes, then odor for 5 minutes. The 60 minutes of ambient air was chosen because studies by Guthrie and Gall (1995) show *c-fos* mRNA expression returns to baseline at this interval. As in the previous experiments, no discernable difference was demonstrated.

CONCLUSION

In these preliminary experiments, I attempted to demonstrate a functional difference between wild-type and mGluR1 mutant mice using *c-fos* mRNA induction as a reporter of neuronal activity in response to odor stimulation. My initial hypothesis was that mGluR1 could be playing one of two roles. mGluR1 may be involved in enhancing the excitability of mitral cells. Alternatively, mGluR1 may be involved in enhancing the stimulation of periglomerular cells through reciprocal synapses thus leading to greater overall inhibition throughout the olfactory bulb. As seen above, neither of the these possibilities could be elucidated despite varying odor concentration, manipulation with an NMDA receptor antagonist and preexposing the mice to the test odor.

Many reasons could account for lack of a finding in these experiments. One reason may be that the role played by mGluR1 is too subtle for the *c-fos* assay. The ionotropic glutamate receptors are generally the key players in exciting a neuron, leaving the metabotropic receptors to modulatory roles. The fact that the *c-fos* assay relied on a long odor exposure, essentially giving a time averaged view of the excitability of the olfactory bulb, was thought by me to be a potential advantage in viewing mGluR1's modulatory role. However, the opposite may be true. A neuron that may have once been excited ten percent of the time may have been excited 60 percent of the time. However, *c-fos* induction as viewed by the qualitative methods of the assay would not have changed in the neuron as both will have been stimulated sufficiently given the long odor induction.

On the other hand, mGluR1's role in modulation of olfactory bulb processing may be more complicated than simply routinely contributing to neuronal activation of olfactory bulb neurons. It may be that AMPA and NMDA receptors more than adequately provide sufficient stimulation of neurons so that in mGluR1 mutant mice routine synaptic transmission is unchanged within the olfactory bulb. However, mGluR1 may be called into play in learning and discriminating odors. Indeed, mGluR1's role in long term potentiation and depression has been shown repeatedly (Aiba et al., 1994; Aiba et al.,

1994; Bashir et al., 1993; Bortolotto et al., 1994; Bortolotto and Collingridge, 1993; Calabresi et al., 1993; Musgrave et al., 1993). The goal of the double odor exposure experiments to determine in a simple way if preexposure to odor altered olfactory bulb processing. As was shown, viewed at the level of the olfactory bulb no change was found. It is likely that only certain neurons or units of neurons change their response patterns in response to a previously identified odor. Therefore, the removal of mGluR1 action within the olfactory bulb may not result in a finding that could be identified by gross examination of *c-fos* mRNA hybridized sections of the olfactory bulb.

Problems inherent in the use of knock out mice point to other reasons for the lack of a finding in these experiments. Because these mice are chronically deficient of mGluR, functional compensation may have occured to mask or distort the true role of mGluR1. There may be enough redundancy within olfactory bulb function that the role of mGluR1 can not be observed. Or, a functionally related receptor may be up-regulated to compensate for the loss of mGluR1. There are examples of such compensation in other knock out mice. Knockout of CREBα and CREBδ is not lethal to mice, largely due to increased levels of CREBβ and the CREB-related protein CREM (Blendy et al., 1996; Hummler et al., 1994).

In the mutant mice, brains develop in the chronic absence of mGluR1. Therefore, compensation could also occur at the level of neuroanatomy. Changes in neuroarchitecture can be seen in other knock out mice. For example, in dopamine D_1 receptor subtype leads to altered morphology of the striatum in which the striosomes seen in wild-type mice are absent. More importantly, changes in neuroanatomy have also been reported in mGluR1 mice. Kano *et al.* have shown that about one third of Purkinje cells in mGluR1 mutant mice are innervated by multiple climbing fibers, unlike the strict one to one relationship seen in wild-type mice (Kano et al., 1997). These findings were made despite the fact that in Nissl-stained sections, the cerebellum of the mGluR1 mutant mouse was indistinguishable from that of the wild-type. While it is unlikely that a neuroanatomical

change would result in a functional compensation that would lead to similar *c-fos* findings between mutant and wild-type, this possibility cannot be excluded.

Thus, I was left with a conundrum. None of the manipulations in the pilot studies gave an indication of a functional change in olfactory bulb processing in mGluR1 deficient mice. Observation, tyrosine hydroxylase staining and hybridization for *c-fos* mRNA all seemed to indicate that the mice responded appropriately to smell. It was clear that the absence of mGluR1 in the cerebellum had profound consequences; the mice had ataxic gait and intentional tremor. But this did not seem to be the case in the olfactory bulb. Additionally, the lack of any effect did not provide any clue to the direction the experiments should head. It was unclear whether I should attempt to quantify the amount of *c-fos* mRNA induction, to attempt an olfactory learning protocol or to focus on potential anatomical differences as seen in the cerebellum. In any case, there was no promise of a robust result.

Fortunately, the pilot experiments did reveal a striking change in olfactory bulb processing with the noncompetitive NMDA antagonist MK-801. These findings compelled me to collaborate with Dr. Nathan Schoppa, a post-doctoral in the laboratory of Dr. Gary Westbrook, who was finding similar results in olfactory bulb patch-clamp recordings. It is for these reasons that Chapter 3 focuses on olfactory bulb responses to odor in the presence and absence of NMDA antagonists and concludes that dendrodendritic inhibition between mitral and granule cells is driven by NMDA receptors.

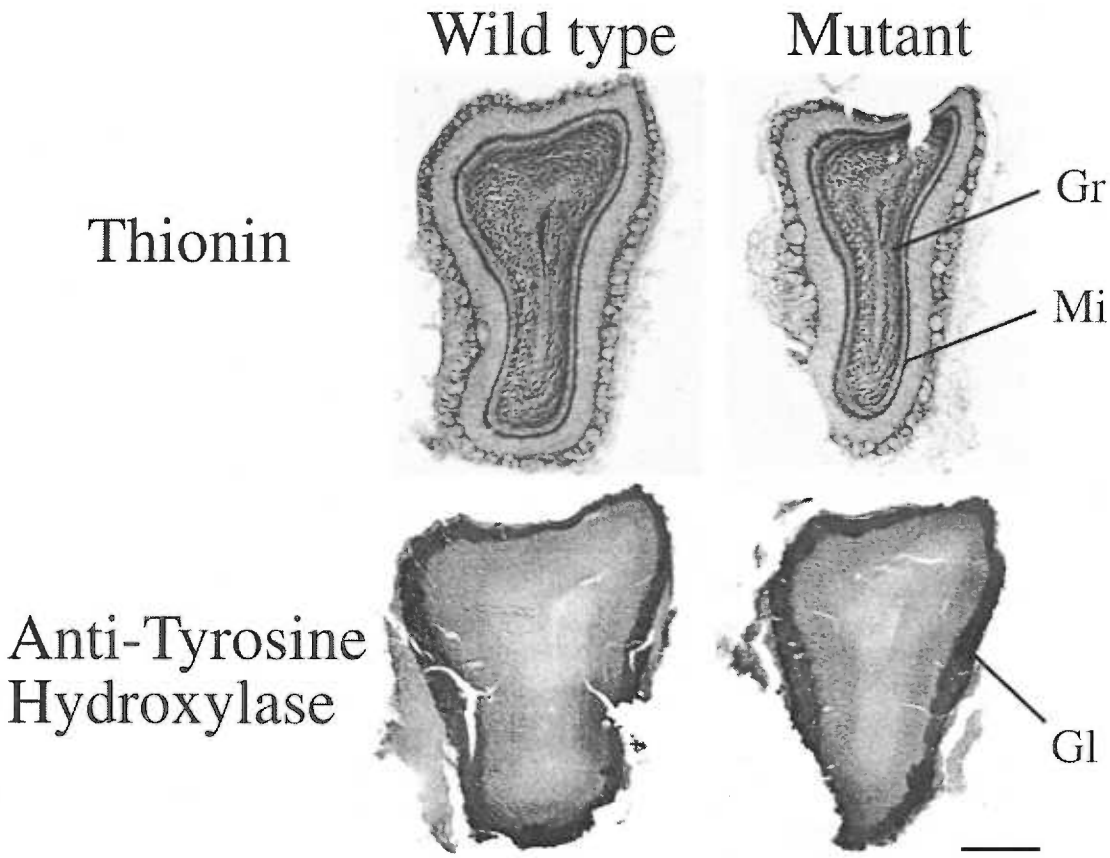

Figure 1. Thionin stain and anti-tyrosine hydroxylase immunohistochemistry of wild type and mGluR1 mutant mice. Top panels. Thionin-stained olfactory bulb coronal sections of both wild-type (left column) and mGluR1 mutant mice (right column) reveal similar glomerular, external plexiform, mitral (Mi) and granule cell (Gr) lavers. Bottom panels. Likewise, anti-tyrosine hydroxylase immunostaining appears equally dense in periglomerular regions (Gl) in coronal sections of wild type and mGluR1 mutant mice suggesting adequate neuronal stimulation at the level of the glomerulus. Scale, 500 μm.

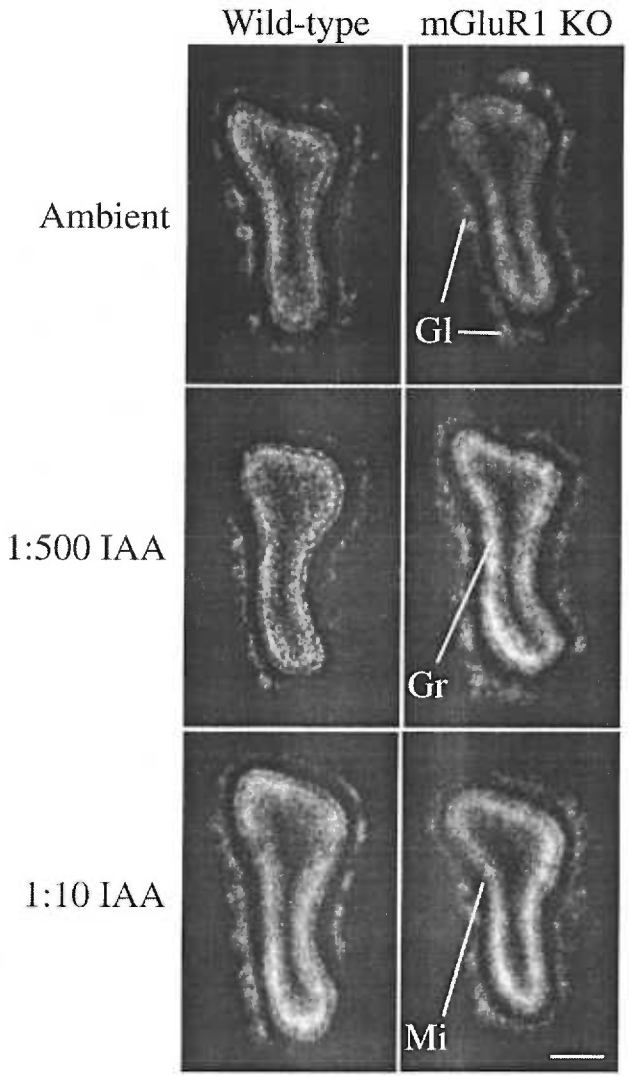

Figure 2. Comparison of induction of *c-fos* mRNA in the olfactory bulb of wild type and mGluR1 mutant mice. Autoradiograms of *in situ* hybridization with a ^{35}S antisense probe to *c-fos* mRNA were compared in three different odor conditions. Coronal olfactory bulb sections from 6 different mice are shown. Sections are oriented with dorsal up and lateral to the right.
Upper panels: In filtered air (ambient), light patchy labeling was present in both wild type (left column) and mGluR1 mutant (labelled mGluR1 KO, right column) mice.
Middle panels: At 1:500 dilution of IAA, the number of glomeruli surrounded by periglomerular cells positive for c-fos induction is about the same in both sections. Within the granule cell layer (Gr), mGluR1 mutants appeared to have greater abundance of c-fos hybridization than wild-type. This finding was inconsistent, however.
Lower panels: At a 1:10 dilution of IAA, periglomerular, mitral (Mi) and granule cells layers of both wild type and mGluR1 mutant mice show broad c-fos mRNA induction.

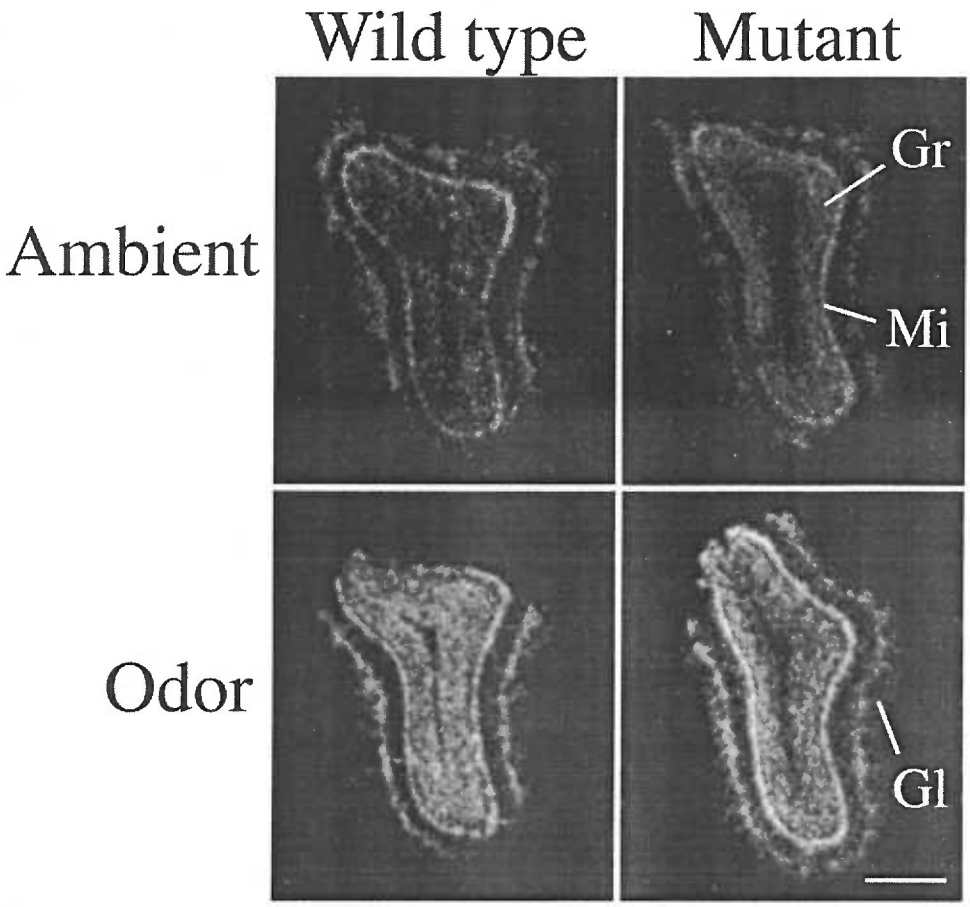

Figure 3. Autoradiograms of *in situ* hybridization with a ^{35}S antisense probe to *c-fos* mRNA in MK-801 (1 mg/kg, i.p.) treated mice. Coronal olfactory bulb sections from 4 different mice are shown with wild type mice shown in left column or mGluR1 mutant mice in right column.
Upper panels: In filtered air (ambient), MK-801 injected mice, the mitral cell layer was uniformly activated (Mi) in both wild type and mGluR1 mutant mice. The coronal olfactory bulb section of the mGluR1 mutant mouse (upper right) appears to have increased c-fos hybridization in the granule cell layer (Gr). However, other sections do not demonstrate this finding.
Lower panels: In 1:10 IAA exposed (labelled odor), MK-801 treated mice of both groups, there was intense labeling in granule and mitral layers. Increased labeling of juxtaglomerular cells (Gl) was also apparent in both wild type and mGluR1 mutant mice without discernable difference.

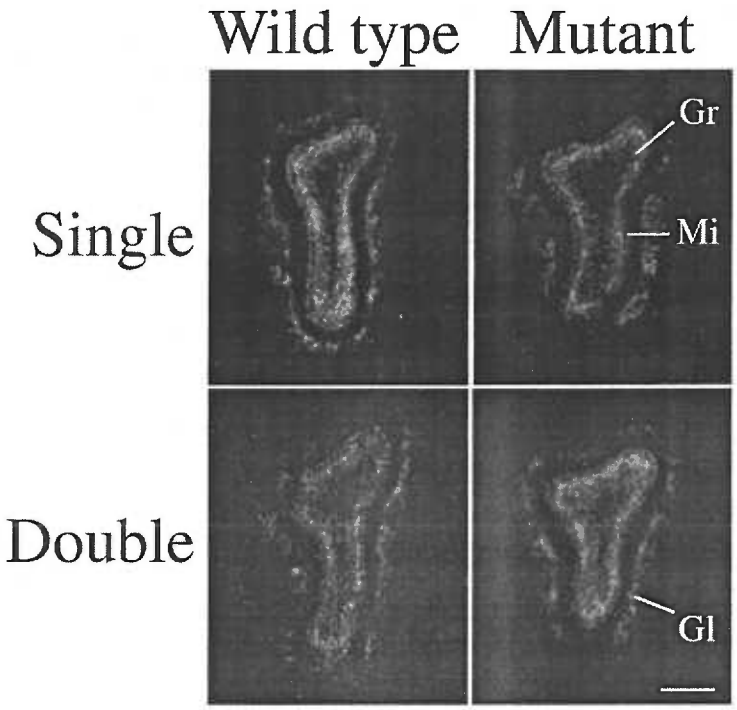

Figure 4. Autoradiograms of *in situ* hybridization with a ^{35}S antisense probe to *c-fos* mRNA in single and double IAA exposed mice. Coronal olfactory bulb sections from 4 different mice are shown with wild type mice shown in left column or mGluR1 mutant mice in right column.
Upper panels: In mice of both groups given a single 5 minute exposure of 1:10 IAA, broad areas of the granule cell layer (Gr) as well as patches of the mitral (Mi) and glomerular cell layer demonstrated hybridization to the *c-fos* mRNA probe.
Lower panels: In mice of both groups exposed to two 5 minute exposures of 1:10 IAA separated by 1 hour of filtered air, the same qualitative differences are seen, including hybridization to selected periglomerular cells (Gl).

Section: Cellular and Molecular Neuroscience

Senior Editor: Dr. David Van Essen

Dendrodendritic inhibition in the olfactory bulb is driven by *N*-methyl-D-aspartate receptors

N. E. Schoppa*, J. M. Kinzie*, Y. Sahara*, T. P. Segerson†, and G. L. Westbrook*

*Vollum Institute, Oregon Health Sciences University

†Department of Medicine, Oregon Health Sciences University

Portland, OR 97201 USA

Abbreviated title: Dendrodendritic inhibition in the olfactory bulb.

Address for correspondence:

Nathan E. Schoppa
Vollum Institute
Oregon Health Sciences University
3181 SW Sam Jackson Park Road
Portland, OR 97201
phone: (503) 494-5436
fax: (503) 494-6972
email: schoppan@ohsu.edu

Acknowledgments: Supported by NIH 5F32 DC00270-02 (NES) and NS26494 (GLW).

Abstract

At many central excitatory synapses, AMPA receptors relay the electrical signal, whereas activation of NMDA receptors is conditional and serves a modulatory function. We show here quite a different role for NMDA receptors at dendrodendritic synapses between mitral and granule cells in the rat olfactory bulb. In whole-cell patch-clamp recordings in bulb slices, stimulation of mitral cells elicited slowly decaying, $GABA_A$ receptor-mediated reciprocal IPSCs that reflected prolonged GABA release from granule cells. Although granule cells had a normal complement of AMPA and NMDA receptors, the IPSC was completely blocked by the NMDA receptor antagonist D,L-AP-5, suggesting that NMDA receptor activation is an absolute requirement for dendrodendritic inhibition. The AMPA receptor antagonist 1,2,3,4-tetrahydro-6- nitro-2,3-dioxobenzo[f]quinoxaline-7-sulfonamide (NBQX) had no effect on IPSCs in the absence of extracellular magnesium but modestly reduced IPSCs in 1 mM magnesium, indicating that the primary effect of the AMPA receptor-mediated depolarization was to facilitate the unblocking of NMDA receptors. Granule cell voltage recordings indicated that effective spike stimulation in granule cells depended on the slow NMDA receptor kinetics. Granule cells also showed a pronounced delay between synaptic stimulation and action potential generation, suggesting that their intrinsic membrane properties underlie the ineffectiveness of brief AMPA receptor-mediated EPSPs. NMDA receptors also seem to have a central role in dendrodendritic inhibition in vivo, because intraperitoneal dizocilpine maleate (MK-801) injection in young adult rats resulted in disinhibition of mitral cells as measured by the generation of *c-fos* mRNA. The unique dependence of dendrodendritic inhibition on slow EPSPs generated by NMDA receptors suggests that olfactory information processing depends on long-lasting reciprocal and lateral inhibition.

Key words: olfactory bulb; dendrodendritic synapses; granule cell; mitral cell; AMPA receptor; NMDA receptor; GABA receptor; synaptic integration; dendrites

Introduction

The unique circuitry of the olfactory bulb suggests that dendrodendritic synaptic interactions there have a profound influence on sensory processing (Shepherd and Greer, 1990; Scott et al., 1993). Olfactory information is mapped onto the glomerular layer of the bulb by olfactory receptor neurons that contact periglomerular cells as well as the primary dendrites of mitral and tufted cells, whose axons provide the output from the bulb. The output from the glomerular layer is transmitted by action potentials to the mitral cell soma (Bischofberger and Jonas, 1997; Chen et al., 1997) and is backpropagated into the primary and secondary dendrites to dendrodendritic synaptic contacts with periglomerular and granule cells. Because granule cells vastly outnumber mitral cells, the activation of a single mitral cell results in robust reciprocal dendrodendritic inhibition (Jahr and Nicoll, 1982). Also, a single granule cell is believed to form contacts with a large number of mitral cells, providing the mechanism for lateral inhibition of adjacent mitral cells. Thus, the temporal and spatial shaping of olfactory bulb output is strongly influenced by the amplitude and duration of dendrodendritic inhibition.

Mitral–granule cell dendrodendritic synapses are reciprocal (Rall et al., 1966; Price and Powell, 1970), consisting of an excitatory synapse directly adjacent to an inhibitory granule-to-mitral cell synapse. Aspiny mitral cell secondary dendrites contact granule cell spines in the external plexiform layer. Dendrodendritic synapses use the same transmitters and receptors that typical axodendritic synapses use, with the excitatory granule cell postsynaptic response mediated by AMPA and NMDA types of glutamate receptors (Trombley and Shepherd, 1992, 1993; Wellis and Kauer, 1994) and the inhibitory mitral cell response mediated by $GABA_A$ receptors (Nicoll, 1971; Nowycky et al., 1981; Jahr and Nicoll, 1982; Wellis and Kauer, 1993). However, the morphology of dendrodendritic synapses suggests that their activation may be atypical. For example, little is known about the mechanisms of glutamate release from dendrites. Likewise, the location of GABA release sites immediately adjacent to postsynaptic glutamate receptors suggests that GABA

release from the granule cell spine could be driven by local depolarizations in the absence of action potentials (Woolf et al., 1991; Scott et al., 1993). Such factors could result in graded or prolonged dendrodendritic inhibition. Consistent with this possibility, $GABA_A$ receptor-mediated IPSPs on mitral cells are prolonged (e.g., Nowycky et al., 1981) compared with that on other central GABAergic synapses.

We examined dendrodendritic inhibition between mitral and granule cells using whole-cell current- and voltage-clamp recordings of synaptic responses in rat olfactory bulb slices. We also examined granule and mitral cell activation in vivo using *c-fos* mRNA as a marker of cellular activation. Our experiments indicated that dendrodendritic inhibition requires the activation of NMDA receptors, despite the fact that granule cells appear to have a normal complement of AMPA and NMDA receptors.

Materials and Methods

Preparation of slices

Olfactory bulb slices were prepared from 9- to 16-day-old Sprague Dawley rats that were anesthetized with halothane and then killed by decapitation. Bulbs were rapidly removed and placed in ice-cold oxygenated (95% O2 and 5% CO2) saline solution, which was similar to our standard recording bath solution (see below) except that 2 mM CaCl2 was replaced with 1 mM CaCl2 and 2 mM MgCl2 . Before cutting slices, we separated the two bulbs from each other with a razor blade and glued a block that included one bulb and a small portion of the frontal cortex to a stage with cyanoacrylate glue along the ventral surface of the bulb. Horizontal slices (400 μm) were cut using a vibrating microslicer (Vibratome 1000; Technical Products International, Redding, CA) and were incubated in a holding chamber for 30 min at 37°C. Subsequently, the slices were stored at room temperature.

Slices were placed on an upright Zeiss Axioskop microscope with infrared (IR) differential interference contrast optics (filter, 850 nm) videomicroscopy and a CCD camera (C2400; Hamamatsu, Hamamatsu City, Japan) after the standard IR filter was removed (Stuart et al., 1993). Cells were visualized with a 40X Zeiss water immersion (0.75 numerical aperture) lens. Mitral and granule cells could be discriminated easily on the basis of morphology (Shepherd and Greer, 1990). All experiments were done at room temperature (20 –24°C).

Voltage-clamp recordings

Patch seal formation and whole-cell patch recordings from mitral and granule cells in the slice were obtained using previously described methods (Stuart et al., 1993). For all experiments, the base extracellular bath solution was oxygenated (95% O2 and 5% CO2) and contained (in mM): 125 NaCl, 25 NaHCO3, 1.25 NaH2 PO4, 25 glucose, 2.5 KCl,

and 2 CaCl2 , pH 7.3. Our standard bath solution contained no added Mg^{2+}, although in some experiments, as indicated, 0.030 –1 mM Mg^{2+} was added. Measurements of granule cell EPSCs were made with 50 μM picrotoxin added to the bath to inhibit $GABA_A$ - mediated responses (Wellis and Kauer, 1994). Granule cell miniature EPSCs (mEPSCs) were recorded also with tetrodotoxin (TTX; 1 μM) and Cd (10 μM) added. This concentration of Cd blocks most neuronal calcium current (Lorenzon and Foehring, 1995) without significantly affecting permeation through NMDA receptors (Mayer et al., 1989). Patch pipettes were fabricated from borosilicate glass (TW150F; WPI, Sarasota, FL) and were pulled with a conventional two-step puller (Narishige, Tokyo, Japan) to a resistance of 1–3 MΩ in mitral cell recordings and 3–10 MΩ in recordings from granule cells. Mitral cell IPSC measurements were made with a pipette solution containing (in mM): 125 KCl, 2 MgCl, 2 CaCl2 , 10 EGTA, 2 NaATP, 0.5 NaGTP, and 10 HEPES, adjusted to pH 7.3 with KOH. Granule cell EPSC measurements were made with equimolar replacement of the pipette KCl with Cs methane-sulfonate (CsMeSO4).

Current signals recorded with an Axopatch 200A amplifier (Axon Instruments, Foster City, CA) were filtered at 1–5 kHz using an eight-pole Bessel filter and were digitized at 1–10 kHz. Data were acquired on a IBM 486 clone using PCLAMP version 6 (Axon Instruments). In all recordings, the membrane voltage Vm and the access resistance Rs were constantly monitored. Data acquisition was terminated when Vm was more positive than -48 mV or Rs obtained values >15 MΩ. No series resistance compensation was used, because the voltage error from the series resistance was expected to be <10 mV for most recordings. The reported membrane potentials were corrected for junction potentials, which were estimated to be <8 mV, for the solutions used. The holding potential for the current recordings was between -70 and -80 mV.

Electrical stimulation of the glomeruli was conducted with a bipolar tungsten electrode (tip separation of 200 μm; Frederick Haer and Company, Brunswick, ME) placed just above the slice in the glomerular layer. Stimulus pulses were generated by the

computer, which triggered a stimulus isolation unit (S-100; Winston Electronics, Millbrae, CA). Maximal 100 V stimulation (with a duration of 100 μsec) was used, unless otherwise indicated. Focal mitral cell stimulation was done by placing a 2–3 MΩ patch pipette filled with extracellular solution above the soma of a mitral cell located 150 μm or less from the granule cell from which currents were recorded. Maximal 100 V stimulation (with a duration of 100 μsec) was also used for these recordings.

Drug solutions were bath-applied. Maximally effective concentrations of the drug solutions were achieved within the first few minutes after the addition of the drugs (see the drug-response time course in Fig. 2 B). Washout of drugs was achieved within 5–10 min.

Drugs were obtained from the following sources: picrotoxin and TTX were from Sigma (St. Louis, MO); D,L-2-amino-5-phosphonopentanoic acid (D,L-AP-5), bicuculline, 6-cyano-7-nitroquinoxaline-2,3-dione (CNQX), (R, S)-3-(2-carboxypiperazin-4-yl)-propyl-1-phosphonic acid (CPP), 2-hydroxysaclofen, and 1,2,3,4-tetrahydro-6-nitro-2,3-dioxobenzo[f]quinoxaline-7-sulfonamide (NBQX) were from Tocris (Ballwin, MO); and dizocilpine maleate (MK-801) was a gift from Merck, Sharp, and Dohme (West Point, PA).

Granule cell current-clamp recordings

Voltage recordings from granule cells were made with the current-clamp facility of the Axopatch 200A amplifier. Solutions were identical to those used in the measurements of granule cell EPSCs, with the exception of an equimolar replacement of the CsMeSO4 in the pipette with Kgluconate. Pipette resistances were 8 –12 MΩ. In recordings from small cells like granule cells, care is required for the compensation of the pipette capacitance. In our experiments, these currents were minimized by using a shallow bath and, in some recordings, by coating the patch pipette with Sylgard; the currents were completely compensated in the cell-attached configuration. From the voltage recorded immediately after patch membrane rupture, we estimated that granule cells had an average resting

potential of -66 ± 2 mV (n=32). For the duration of the recording, a small 5–10 pA negative current was sometimes injected to hold the cell continuously at a voltage between --65 and -75 mV. Step current injections of 10 pA from rest yielded estimates of the membrane time constant τ_m (59 ± 14 msec; n=12) and the input resistance (0.98 ± 0.17 GΩ; n=12).

Data analysis and statistics

All analyses were done using AXO-GRAPH (Axon Instruments) on a Macintosh computer. Estimates of the IPSC charge were made by subtracting the holding current and then numerically integrating the remaining current beginning at the time at which a stimulus was applied. The detection of IPSCs and mEPSCs was done by evaluating the error between the data and a sliding double exponential template function, with the specified time constants. For all experiments, statistical significance was determined using standard t tests within Microsoft EXCEL (Redmond, WA). In the displayed histograms (see Figs. 2C,4C), the numbers above the histogram bars reflect the number of cells for each condition. The response for each cell was the average from 10 or more stimulus-evoked IPSCs or EPSPs. Asterisk s denote statistical significance.

In vivo analysis of *c-fos* mRNA activation

Male Sprague-Dawley rats at postnatal stages P10 to P12 (n=2 per treatment) and p19 to P21 (n=4 per treatment) were injected with 1 mg/kg MK-801 or saline. Rats were then placed in a Buchner funnel (160 mm) covered by a glass funnel (155 mm) into which flowed 10 l/min. charcoal filtered, humidified air for 90 minutes. Filtered air or a 1:10 dilution of isoamyl acetate saturated air (approximately 22 μM) was then supplied to the chamber for 5 minutes followed by 15 minutes of filtered air. Rats were deeply anesthetized with pentobarbital and perfused transcardially with 100 ml ice-cold saline containing followed by ice-cold 4% paraformaldehyde in 0.1 M sodium borate (pH 9.5).

The brains were removed quickly and post-fixed overnight at 4°C in 4% paraformaldehyde in borate buffer (pH 9.5) containing 10% sucrose.

Coronal freezing microtome sections (25 μm) of the olfactory bulb were collected PBS, mounted onto Poly-Prep slides (Sigma) and incubated for 15 min in 4% paraformaldehyde in 0.1 M PBS, washed twice in 0.1 M PBS, and treated for 30 min at 37°C in 10 μg/ml proteinase K in 100 mM Tris/50 mM EDTA (pH 8), followed by 0.0025% acetic anhydride in 0.1 M triethanolamine at room temperature. The sections were then washed in 2X SSC (1X SSC= 0.15 M NaCl, 0.015 M $Na_3C_6H_5O_7$), dehydrated in increasing concentrations of ethanol, and vacuum-dried at room temperature.

The probe for *c-fos* mRNA was generated using a 1.3 kb EcoRI/SacI fragment of *c-fos* subcloned into pGEM3z (from Dr. Phillip Stork, Vollum Instititute). Using linearized template DNA, ^{35}S -labeled antisense *c-fos* cRNA probe was transcribed as described[33], heated to 65°C for 5 min and diluted to 10^7 cpm/ml in hybridization buffer (66% formamide, 260 mM NaCl, 1.3X Denhardt's solution, 13 mM Tris (pH 8.0), 1.3 mM EDTA, 13% dextran sulfate). Hybridization mixture applied to the sections was covered with glass coverslips and sealed using DPX mountant. After incubating at 58°C for 20-24 hr, the slides were soaked in 4X SSC to remove coverslips, then rinsed in 4X SSC (4 times, 5 min each) prior to ribonuclease A treatment (20 μg/ml for 30 min at 37°C). The slides were then rinsed in decreasing concentrations of SSC containing 1 mM DTT to a final stringency of 0.1X SSC, 1 mM DTT for 30 min at 65°C. After dehydrating the sections in increasing concentrations of ethanol, they were vacuum-dried and exposed to DuPont Cronex-4 X-ray film for 3 days. The autoradiograms of hybridized sections were converted to digital images for the generating figures by a Nikon LS3500 scanner at 1670 dot per cm resolution and the images were manipulatedusing Photoshop (Adobe).

Darkfield figures and intensity measurements were taken using emulsion dipped slides. The slides were dipped in NTB-2 liquid photographic emulsion (Kodak), exposed for 3 days, developed with D-19 developer and counter-stained with thionin. Images were

captured using a CCD camera and NIH Image computer program under constant conditions after calibrating the camera to avoid supersaturating pixel intensities. Intensity quantitation was performed using NIH Image. Because granule cells are found immediately medial to the mitral cell layer, a region of interest (ROI) was drawn around mitral cells in bright field images then restored on the corresponding darkfield image and the mean pixel intensity of the ROI was computed. The same procedure was then taken with the granule cell layer in which the ROI was drawn medial to the internal plexiform layer.

Melting temperature (T_m) control experiments of adult rat brain parasagittal sections were performed by hybridization with *c-fos* cRNA probe as described above with modification of wash temperature. Following hybridization and low stringency washes, individual sections were rinsed in 0.1X SSC, 1 mM DTT for 30 min at temperatures ranging between 65°C and 100°C, then treated thereafter as described above. For competition experiments, sections were incubated overnight in either hybridization solution alone, hybridization solution containing 100-fold excess unlabeled *c-fos* probe. Following rinses in 2X SSC, sections were incubated with hybridization mix containing the appropriate unlabeled probe and 10^7 cpm/ml ^{35}S -labeled *c-fos* probe. Subsequent treatments were performed as described above.

RESULTS

The slow time course of the dendrodendritic IPSC is determined by the asynchronous release of GABA from granule cells

To activate dendrodendritic synapses in mitral cells, a bipolar electrode was placed on the surface of the slice in the glomerular layer, where olfactory nerve axons contact the primary dendrites of mitral cells (Fig. 1A). Mitral cells were voltage clamped at 270 mV with KCl-containing patch pipettes. To allow full expression of glutamate receptors that might be involved in the activation of dendrodendritic synapses, we first examined synaptic responses in magnesium-free saline. Maximal glomerular stimulation (100 μsec; 100 V) elicited a large, slowly decaying inward whole-cell current. The current was completely blocked by bicuculline (Fig. 1A;50 μM; n=7) or picrotoxin (50 μM; n=2) but not by the $GABA_B$ receptor antagonist 2-hydroxysaclofen (100 μM; n=3), indicating that the current was mediated by mitral cell $GABA_A$ receptors. The slow IPSCs had a peak amplitude of 1.4 ± 0.3 nA and a decay time constant of 0.41 ± 0.05 sec (n=18). The IPSC amplitude was proportional to stimulus intensity (n=3; data not shown). Given the 200 μm tip separation of the stimulating electrode and the diameter of a single glomerulus (130 μm) (Scott et al., 1993), it seems likely that maximal stimulation activated the ≈25 mitral cells that project to a single glomerulus (see Scott et al., 1993). TTX (1 μM) blocked the IPSC, suggesting that normal afferent pathways were activated by simulation. The prolonged IPSCs we observed are consistent with activation of reciprocal dendrodendritic synapses between mitral and granule cells (Rall et al., 1966; Nowycky et al., 1981; Jahr and Nicoll, 1982). However, activation of granule cells by mitral cell axon collaterals (Shepherd and Greer, 1990) could contaminate the dendrodendritic IPSC. To test this possibility, we recorded IPSCs in response to direct somatic stimulation of a single mitral cell in the presence and absence of TTX (Jahr and Nicoll, 1982). A 2 msec depolarization to 0 mV applied to the mitral cell evoked an action potential that was followed by a flurry of brief

inward synaptic currents (Fig. 1B). The synaptic currents were completely blocked by bicuculline (n=8) or picrotoxin (n=3). The ensemble average of a series of single mitral cell depolarizations produced a composite IPSC (Fig. 1B) that was smaller than the IPSC evoked in the same cell by glomerular stimulation (73 ± 4% reduction; n=17) but that had the same decay time course (τ, 0.46 ± 0.05 vs 0.41 sec; n=21). TTX (1 μM) blocked the IPSC elicited by a 2 msec depolarization (n=7), but longer somatic depolarizations (10 –500 msec) evoked IPSCs (1.2 ± 0.4 nA) that did not differ from the IPSC before the addition of TTX (1.1 ± 0.2 nA). The TTX-insensitive IPSCs are likely to be dendritic in origin because mitral cell dendrites should be much more effectively depolarized than are axons by somatic voltage injections. The TTX-insensitive IPSCs, taken together with morphological data showing that only a subset of mitral cells have axon collaterals in the bulb (Orona et al., 1984), suggest that axon collaterals made little contribution to the IPSCs under our conditions. The decay of the dendrodendritic IPSCs was much slower than was the kinetics of commonly observed stimulus-evoked $GABA_A$ receptor-mediated IPSCs (e.g., Edwards et al., 1990). The long duration of the IPSC did not seem to represent prolonged deactivation kinetics of the $GABA_A$ receptors because, as noted above, single mitral cell stimulation revealed discrete synaptic events with rapid decay time courses. In five cells, the decay time constant of the unitary IPSCs was 18 ± 1 msec (Fig. 1C), which is similar to that of IPSCs observed in other pathways. Likewise, direct stimulation of granule cells with a patch pipette elicited a monophasic IPSC in mitral cells that occurred with a short latency (time-to-peak from stimulus, 5.8 and 7.7 msec; n=2 cells) and with rapid decay (τ, 15 and 22 msec; n=2 cells). These results indicate that the slow kinetics of the dendrodendritic IPSC elicited by mitral cell stimulation reflects the prolonged and asynchronous release of GABA from granule cells.

NMDA receptors, and not AMPA receptors, mediate GABA release from granule cells

The slowly decaying IPSCs in mitral cells are driven by the excitatory synaptic response in granule cells. Most central excitatory synapses have both AMPA and NMDA receptors. Granule cells also express multiple AMPA and NMDA receptor subunits (Keinanen et al., 1990; Petralia and Wenthold, 1992; Watanabe et al., 1993; Petralia et al., 1994). However, bath application of the NMDA receptor antagonist DL-2-amino-5-phosphonopentanoic acid (DL-AP5, 100 μM) completely abolished the IPSC elicited by glomerular stimulation (Fig. 2A and B), whereas the IPSC was insensitive to the AMPA receptor antagonist NBQX (10 μM). The IPSCs typically displayed multiple kinetic components (Fig. 2A), but NBQX did not affect any of these components. The less-selective AMPA receptor antagonist 6-cyano-7-nitroquinoxaline-2,3-dione (CNQX, 10 μM) produced a 24±5% reduction in the IPSC charge (n=7), consistent with its action as a glycine antagonist at NMDA receptors (Lester et al., 1989). A similar glutamate receptor antagonist profile was observed for the IPSC elicited by single mitral cell stimulation (Fig. 2C). Because single mitral cell stimulation bypasses the activation of the olfactory nerve-mitral cell synapse, the complete block by DL-AP5 indicates that NMDA receptors located at dendrodendritic synapses are an absolute requirement for activation of IPSCs in mitral cells.

Because excitatory postsynaptic currents (EPSCs) mediated by NMDA receptors typically persist for hundreds of milliseconds (McBain and Mayer, 1994), the duration of the granule cell EPSC may be responsible for the long duration of the dendrodendritic IPSC. To test this possibility, we examined the effect of the noncompetitive NMDA receptor antagonist MK-801, which can reduce the duration of NMDA receptor-mediated EPSCs by ~50% (Rosenmund et al., 1993). For IPSCs elicited by single mitral cell stimulation, MK-801 (10 μM) reduced the IPSC amplitude while producing a 23±12% (n=10) acceleration of the decay time constant. The faster IPSC kinetics suggest that the kinetics of the granule cell NMDA receptor-mediated EPSC contribute to the long duration of the dendrodendritic IPSC.

AMPA and NMDA receptors are present at dendrodendritic synapses

Although AMPA and NMDA receptors generally are colocalized, there are several examples of "pure" NMDA receptor synapses (Dale and Roberts, 1985; Liao et al., 1995; Durand et al., 1996; Wu et al., 1996; O'Brien et al., 1997). Although granule cells have been reported to have both AMPA and NMDA components in their excitatory responses (Trombley and Shepherd, 1992; Wellis and Kauer, 1994), the disparate effects of NMDA and AMPA receptor antagonists on mitral cell IPSCs could imply that granule cells have many more NMDA receptors than AMPA receptors. To test this possibility, we recorded granule cell EPSCs in response to focal stimulation of a nearby mitral cell (Fig. 3A). The EPSCs had a short latency and displayed a fast component that was completely blocked by CNQX (10 μM; $\tau = 5.5 \pm 1.2$ msec; n=7), as well as a slow component that was blocked by D,L-AP-5 (50 μM). The slow component was well described by two exponentials with time constants of 52 ± 10 and 343 ± 48 msec (n=9). Glomerular stimulation typically elicited short-latency EPSCs with multiple peaks, presumably reflecting asynchrony in the release of glutamate from mitral cells (data not shown). In two cells, the mean latency to the first peak after stimulation was 6.7 and 7.0 msec, whereas the latency to all peaks averaged 27 and 17 msec. The fast components of these EPSCs were clearly blocked by NBQX (n=4 cells). The peak amplitude of the NMDA component of the focally evoked EPSC was smaller than that of the AMPA component (Fig. 3B; $I_{NMDA}/I_{AMPA} = 0.26 \pm 0.05$; n=24), whereas the relative current amplitudes were similar to those of other excitatory synapses (Forsythe and Westbrook, 1988; Hestrin et al., 1990; Silver et al., 1992; Jonas et al., 1993). Thus, the effectiveness of the NMDA receptor in driving dendrodendritic IPSCs is not simply because of a larger number of functional NMDA receptors.

Although the above results indicate that granule cells have both AMPA and NMDA receptors, it is possible that the receptors are segregated such that dendrodendritic inhibition is driven by pure NMDA receptor synapses, whereas the AMPA component of

the evoked EPSC could reflect contributions from mitral cell axon collaterals or centrif ugal fibers. Such a segregation of synapses should be apparent in mEPSCs. However, the small amplitude of pure NMDA receptor mEPSCs makes them difficult to detect (Bekkers and Stevens, 1989). To circumvent this problem, we compared evoked EPSCs with mEPSCs selected using the rapid kinetics characteristic of AMPA receptor-mediated mEPSCs. As shown in Figure 3C (left), mEPSCs selected in this way showed a prominent NMDA receptor-mediated slow component. If the evoked EPSC reflects a composite of different populations of synapses, including pure NMDA receptor synapses, the ensemble average of these mEPSCs should have a smaller NMDA component than does the evoked EPSC because our mEPSC selection criteria excluded pure NMDA receptor-mediated mEPSCs. However, the averaged mEPSCs and the evoked current had the same decay time course (Fig. 3C; n=2), suggesting that most synapses on one granule cell have a similar complement of AMPA and NMDA receptors.

NMDA receptor activation causes stronger granule cell excitation than AMPA receptor activation

At conventional central synapses, the depolarization caused by AMPA receptor-mediated EPSPs drives the short-latency response of the postsynaptic cell. The failure of AMPA receptors to activate dendrodendritic inhibition, despite the presence of typical dual-component EPSCs, suggests that granule cells process incoming excitatory signals in a distinctive manner. One possibility is that the short duration of the AMPA receptor-mediated EPSC limits the voltage response of granule cells. We examined this issue directly in current-clamp recordings in granule cells using potassium gluconate-containing patch pipettes. The amplitude and duration of the evoked EPSP as well as the fraction of stimuli that elicited action potentials were used as measures of the effectiveness of incoming mitral cell activity.

Glomerular stimulation (100 V; 100 msec), identical to that used to record IPSCs in Figure 1, evoked dual-component EPSPs (Fig. 4A, B) with large peak amplitudes and slow decay kinetics (18 ± 2 mV; $t_{1/2}$ = 204 ± 24 msec; n=21). D,L-AP-5 (50 μM) had a variable effect on the peak EPSP amplitude, with an average reduction of 32 ± 18% (n=7), but blocked stimulus-induced action potentials in all cells tested (Fig. 4A,C). In some cells, the peak of the remaining AMPA EPSP component was as large as that of the dual-component EPSP, but the AMPA component nevertheless failed to elicit spiking [Fig. 4A, B (top)]. D,L-AP-5 reduced the duration of the EPSPs by 62 ± 8% (n=7), leaving an AMPA component that had a decay time constant similar to the membrane time constant (τ = 62 ± 15 and τ_m = 59 ± 14 msec, respectively; n=12), as expected for the voltage response to a fast-decaying current input. In contrast, NBQX (10 μM) did not affect the peak amplitude or duration of the EPSP. Furthermore, the remaining NMDA receptor-mediated EPSP was just as effective at eliciting action potentials as was the dual-component response (Fig. 4C). These results indicate that AMPA receptors are less effective at eliciting granule cell excitation than are NMDA receptors, despite their similar amplitudes.

We next considered whether the longer duration of the NMDA receptor-mediated EPSP was critical for granule cell excitation. One clue to this possibility was their long latency to action potential firing. Even with suprathreshold dual-component depolarizations, there was a pronounced delay (72 ± 14 msec; n=7 cells) before the onset of action potentials, as seen in the responses to five stimuli in Figure 4A. This suggests that the AMPA receptor-mediated EPSP was not of sufficient duration to elicit an action potential, although the peak amplitude of the AMPA component in this cell was "suprathreshold." Short somatic current injections (2–5 msec; 50–100 pA; n=3) were similarly ineffective. The depolarizations induced by these current pulses were larger than those elicited by long current injections (400–500 msec; 10–20 pA) that were effective in

generating spikes. Thus, the granule cell membrane appears to have an intrinsic shunt that prevents action potential firing in response to a short-duration current input.

Although the complete block of EPSP-evoked action potentials in granule cells by D,L-AP-5 matched the block of the dendrodendritic IPSCs in mitral cells, this correlation does not imply that NMDA receptor-driven action potentials are required for dendrodendritic inhibition. For example, as discussed above, IPSCs could be elicited by single mitral cell stimulation in the presence of TTX. However, natural odorant stimulation does elicit action potentials in granule cells (Wellis and Scott, 1990), as did the same glomerular stimulation that elicited the IPSCs in our experiments. In 11 of 18 granule cells, glomerular stimulation drove action potentials in at least 20% of the trials. Interestingly, dendrodendritic inhibition evoked by both natural stimuli and glomerular stimulation involves both reciprocal and lateral components. Action potentials should markedly augment the dendritic spread of a voltage signal in the granule cell, which may be particularly important for lateral inhibition (Woolf et al., 1991; Scott et al., 1993).

Dendrodendritic inhibition in the presence of extracellular magnesium

Our experiments thus far have shown that NMDA receptor activation is required for dendrodendritic inhibition. However, no magnesium was added to the extracellular bath in these experiments. Magnesium causes a potent voltage-dependent block of the NMDA receptor channel (Mayer et al., 1984; Nowak et al., 1984), but the addition of magnesium (30 –1000 μM) did not eliminate the mitral cell IPSC evoked by glomerular stimulation (Fig. 5A, B). Both the amplitude and duration of these IPSCs were reduced by 1 mM Mg^{2+}; the remaining charge was 23 ± 4% of control (n=5). Furthermore, dual-component granule cell EPSPs in 1 mM Mg^{2+} were large (15 ± 2 mV; n=26) and frequently elicited action potential firing in granule cells (Fig. 4C). Thus, granule cell excitation and subsequent mitral cell inhibition in response to glomerular stimulation remain intact in the presence of physiological concentrations of magnesium.

Extracellular magnesium could nevertheless change the relative effectiveness of AMPA and NMDA receptors in mediating dendrodendritic inhibition. However, D,L-AP-5 (50 μM) caused a nearly complete (89 ± 4%) block of mitral cell IPSC in 1 mM Mg^{2+} (Fig. 5C; n=11), with similarly large effects on granule cell excitation (Fig. 4C). The small remaining current had a rapid decay time course ($\tau = 6.8 \pm 2.6$ msec; n=3), suggesting that it was attributable to an AMPA receptor-mediated EPSC at the olfactory nerve–mitral cell synapse. In contrast to Mg^{2+}-free conditions, NBQX (10 μM) caused a modest reduction in the IPSC (34 ± 9%; n=18), as well as reductions in granule cell excitability (Fig. 4C). The effect of NBQX on the IPSC was, however, highly variable, as shown for two cells in Figure 5C. There was a modest negative correlation (r =-0.44; n=18) between the magnitude of the NBQX-induced block of the IPSC and the amplitude of the IPSC (Fig. 5D). These results imply that dendrodendritic inhibition in the presence of Mg^{2+} relies completely on the activation of granule cell NMDA receptors, whereas AMPA receptors play a facilitatory role by causing relief of the magnesium block of NMDA receptors.

The negligible effect that NBQX had on IPSCs in many cells, even in magnesium, implies that NMDA receptor activation is capable of eliciting IPSCs in the absence of AMPA receptor activation. This result was somewhat surprising given that at most central synapses, 1 mM Mg^{2+} blocks nearly all of the NMDA receptor-mediated EPSC at voltages near the granule cell resting potential (266 ± 2 mV; n=32). However, some recombinant NMDA receptors have a reduced sensitivity to magnesium (see McBain and Mayer, 1994). To test the magnesium sensitivity of granule cell NMDA receptors, we measured granule cell EPSCs across a wide voltage range in response to focal mitral cell stimulation in the absence and presence of magnesium. The degree of block of the NMDA component attributable to 1 mM Mg^{2+} , as estimated from the current at 30–40 msec after stimulus, was voltage-dependent, averaging 44 ± 5% at 228 mV (n=5), 78 ± 5% at 248 mV (n=3), and 96 ± 2% at 278 mV (n=3). This block is very similar to that of the highly magnesium-sensitive receptors containing NMDAR-2A and 2B subunits (Monyer et al., 1994), as well

as to the magnesium sensitivity of EPSCs at other synapses (Hestrin et al., 1990). The convergence of many mitral cells onto single granule cells, however, may provide a mechanism for relieving the magnesium block of the NMDA receptor during glomerular stimulation. Given the high input resistances of granule cells (0.98 ± 0.17 GΩ; n=12), the activation of several mitral cell inputs should provide sufficient current through NMDA receptors to depolarize the granule cell. Consistent with such a mechanism, the block of mitral cell IPSCs elicited by glomerular stimulation was much less than that of IPSCs induced by single mitral cell stimulation (Fig. 5B). These results imply that NMDA receptors can drive dendrodendritic inhibition not because of a low intrinsic magnesium sensitivity but because of the position of the granule cell within the circuitry of the olfactory bulb.

MK-801 blocks dendrodendritic inhibition in vivo

While the above experiments provide convincing evidence that NMDA receptor activation is required for dendrodendritic inhibition in brain slices, it is difficult to precisely mimic natural stimulation conditions *in vitro*. For example, the stimulus strength and other network properties of the bulb could conceivably influence the impact of voltage-dependent NMDA receptors on dendrodendritic inhibition. Thus, we examined the effects of NMDA receptor blockade on the activation of olfactory bulb circuits in 21 day-old male rats using the immediate early gene *c-fos* as a measure of cellular activation. Because *c-fos* is induced by a rise in intracellular calcium (Sheng et al., 1990), its induction has been widely used as an assay for studying the excitability of populations of neurons within many different brain regions (Morgan and Curran, 1991). While *c-fos* mRNA expression is not a linear function of synaptic activity or action potential generation (Fields et al., 1997), it can be used to compare the relative activation of different cell groups. In particular, if NMDA receptors are required for dendrodendritic inhibition, then block of these receptors should remove inhibition and result in increased *c-fos* mRNA expression in mitral cells.

c-fos mRNA probe is specific

Two control experiments were conducted to determine the specificity of the ^{35}S antisense RNA *c-fos* probe (Fig 6). First, T_m analysis of the *c-fos* probe demonstrated that the probe was removed from all cells of the olfactory bulb when the hybridized sections were washed in the narrow temperature range of 95-100°C rather than being gradually removed over a wider temperature range, indicating that the *c-fos* probe hybridizes specifically to one species of mRNA. Second, an unlabeled *c-fos* RNA probe used in 100-fold excess blocked hybidization by the labelled *c-fos* probe.

c-fos distribution pattern is altered with MK-801

As seen in the low power autoradiographs in Figure 7, the basal *c-fos* levels of rats exposed to ambient air prior to perfusion is general quite low with only occasion isolated cells demonstrating appreciable levels of *c-fos* mRNA (Fig 7a). We then exposed rats to the general odorant isoamyl acetate (IAA), that induces *c-fos* in periglomerular and granule cells throughout the bulb (Guthrie et al., 1993). Following a 5 minute exposure to a 1:10 dilution of IAA, juxtaglomerular cells surrounding individual glomerli became positive for *c-fos* mRNA expression (Fig 7b). Deep to these activated glomeruli are wide pockets of *c-fos* mRNA expressing granule cells. Areas of activated periglomerular and granule cells coincide; areas of the olfactory bulb not containing *c-fos* induced periglomerular cells do not have a large population of activated granule cells. This finding points to the topographical nature of odorant processing in the olfactory bulb. Although this concentration of IAA tends to induce many olfactory bulb neurons, there is a specific pattern of activation in the bulb with regions with and without neuronal *c-fos* mRNA activation.

The prominent feature seen *in situ* hybridization for *c-fos* mRNA in rats injected with the non-competitive NMDA antagonist MK-801 (1 mg/kg, i.p.) but not exposed to

odor is the presence of a ring of increased *c-fos* expression deep to the external plexiform layer (Fig 7c). This ring, also seen by Wilson *et al.* (1996), represents the cell bodies of the mitral cells. There are two additional features seen. One it the presence of occasional pockets of above baseline granule cell expression. The other is the rather uniform expression of *c-fos* mRNA in juxtaglomerular cells throughout the olfactory bulb.

A pattern of uniform *c-fos* mRNA induction is seen in rats injected with MK-801 and exposed to IAA (Fig 7d). As with MK-801/no odor condition (Fig 7c), a ring of induction representing the mitral cell layer can be seen, as well as the uniform juxtaglomerular activation. Additionally, the entire granule cell layer expresses *c-fos* mRNA. Unlike, odor exposed, uninjected rats, all topographical elements of odor stimulation seem to be lost.

A similar pattern with a competitive NMDA antagonist

In order to determine if the effect of MK-801 on *c-fos* mRNA induction is the result of its action on the NMDA receptor, the experiment was next performed with CPP, a competitive NMDA antagonist (Fig 8). Like MK-801, unstimulated olfactory bulbs demonstrated a ring of activated mitral cells. The degree of activated granule cells was increased in CPP injected rats, however this may be do to the reduced potency of the drug (Harris et al., 1986). In IAA stimulated rats given CPP, the pattern matches that of MK-801 injected rats. All levels of the olfactory bulb are highly activated with the exception of cells directly apposed to the glomeruli.

Darkfield examination of *c-fos* hybridized sections

To examine *c-fos* mRNA expression within cell groups, the sections shown in Figure 7 were analyzed at higher magnification. Figure 9 shows brightfield and darkfield views of thionin-stained, emulsion-dipped sections, along with profile plots of mean intensity values along the horizontal axis of the darkfield image. Consistent with the low

magnification views, the ambient air, non-MK-801 treated sections have only a few *c-fos* mRNA induced cells, mostly localized to periglomerular cells and cells of the superficial part of the granule cell layer (Fig 3a). In contrast, sections from IAA stimulated olfactory bulbs have individual glomeruli that are surrounded by *c-fos* mRNA induced periglomerular cells, whereas other glomeruli do not. Additionally, deep to the activated glomeruli are *c-fos* mRNA containing granule cells (Fig 3c). The peak of the intensity in the granule cell layer lies in granule cells just deep to the internal plexiform layer.

In MK-801 treated, non-IAA stimulated olfactory bulbs, the mitral cell layer is the most intensely hybridized region of the olfactory bulb. Because of the harsh treatment of *in situ* hybridization, mitral cells do not stain well for thionin; hence, the lack of correspondence of the intensely labeled band in the darkfield image to a layer of thionin stained cells in the brightfield image in Figure 3b. Additionally, cells in the external plexiform layer, most likely tufted cells, intensely hybridized to the antisense *c-fos* probe. Large numbers of granule, mitral and tufted cells in the MK-801, IAA stimulated olfactory bulbs contained *c-fos* mRNA (Fig 3d). However, like the MK-801 injection with odor, there were no glomeruli surrounded by activated periglomerular cells.

MK-801 increased the absolute level of granule cell activation as well as mitral cell activation, but this was to be expected because blocking granule cell NMDA receptors should relieve granule cell to granule cell inhibition (Wellis et al., 1989). The ratio of the mean intensity values of the mitral cell layer to a layer of granule cells deep to the internal plexiform layer confirmed that MK-801 produced a significant increase in mitral cell *c-fos* expression. MK-801 increased the mitral/granule intensity ratio from 0.86±0.12 to 1.36±0.16 in ambient air and from 0.47±0.01 to 1.03±0.06 in odor-stimulated animals (n=4, all groups). These data indicate that NMDA receptors play a key role in dendrodendritic inhibition *in vivo*.

Overall distribution pattern in 10-12 day old rats

The electrophysiological evidence presented in this paper are from 9-16 day-old Sprague-Dawley rats. Previous studies indicate that the *c-fos* response of 10-12 day old rats differs from 21 day old rats (Guthrie and Gall, 1995). Figure 10 demonstrates results from control and MK-801 injected rats exposed to ambient and 1:10 dilution of IAA. All four conditions were indistinguishable with wide-spanning *c-fos* mRNA expression in all olfactory bulb layers. The lack of apparent lateral inhibition seen with these *c-fos* studies may stem from the observation that most periglomerular and granule cells are generated during the first three postnatal weeks (Brunjes and Frazier, 1986).

Discussion

The most striking features of dendrodendritic inhibition in our experiments were its prolonged duration and its absolute dependence on NMDA receptor activation. Dendrodendritic IPSCs were longer than $GABA_A$ receptor-mediated inhibition in other brain regions but are consistent with earlier studies of inhibition in mitral cells (Nowycky et al., 1981; Jahr and Nicoll, 1982; Wellis and Kauer, 1993). The IPSC duration was defined by prolonged activation of granule cells in response to mitral cell stimulation. Our results suggest that the specific properties of NMDA receptors can shape the network properties of the olfactory bulb.

Is the NMDA receptor dependence a general property of dendrodendritic synapses?

NMDA receptors were required for triggering GABA release from granule cells, whereas AMPA receptor activation by itself was functionally ineffective. We considered several factors that could have influenced the dependence of dendrodendritic IPSCs on NMDA receptor activation in our experiments including the stimulus strength, the effects of extracellular magnesium, and the age of the animals. However, these factors did not affect the basic result. For example, in experiments done in the absence of extracellular magnesium, stimulation of a single mitral cell or many mitral cells by glomerular stimulation produced IPSCs that were completely blocked by D,L-AP-5. As expected, extracellular magnesium reduced the NMDA response in granule cells, but the remaining glomerular stimulation-evoked IPSC was still completely blocked by D,L-AP-5. On the other hand, NBQX reduced the IPSC only in magnesium-containing solutions. The magnesium dependence of the NBQX sensitivity indicates that an AMPA receptor-mediated depolarization does not trigger GABA release but instead facilitates the NMDA response by reducing magnesium block. For technical reasons, we used slices from young rats (P9–P16). Granule cell maturation and synaptogenesis are still ongoing during this period

(Rosselli-Austin and Altman, 1979), and NMDA receptors may precede AMPA receptors at some synapses (Durand et al., 1996; Wu et al., 1996). However, granule cell EPSCs had both AMPA and NMDA components (see also Trombley and Shepherd, 1992; Wellis and Kauer, 1994). Likewise, the disinhibition of mitral cell *c-fos* expression by MK-801 was actually more prominent at 21 d than at 12 d (Fig. 10), indicating that the critical role of NMDA receptors extends at least to the young adult.

We were initially surprised that the IPSCs were completely dependent on NMDA receptor activation, although previous results did suggest that NMDA receptors are involved in dendrodendritic inhibition. For example, a-aminoadipate, a somewhat selective NMDA antagonist, completely blocked dendrodendritic IPSCs in the turtle olfactory bulb (Nicoll and Jahr, 1982). Also, Wilson et al. (1996) found that MK-801 increased basal *c-fos* expression in mitral cells in rats exposed to clean air. However, incomplete block of mitral cell IPSCs by AP-5 was observed by Wellis and Kauer (1993) in the salamander olfactory bulb. Whether species differences are significant in this regard remains unclear. Recently, Isaacson and Strowbridge (1998) reported incomplete block of mitral cell IPSCs by AP-5 in the rat bulb. However, these authors measured TTX-insensitive IPSCs in response to prolonged mitral cell depolarizations using CsCl-filled patch pipettes. The properties of glutamate release under these conditions may differ from that in our experiments.

Dendrodendritic synapses compared with conventional synapses

The critical role of NMDA receptor activation in dendrodendritic inhibition differs fundamentally from the properties of most excitatory synapses. At conventional axosomatic or axodendritic synapses, postsynaptic AMPA receptor activation is generally sufficient to drive short-latency firing of action potentials, whereas NMDA receptors require coincident depolarization or a train of depolarizations to relieve magnesium block and become fully activated. The requirement for ongoing electrical activity fits well with a modulatory role of

NMDA receptors (Bliss and Collingridge, 1993). In contrast, at dendrodendritic synapses, NMDA receptors are necessary for information transfer, whereas AMPA receptors serve a facilitatory role.

Conventional axodendritic synapses do exist in which NMDA receptor activation is critical for information transfer, for example, in the thalamus, spinal cord, and cerebellum (Salt, 1986; Dickenson and Sullivan, 1990; D'Angelo et al., 1995). Dendrodendritic synapses are unusual, however, in that they are critical for action potentials as well as inhibition evoked by a single stimulus, whereas a train of stimuli are required for NMDA receptor-mediated action potentials at other synapses. The basis for this difference may be the anatomical convergence of a large number of mitral cells onto single granule cells, allowing a buildup of an NMDA response in granule cells during a single stimulus. Dendrodendritic NMDA receptors may also integrate responses to a stimulus train, as seen at other synapses.

Despite the specialized anatomical features of dendrodendritic synapses, many functional aspects of synaptic transmission appear similar to other central synapses. For example, focal mitral cell stimulation elicited fast-deactivating AMPA receptor-mediated EPSCs in granule cells (Fig. 3A), implying that glutamate release is brief, as observed at other fast-acting synapses (Clements et al., 1992). Focal granule cell stimulation also elicited fast-decaying IPSCs in mitral cells, suggesting that mitral cell $GABA_A$ receptors have conventional kinetics and, moreover, that the mechanics of GABA release from granule cell dendrites are conventional, given the appropriate stimulus.

What is special at dendrodendritic synapses—the NMDA receptor or the granule cell response?

Based on the properties of the granule cell EPSCs, the number of NMDA receptors or their magnesium sensitivity did not explain their preferential activation of dendrodendritic inhibition. NMDA receptors also have a high calcium permeability (Mayer

and Westbrook, 1987; Ascher and Nowak, 1988), whereas most AMPA receptors including those found in bulb interneurons (Jardemark et al., 1997) have a low calcium permeability (Hollman and Heinemann, 1994). The proximity between granule cell glutamate receptors and GABA release sites on dendrodendritic synapses raises the possibility that calcium influx through NMDA receptors directly triggers GABA release. This mechanism would, however, be inconsistent with the calcium sensitivity of exocytosis at other synapses, where vesicle fusion occurs in response to >100 μM calcium within 100 nm of voltage-gated calcium channels (Llinas et al., 1992; Zucker, 1993). In contrast, GABA release sites on granule cell dendritic spines are up to 1 μm from the postsynaptic density (Price and Powell, 1970).

However, NMDA receptors could be located at presynaptic terminals of granule cells, as reported at some axon terminals (Berretta and Jones, 1996). Moreover, some central synapses display a slow component of transmitter release, perhaps mediated by highly calcium-sensitive protein(s) responding to residual calcium (Goda and Stevens, 1994). In principle, residual calcium derived from the NMDA receptor could mediate such a response. Although we cannot exclude the NMDA "calcium hypothesis," we favor the possibility that the calcium that triggers GABA release is derived from voltage-gated calcium channels that are preferentially opened by an NMDA receptor-mediated depolarization. The failure of TTX to block mitral cell IPSCs evoked by single mitral cell stimulation implies that action potentials are not required for this release. In the absence of action potentials, the voltage in an activated spine would be expected to be near 0 mV (Koch and Poggio, 1983). Because such a depolarization is less than an action potential, a longer EPSP might be required to account for slower calcium channel-opening kinetics.

Because of the lag to action potential generation in granule cells, a prolonged NMDA receptor-mediated EPSP was also required for spiking, which might be particularly critical for lateral inhibition. The firing lag raises the possibility that an inactivating potassium conductance in the granule cell, like that reported in some other neurons (Storm,

1988; Hoffman et al., 1997; Ruszna´k et al., 1997), may shape the granule cell response. Thus, the intrinsic properties of the whole granule cell membrane might be better matched to a slow NMDA depolarization than to the brief AMPA receptor-mediated EPSP.

Implications for olfactory processing

The long duration of dendrodendritic IPSCs and their dependence on NMDA receptors have important implications for sensory processing in the olfactory bulb. Although the *c-fos* experiments are qualitative, they do provide a means to evaluate dendrodendritic inhibition in response to natural stimuli. The MK-801-induced enhancement of *c-fos* expression in mitral cells is consistent with a reduction of dendrodendritic inhibition. Although we did not test the effects of AMPA receptor antagonists in vivo, the disinhibition observed in MK-801 indicates that granule cell AMPA receptors drive less dendrodendritic inhibition than does NMDA receptor activation. MK-801 did not prevent the odorant-induced increase in *c-fos* expression in granule cells, indicating that AMPA receptor-mediated depolarizations resulted in sufficient calcium entry to activate *c-fos* mRNA (<1 μM peak $[Ca^{2+}]$; Fields et al., 1997); however, this calcium may not be sufficient to trigger GABA release. Only a subset of glomeruli were activated by isoamyl acetate in control animals, but there was a generalized activation of glomeruli after MK-801. The loss of spatial specificity suggests that NMDA receptor activation is critical for lateral inhibition in the glomerular layer (see also Guthrie et al., 1993). The uniform activation by odorant of the granule cell layer after MK-801 also suggests that elements of both reciprocal and lateral inhibition depend on NMDA receptors.

The properties of the NMDA response seem well adapted to influence sensory processing in the olfactory bulb. For example, their voltage dependence may insure that lateral inhibition occurs only from mitral cells that respond strongly to an odor. Spontaneously active mitral cells or those that respond weakly to an odor may not provide sufficiently robust excitation of granule cells to relieve the magnesium block of the NMDA

receptor. The slow kinetics of the NMDA receptor-mediated EPSC is a major determinant of the duration of dendrodendritic IPSCs. Prolonged IPSCs are also expected to augment the spatial signal-to-noise ratio. Mitral cells can fire spontaneously at 10–20 Hz (e.g., Harrison and Scott, 1986); thus, their effective suppression requires inhibition lasting $100 msec. Prolonged IPSCs might also more effectively suppress odor-induced activity in other mitral cells, whose odor-induced spiking can be delayed or asynchronous (Hamilton and Kauer, 1989). The time course of the reciprocal inhibitory output might also be critical for the synchronized oscillatory pattern observed in odor responses (Tank et al., 1994) that have been shown in honeybees to be essential for odor discrimination (Stopfer et al., 1997).

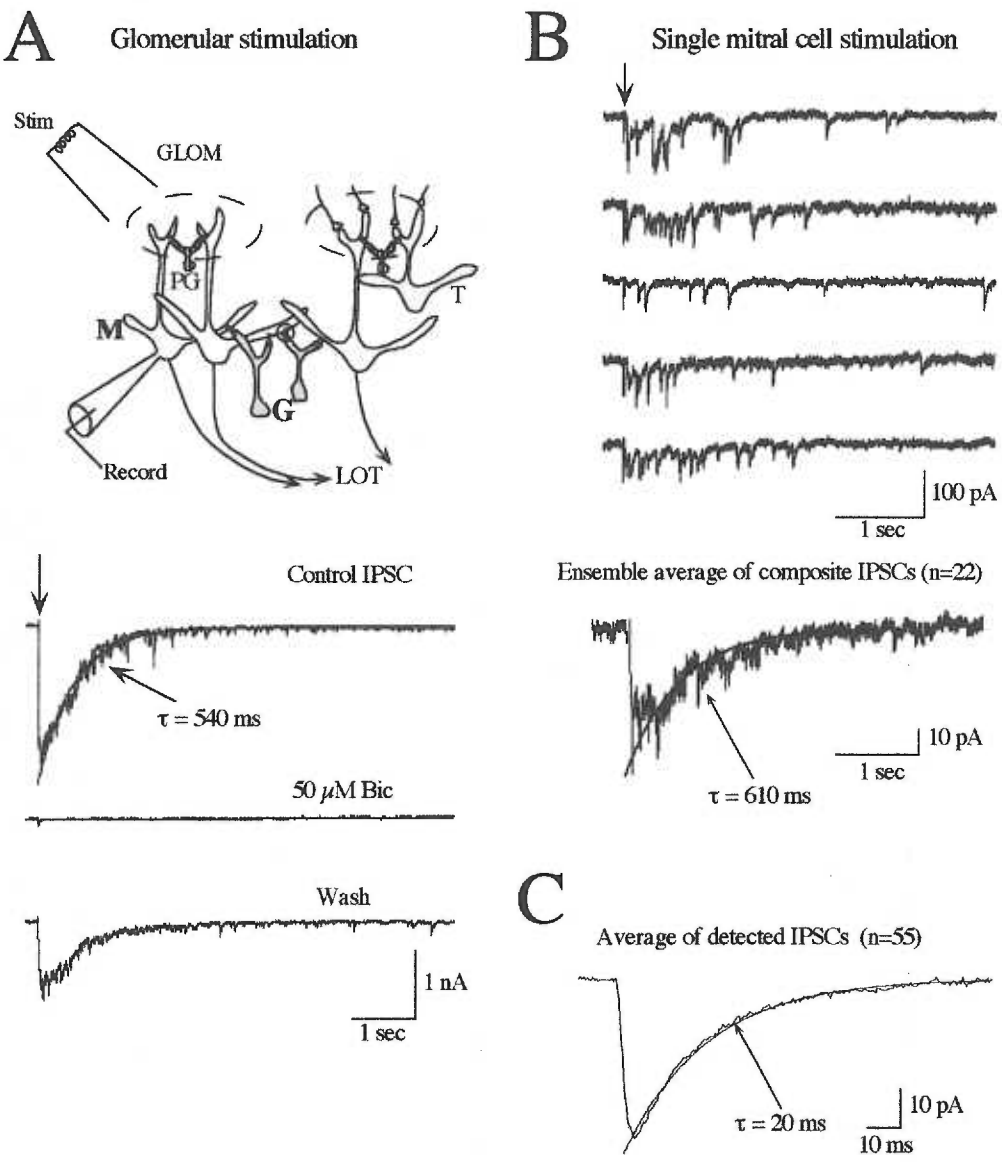

Figure 1. The kinetics of the dendrodendritic inhibition are determined by the asynchronous release of GABA from granule cells. (*A*) Bipolar stimulation in the glomerular layer (GLOM) elicited a long-lasting inward current in the mitral cell (M), when recordings were made with a NaCl extracellular solution with no added magnesium. The current was blocked by bicuculline (Bic; 50 μM), indicating that it reflects a GABAA receptor-mediated IPSC caused by the release of GABA from granule cells (G) at reciprocal dendrodendritic synapses (circled). Periglomerular cells (PG), tufted cells (T), and the lateral olfactory tract (LOT) are also shown. Cell 971126c2. (*B*) Direct somatic stimulation of a mitral cell with the recording pipette also elicited an IPSC, shown here as 5 raw data traces. The traces showed unitary IPSCs with fast kinetics, but the averaged, composite IPSC (bottom) had a slow decay (t=0.61 s) similar to the IPSC elicited by glomerular stimulation. The action-potential mediated sodium current was deleted from these traces for clarity. Cell 97508c4. (*C*) The average of 55 unitary IPSCs in the recording in Part B had a decay time constant of 20 ms. Unitary IPSCs were detected with a template comprised of rising and decaying exponentials (t=3 ms and 30 ms, respectively).

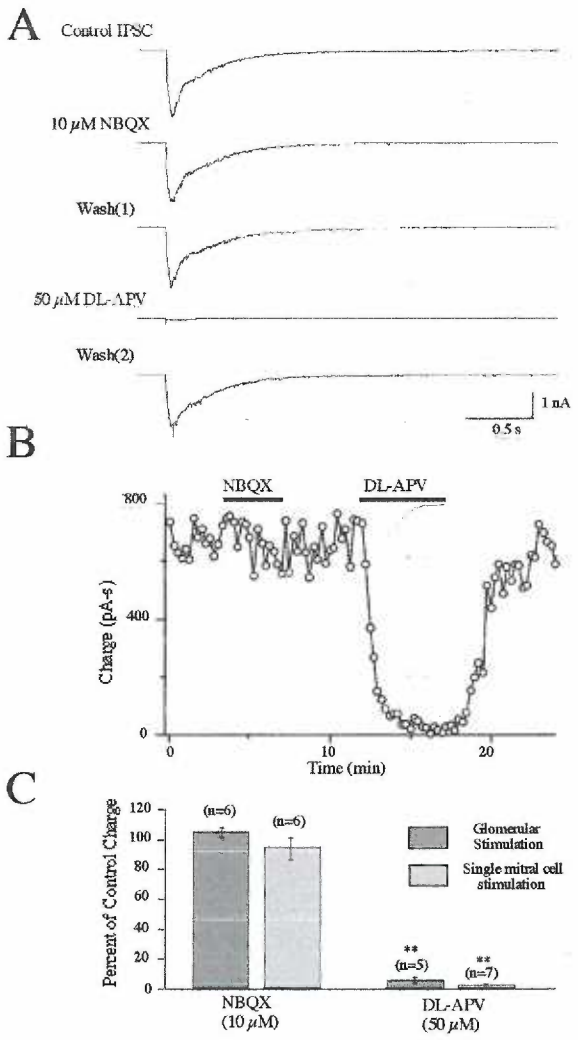

Figure 2. Dendrodendritic inhibition requires the activation of NMDA receptors. (*A*, *B*) The glomerular stimulation-evoked IPSC was insensitive to the AMPA receptor antagonist NBQX (10 μM) but was completely blocked by the NMDA receptor antagonist DL-AP5 (50 μM). Each displayed trace reflects an average of 10-20 traces. The effect of DL-AP5 on the IPSCs occurred rapidly and was reversible within 5 minutes after the removal of the drug. Cell 971016c5. (*C*) Histogram summarizing the effects of NBQX and DL-AP5 on the IPSCs. Similar glutamate receptor pharmacological profiles were observed for the IPSCs evoked by glomerular stimulation and single mitral cell stimulation. Quantification of drug effects was done by integrating the IPSC, yielding a charge value.

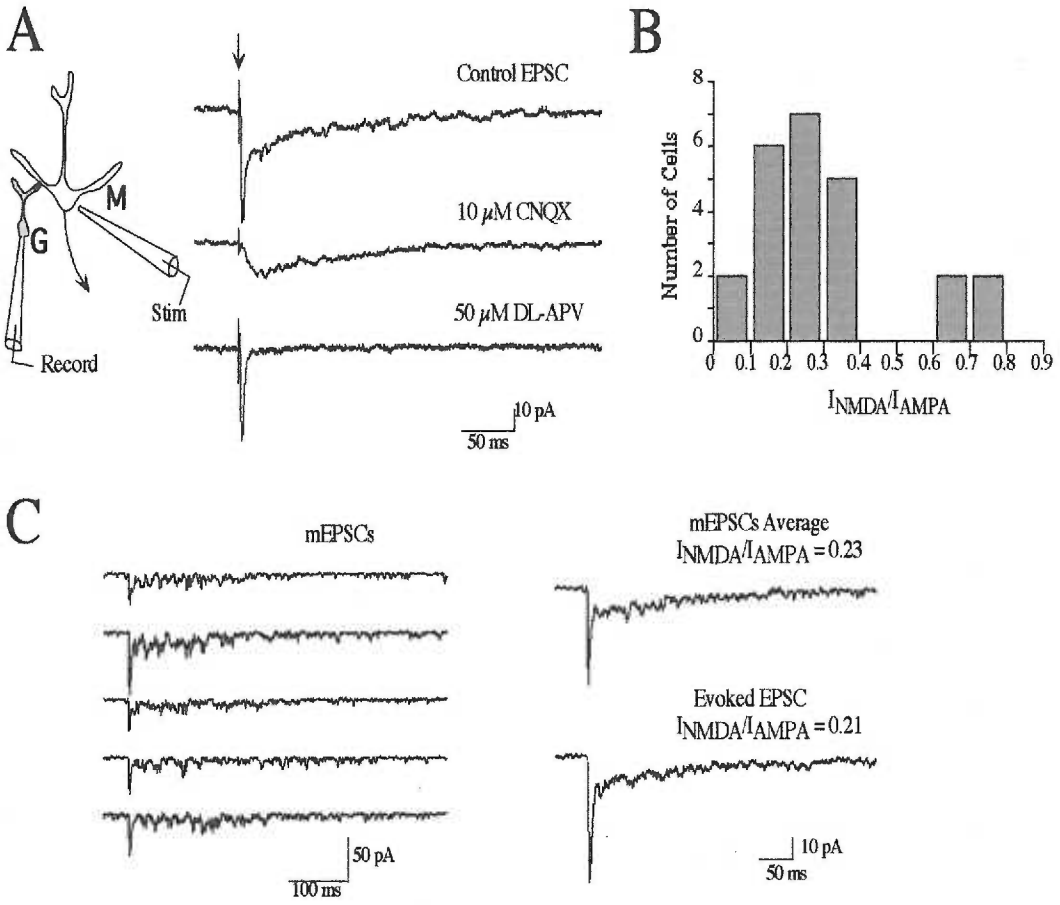

Figure 3. Granule cell EPSCs at dendrodendritic synapses have both AMPA and NMDA components. (*A*) Focal mitral cell (M) stimulation evoked EPSCs in a granule cell (G) with a CNQX-sensitive, rapidly decaying AMPA receptor-mediated component, as well as a DL-AP5-sensitive, slowly decaying NMDA component. The extracellular solution contained no added magnesium. Cell 97617c4. (*B*) The amplitude of the NMDA component was about one-fourth of the AMPA component. In 24 cells, the ratio of the NMDA and AMPA receptor-mediated currents (INMDA/IAMPA) was taken from the peak current (IAMPA) and the mean current 20-25 ms post-stimulus (INMDA). (*C*) Miniature excitatory synaptic currents (mEPSCs) in granule cells were recorded in TTX (1 μM) and cadmium (Cd2+; 10 μM). Five examples from one cell are shown (left) that were detected using a template that approximated an AMPA mEPSC: a sum of two exponentials with rising and decay components (t=0.3 and 3 ms, respectively). The averaged mEPSCs (n=15; right, top) had the same time course as the evoked EPSC in the same cell (right, bottom), implying that there are few 'pure' NMDA synapses (see Results). Cell 97812c3.

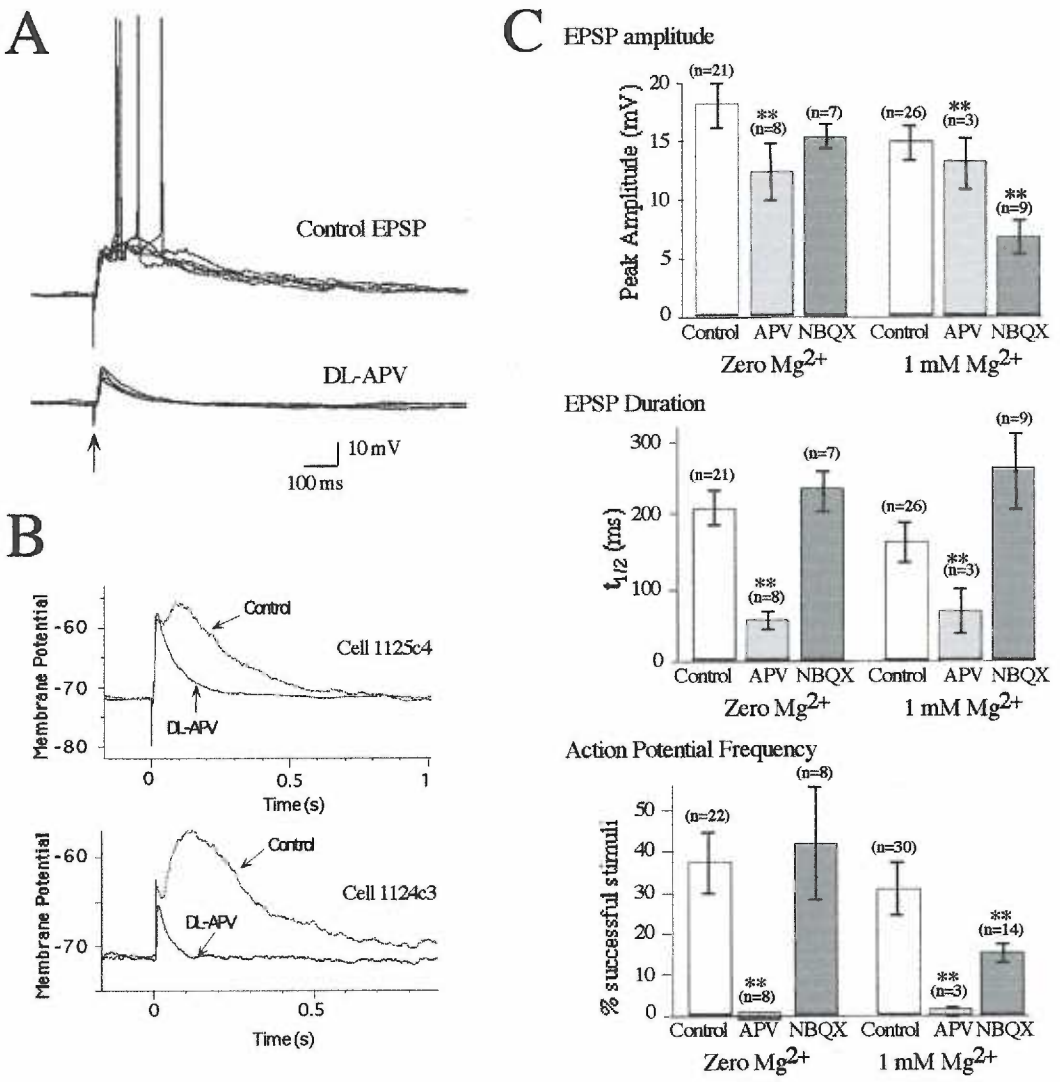

Figure 4. Stimulus-evoked action potentials in granule cells require NMDA receptor activation. (*A*) Glomerular stimulation evoked large dual component EPSPs in granule cells (top), as well as action potentials. Action potentials were abolished by DL-AP5 (50 μM; bottom). Five responses before and after application of DL-AP5 for the same cell are superimposed. Firing under control conditions followed a delay, averaging 61 ms in this cell in 13 trials. The bath had no added extracellular magnesium. Cell 1125c4. (*B*) For the cell in Part A, the peak of the EPSP in DL-AP5 (top) was similar to that of the dual component EPSP; however, the duration, expressed as the time t1/2 for 50% decay of the voltage signal from peak, was reduced from 195 to 51 ms. In a different cell (bottom), DL-AP5 reduced the amplitude and duration of the EPSP. Only voltage responses that did not elicit action potentials were selected for averaging. (*C*) In the absence of extracellular magnesium, DL-AP5 had variable effects on the EPSP amplitude (top), but consistently reduced the duration, t1/2, of the EPSP (middle) and action potential firing frequency (bottom). NBQX had little effect on the granule cell voltage responses in no magnesium, but had modest effects on the EPSP amplitude and firing frequency in 1 mM Mg2+.

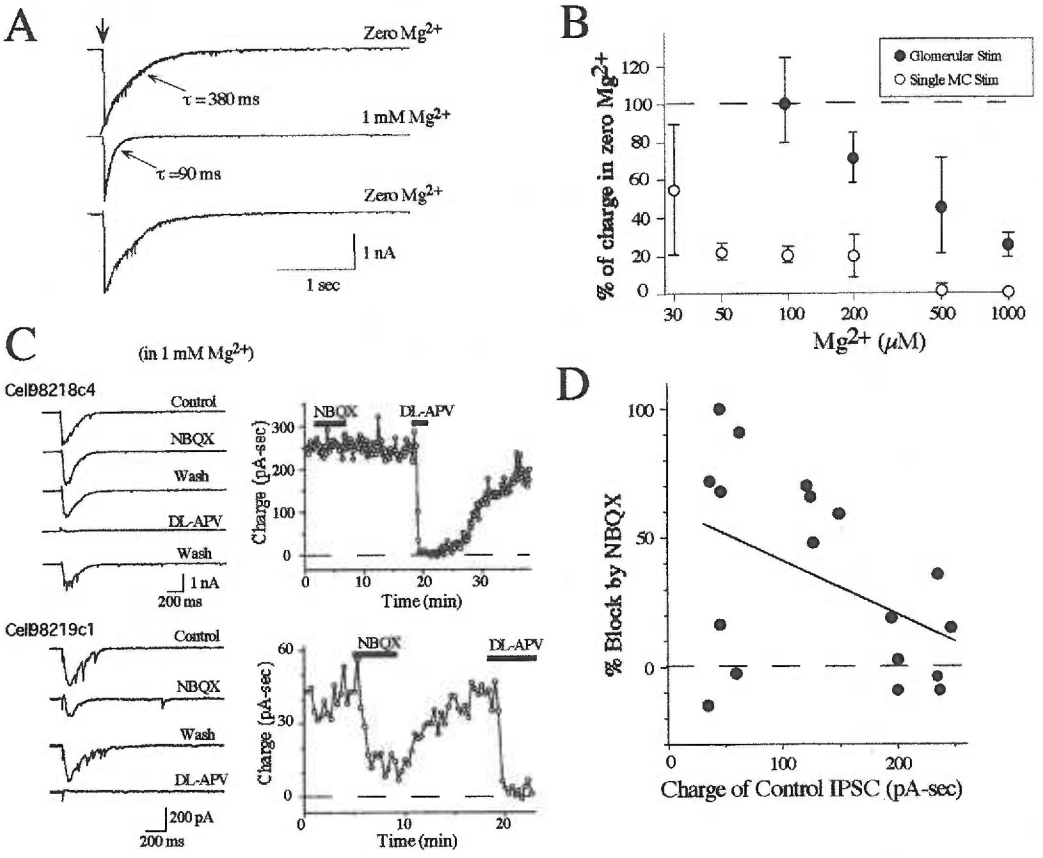

Figure 5. Mitral cell IPSCs require NMDA receptor activation in the presence of extracellular Mg2+. (*A*) The addition of 1 mM Mg2+ to the bath reduced the size and duration of the mitral cell IPSC evoked by glomerular stimulation. Each trace reflects the average of 8-15 responses. Cell 971103c4. (*B*) IPSCs induced by glomerular stimulation displayed a dose-dependent blockade by magnesium (filled circles), but 23% of the IPSC charge remained in 1 mM Mg2+. The magnesium-sensitivity of IPSCs evoked by single mitral cell stimulation (open circles) was markedly higher. Each plotted value reflects 2-8 experiments. (*C*) In the continuous presence of 1 mM Mg2+, IPSCs evoked by glomerular stimulation were completely blocked by DL-AP5 (50 μM), but had varying responses to NBQX (10 μM). Data from two experiments are shown (top and bottom). (*D*) In measurements made in 18 mitral cells in magnesium, there was a modest negative correlation (r=–0.44) between the size of the control IPSC and the magnitude of the NBQX effect, implying that AMPA receptors play a role in facilitating dendrodendritic inhibition under conditions of weaker stimulation.

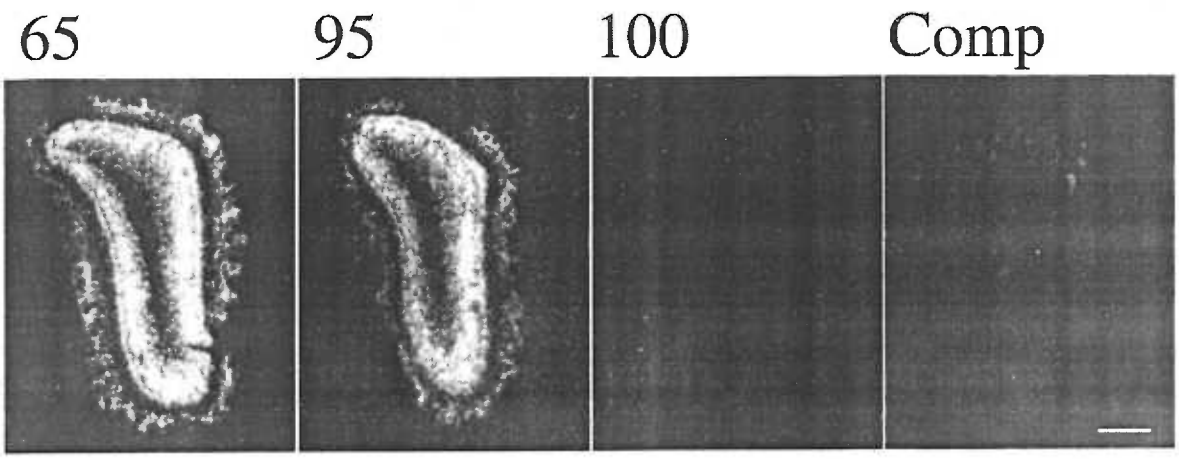

Figure 6. Control experiments of the *c-fos* probe. Autoradiograms of *in situ* hybridization with a ^{35}S antisense probe to *c-fos* mRNA were performed on one PN 21 rat exposed to 1:10 concentration of IAA. Following hybridization and low stringency washes, individual sections were rinsed in 0.1X SSC, 1 mM DTT for 30 min at temperatures at 65°C (labeled 65), 95°C (95) and 100°C (100). Washes at 65°C and 95°C displayed similar hybridization patterns, whereas 100°C had virtually no hybridization. Likewise, prehybridzation with 100-fold excess unlabeled antisense RNA probe successfully prevented hybridization of the ^{35}S antisense probe (labeled Comp). Scale, 500 μm.

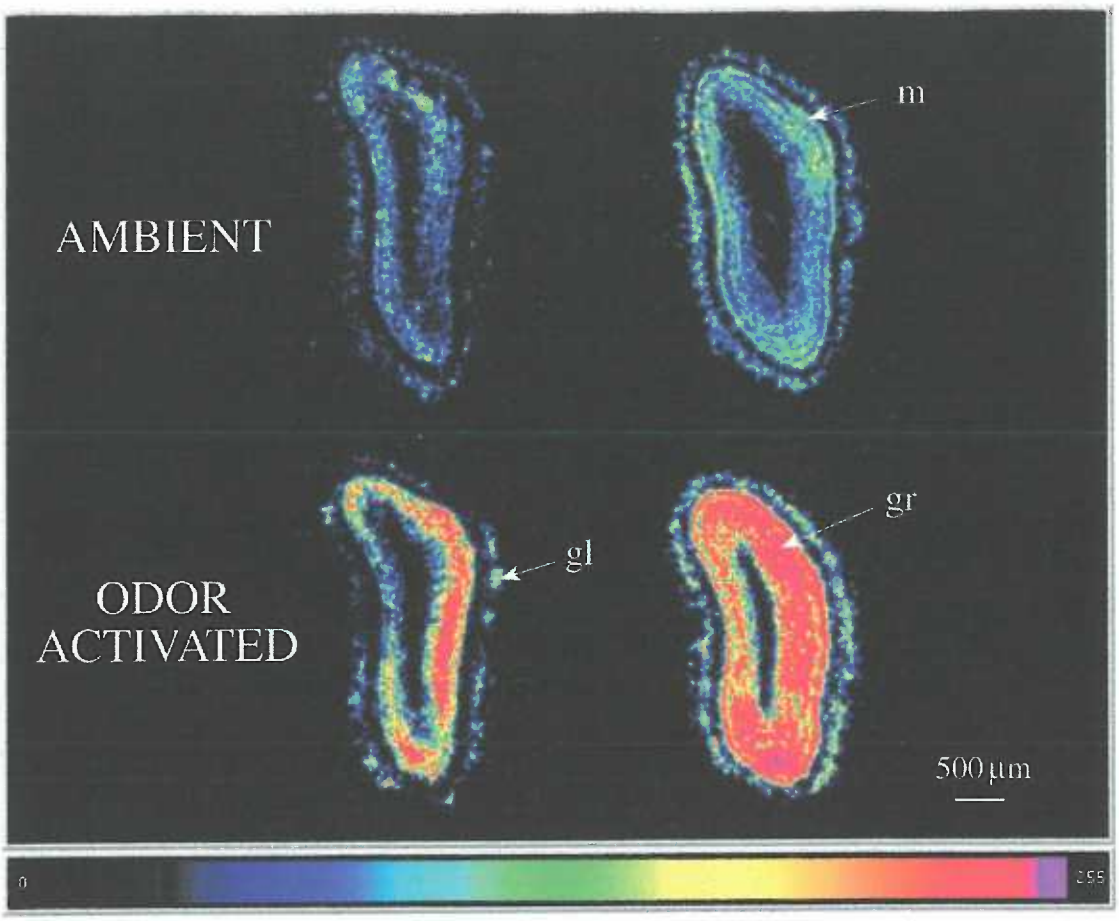

Figure 7. Induction of *c-fos* mRNA in the olfactory bulb *in vivo*. Pseudocolored autoradiograms of *in situ* hybridization with a ^{35}S antisense probe to *c-fos* mRNA were compared in four different drug/odor conditions. Coronal olfactory bulb sections from 4 different PN 21 rats are shown. Sections are oriented with dorsal up and lateral to the right.
Upper left: In filtered air (ambient), only light patchy labeling was present (two blebs of highest intensity are tissue folds).
Lower left: The odor-activated rat showed intense labeling of the granule cell layer (gr) as well as scattered labeling in the glomerular layer (gl).
Upper right: In MK-801 injected rats in filtered air, the mitral cell layer was uniformly activated (m).
Lower right: In MK-801/odor-activated rats, there was intense labeling in granule and mitral layers. Increased labeling of glomeruli was also apparent.

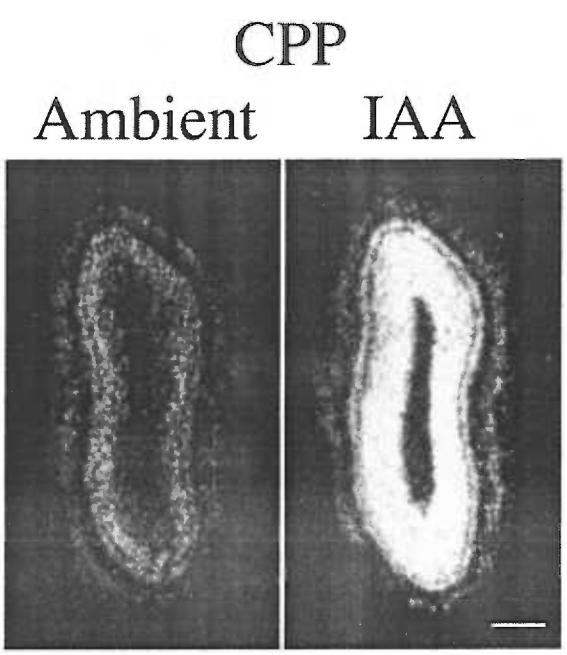

Figure 8. Effect of CPP on induction of *c-fos* mRNA in the olfactory bulb.
Autoradiograms of *in situ* hybridization with a ^{35}S antisense probe to *c-fos* mRNA were compared between ambient and 1:10 IAA exposure. Coronal olfactory bulb sections from 2 different PN 21 rats are shown.
Left: In CPP injected rats in filtered air, the mitral cell layer was uniformly activated.
Right: In CPP/odor-activated rats, there was intense labeling in granule and mitral layers. Increased labeling of glomeruli was also apparent.

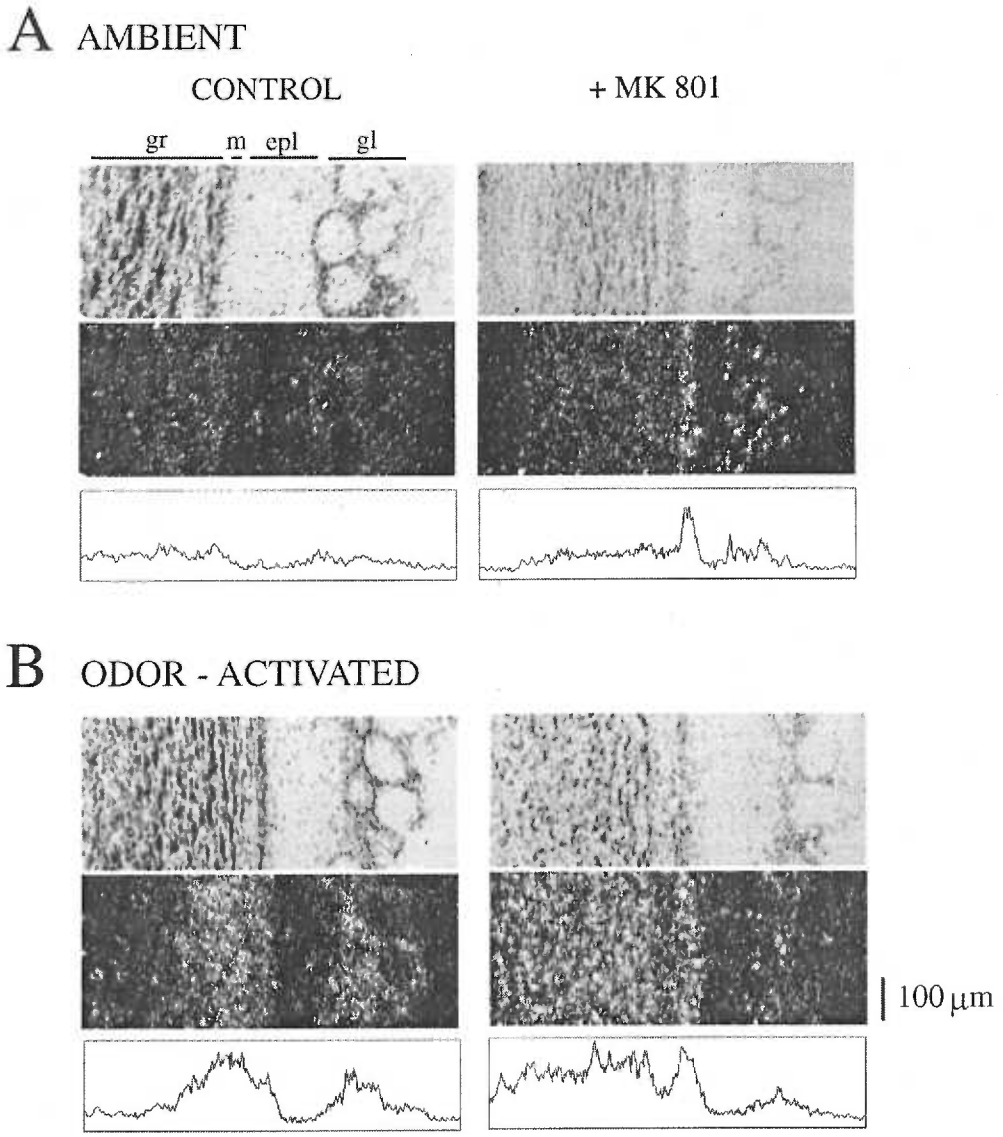

Figure 9. MK-801 increases the magnitude of *c-fos* expression in mitral cells, consistent with a reduction in dendrodendritic inhibition. Higher magnification photomicrographs of emulsion-dipped slides for the filtered air (A, ambient) and odor-activated rats (B) as in Figure 7. For each condition, the top panel is brightfield, middle panel is darkfield, and bottom panel is a profile plot of average pixel intensity in the vertical axis of the darkfield image. Intensities from 0-150 were plotted (total scale 0-255). In filtered air, MK-801 caused a marked increase in the labeling of mitral cells (m), as well as labeling of scattered tufted cells in the external plexiform layer (epl; top right). In the absence of MK-801, odor-activated rats showed labeling in the superficial half of the granule cell layer (gr), as well as of periglomerular cells surrounding individual glomeruli in the glomerular layer (gl; bottom left). MK-801 induced a peak of intense mitral cell labeling in odor-activated rats that was not present without MK-801 (bottom right). Labeling was extended throughout the granule cell layer. Mitral cells did not stain well for thionin under the conditions used for *in situ* hybridization. This explains the absence of a layer of thionin-stained mitral cells in the brightfield image of the bulb from rats exposed to filtered air and MK-801 (top right).

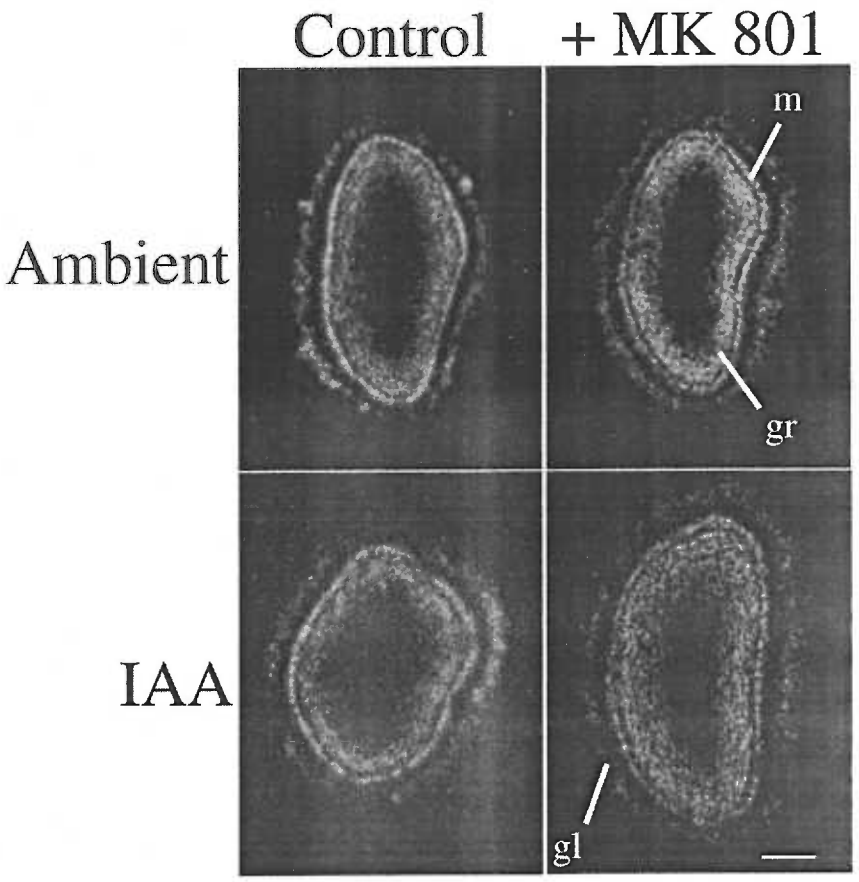

Figure 10. Induction of *c-fos* mRNA in PN 10-12. Autoradiograms of coronal sections comparing four different drug/odor combinations with MK-801 and 1:10 IAA. All four conditions demonstrate widespread *c-fos* mRNA induction in all areas of the olfactory bulb. Scale, 500 μm.
Upper left: Filtered air (ambient).
Lower Left: Odor activated rat (IAA).
Upper Right: MK-801 injected (+MK 801).
Lower Right: Odor activated and MK-801 injected.

CONCLUSION

In this thesis, I have discussed the cloning of the metabotropic glutamate receptor subtype 7 and its initial characterization as a receptor sensitive to L-AP4, a glutamate analog previously shown to stimulate a subclass of mGluRs in olfactory bulb mitral cells. In chapter 1, the anatomical distribution of mGluR7 mRNA expression by *in situ* hybridization in the developing and adult rat central nervous systems was discussed. The results demonstrated that mGluR7 mRNA is among the most widely distributed of mGluRs in the rat nervous system and that mGluR7 mRNA is expressed in most neuronal groups known to respond to L-AP4 including mitral cells of the olfactory bulb. Additionally, mGluR7 mRNA was found to be abundantly expressed at all levels of olfactory circuitry. Chapter 2 discussed the immunolocalization of mGluR7 in the olfactory system. The results indicated that mGluR7 is primarily presynaptic, including in mitral cell axons. However, the postsynaptic localization of mGluR7 at selected synapses indicates that mGluR7 is not targeted exclusively to axonal compartments. The prologue to chapter 3 discussed attempts to demonstrate a functional difference in olfactory information processing in mice deficient in mGluR1, a receptor subtype found abundantly within the olfactory bulb. Finally, chapter 3 discussed a collaborative project demonstrating that dendrodendritic inhibition in the olfactory bulb is driven by NMDA, not AMPA, receptors using electrophysiological and *in vivo* techniques. The findings suggest that olfactory information processing depends on long-lasting reciprocal and lateral inhibition.

In this section, I wish to comment on additional findings that have shed light on the functions of glutamate receptors in the olfactory system.

Cloning of mGluR8, another mitral cell L-AP4 receptor

The immunohistochemistry data shown in chapter 2 indicated that mGluR7 is located presynaptically in mitral cell axons. However, during the course of the immunohistochemistry work, our laboratories characterized another L-AP4 sensitive

receptor, mGluR8 (Saugstad et al., 1997). I performed *in situ* hybridization studies that showed rat mGluR8 mRNA has a highly restricted expression pattern compared with that of mGluR4 and mGluR7. However, there was prominent expression within olfactory areas, as well as piriform cortex and pontine gray, and lateral reticular nucleus (Figure 1). In the main olfactory bulb, the mitral cell layer demonstrated intense hybridization, although there was also abundant expression in the granule cell layer (Figure 1B). Work by Kinoshita, et al., has shown that, like mGluR7, mGluR8 is localized presynaptically at mitral cell axon terminals (Kinoshita et al., 1996). Therefore, mitral cells express two L-AP4-specific mGluRs that are candidates to mediate presynaptic inhibition of transmitter release in mitral cell axon terminals.

Coexpression of these two receptors in mitral cells could suggest either redundancy of function or distinct roles of the receptors based on differences in function or localization. While there is no current evidence that mGluR7 and mGluR8 are differentially localized with mitral cells, our characterization suggests different roles for mGluR7 and mGluR8

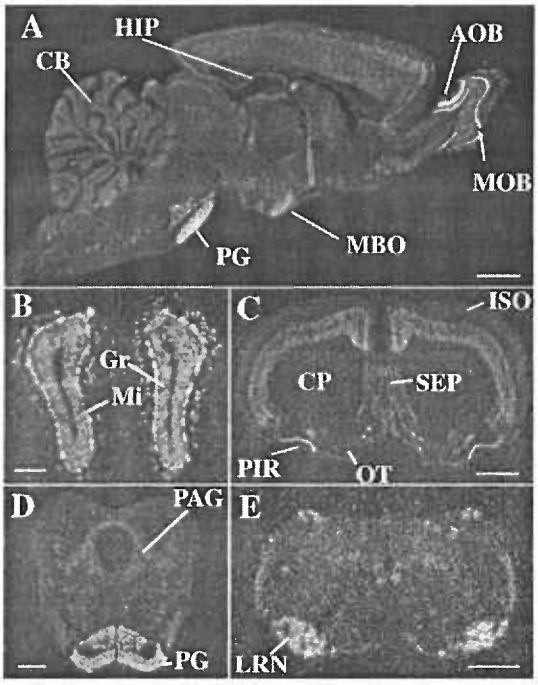

Figure 1: *In situ* hybridization of adult rat brain sections hybridized with an mGluR8 antisense cRNA probe. A, Parasagittal section revealing hybridization in the main (MOB) and accessory (AOB) olfactory bulbs and the pontine gray (PG). Relatively less hybridization was seen in the mammillary body (MBO), the cerebellum (CB), and the hippocampus (HIP). Scale bar, 2mm. B, Coronal section of the MOB. Mi, mitral cell layer; Gr, granule cell layer. Scale bar, 0.5 mm. C, Coronal section showing hybidization in piriform cortex (PIR), Septum (SEP), and deep layers of the isocortex (ISO). Far less staining was seen in the olfactory tubercle (OT) and the caudoputamen (CP). Scale bar, 2 mm. D, Coronal section at the level of the PG. PAG, periaqueductal gray. Scale bar, 1mm. E, Coronal section of the lateral reticular nucleus (LRN). Scale bar, 1mm.

(Kinzie et al., 1998). Responses in oocytes and in CHO cells (Saugstad et al., 1997) show that these two mGluRs differ markedly in their sensitivity to glutamate. Therefore, if mGluR7 and mGluR8 are colocalized to the release site, the apparent difference in their agonist affinities may be crucial to differences in their function. Under low probability of transmitter release, synaptic glutamate concentration may be sufficient to activate both mGluR7 and mGluR8, but excitation, and therefore, autoinhibition, would be restricted to those terminals where release occurred (Figure 2). However, under high release conditions with strong or repetitive stimulation, sufficient concentrations of glutamate may reach terminals in adjacent, quiescent synapses, thus inducing heterosynaptic inhibition through the action of high affinity mGluR8 receptors. As input to the olfactory cortex is highly distributed, such a differential role for mGluR7 and mGluR8 in homosynaptic and heterosynaptic inhibition could serve an important role in selection of asynchronous input at pyramidal cells of the olfactory cortex. Alternatively, mGluR7 and mGluR8 may act as a two-step inhibitory autofeedback mechanism. mGluR8 may be activated in routine

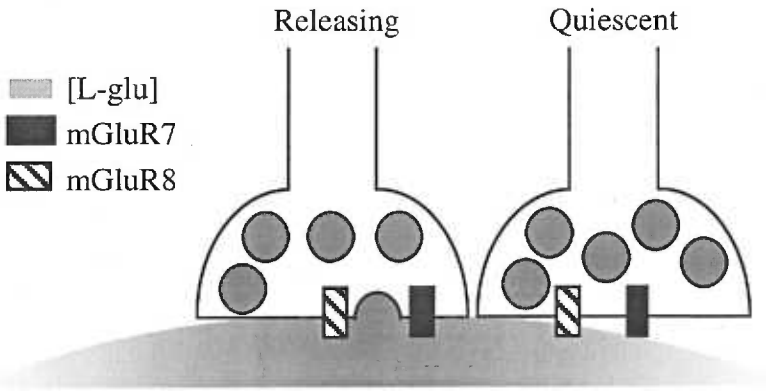

Figure 2: Schematic depiction of adjacent axon terminals making synaptic contact with the same dendrite, showing localization of mGluR7 and mGluR8 in the active zone, with mGluR2 in the preterminal axon. In this scheme, homosynaptic activation results in concentrations of glutamate sufficient to activate both low (mGluR7) and high (mGluR8) affinity receptors in the active zone. Heterosynaptic activation of an adjacent quiescent synapse by lower concentrations of "leaked" glutamate is only capable of activating mGluR8. mGluR2 in the preterminal axon is not activated, but may be positioned to affect the shape of the action potential when exposed to glutamate either from neuronal or glial sources.

synaptic transmission while mGluR7 becomes activated in times of intense, repeated synaptic transmission.

An *in vivo* function for an mGluR?

Despite the lack of a deficit in olfactory signalling in*c-fos* experiments in mGluR1 mutant mice, the *c-fos* assay can be powerful. It allows an *in vivo* analysis of a multiple neurons thereby a snapshot of a network in action. Therefore, even though there was an absence of a robust finding for the analysis of mGluR1, the *c-fos* assay may still prove useful in the examination of mGluR function.

As mentioned in the introduction, mGluR2 has already been extensively studied in the olfactory system. mGluR2 is localized to granule cell dendrites of the main and accessory olfactory bulb. Electrophysiologic studies have shown that mGluR2 is involved in the inhibition of GABA-induced IPSPs of accessory olfactory bulb mitral cells (Hayashi et al., 1993) by inhibiting GABA release from granule cells. Additionally, these receptors have been shown to involved in the formation of an olfactory memory.

In light of the findings in chapter 3 of this thesis, the mGluR2 results are curious. We have shown that, like the stimulation of mGluR2, the inhibition of NMDA receptors can inhibit GABA-induced IPSPs in mitral cells. However, unlike mGluR2 agonists, NMDA antagonists such as AP5 and MK-801 have no effect on formation of olfactory memory formation to the pheromones of the male that mates with them (Brennan and Keverne, 1989).

This apparent conflict may be resolved by the use of the *c-fos* induction assay and the use of LY354740, a potent mGluR2 agonist that crosses the blood-brain barrier (Helton et al., 1998). If mGluR2 acts by inhibiting GABA release from granule cells, a pattern of *c-fos* mRNA induction much like that seen with MK-801 in the main olfactory bulb would be expected: global mitral cell disinhibition. However, the *c-fos* induction experiments may also show that, unlike the main olfactory bulb, NMDA receptors are not the driving force

of GABA mediated feedback inhibition and therefore demonstrate functional differences between the two olfactory systems, although there is evidence to refute this (McLellan et al., 1998).

A Clinical Role for mGluRs?

Finally, I would like to mention the possible clinical importance of mGluRs. My interests in neuroscience and medical research have stemmed from my interest advancing our knowledge in the fields of neurology and psychiatry. When I began my research, there was no clear indication that mGluRs would be important in these fields. But it was clear to me that studying the modulatory functions of the most prominent excitatory neurotransmitter receptor in the brain had to be important. Preliminary results appear to bear this out based on the effects of the mGluR2 agonist LY354740 which can cross the blood-brain barrier.

Phencyclidine (PCP) induces schizophrenia-like symptoms in healthy people including hallucinations. Moghaddam and Adams (1998) have shown that PCP other psychotomimetic NMDA antagonists increase glutamate efflux from presynaptic terminals and thus may produce their effects by potentiating glutamatergic neurotransmission at non-NMDA receptors. One problem with targeting the ionotropic receptors in a clinical setting is that these receptors are involved neurotransmission throughout the nervous system. Therefore, modulating glutamatergic neurotransmission through the mGluRs is an attractive alternative. Because mGluR2 is localized presynaptically and inhibits neurotransmitter release, LY354740 was evaluated in the ability to attenuate the effects of PCP. In rats given PCP, the increase in glutamate efflux in the prefrontal cortex produced by PCP was abolished. Additionally, LY354740 nearly abolished PCP-induced locomotor activity and significantly reduced stereotypic behaviors such as head rolling. Therefore, modulating neurotransmission through mGluRs may offer a new route to treating schizophrenia.

The drug LY354740 has also been shown to be anxiolytic in mice in fear potentiated startle and elevated plus maze models without the sedating effects associated with routinely used anxiolytics such the benzodiazepine diazepam (Helton et al., 1998). Presumably, the mechanism of action is through the inhibition of glutamate release because antagonists to both AMPA and NMDA receptors produce similar anxiolytic effects.

The activation of mGluR2 has also been shown to reverse Parkinson-like muscle rigidity associated with haloperidol (Konieczny et al., 1998). Muscle rigidity induced by haloperidol has been proposed to be caused by the blockade of striatal dopamine D2 receptors of the stiatopallidal pathway. The loss of the inhibitory influence of dopamine results in a functional prevalence in the excitatory effects of glutamate in striatopallidal neurons as well as neurons in the substantia nigra and globus pallidus. Therefore activation of mGluR2 in inhibiting glutamate release may control this functional prevalence.

Since I began my studies on metabotropic glutamate receptors a great deal has been learned about this family of receptors including the characterization of different subtypes, their pharmacology, their localization and their function. The coming years should see a tremendous payoff for this work in our understanding of how mGluRs act in neuronal systems and as targets for therapeutic intervention.

References

Abe, T., Sugihara, H., Nawa, H., Shigemoto, R., Mizuno, N., and Nakanishi, S. (1992). Molecular characterization of a novel metabotropic glutamate receptor mGluR5 coupled to inositol phosphate/Ca2+ signal transduction. J. Biol. Chem. 267, 13361-13368.

Aiba, A., Chen, C., Herrup, K., Rosenmund, C., Stevens, C. F., and Tonegawa, S. (1994). Reduced hippocampal long-term potentiation and context-specific deficit in associative learning in mGluR1 mutant mice. Cell *79*, 365-75.

Aiba, A., Kano, M., Chen, C., Stanton, M. E., Fox, G. D., Herrup, K., Zwingman, T. A., and Tonegawa, S. (1994). Deficient cerebellar long-term depression and impaired motor learning in mGluR1 mutant mice. Cell *79*, 377-88.

Anson, J., and Collins, G. G. (1987). Possible presynaptic actions of 2-amino-4-phosphonobutyrate in rat olfactory cortex. Br. J. Pharmacol. 91, 753-761.

Ascher, P., and Nowak, L. (1988). The role of divalent cations in the N-methyl-D-aspartate responses of mouse central neurones in culture. Journal of Physiology *399*, 247-66.

Bashir, Z. I., Bortolotto, Z. A., Davies, C. H., Berretta, N., Irving, A. J., Seal, A. J., Henley, J. M., Jane, D. E., Watkins, J. C., and Collingridge, G. L. (1993). Induction of LTP in the hippocampus needs synaptic activation of glutamate metabotropic receptors. Nature *363*, 347-50.

Baude, A., Nusser, Z., Roberts, J. D., Mulvihill, E., McIlhinney, R. A., and Somogyi, P. (1993). The metabotropic glutamate receptor (mGluR1 alpha) is concentrated at perisynaptic membrane of neuronal subpopulations as detected by immunogold reaction. Neuron 11, 771-87.

Bekkers, J. M., and Stevens, C. F. (1989). NMDA and non-NMDA receptors are co-localized at individual excitatory synapses in cultured rat hippocampus. Nature *341*, 230-3.

Berretta, N., and Jones, R. S. (1996). Tonic facilitation of glutamate release by presynaptic N-methyl-D-aspartate autoreceptors in the entorhinal cortex. Neuroscience *75*, 339-44.

Bischofberger, J., and Jonas, P. (1997). Action potential propagation into the presynaptic dendrites of rat mitral cells. Journal of Physiology *504*, 359-65.

Bliss, T. V., and Collingridge, G. L. (1993). A synaptic model of memory: long-term potentiation in the hippocampus. Nature *361*, 31-9.

Bortolotto, Z. A., and Collingridge, G. L. (1993). Characterisation of LTP induced by the activation of glutamate metabotropic receptors in area CA1 of the hippocampus. Neuropharmacology *32*, 1-9.

Bortolotto, Z. A., Bashir, Z. I., Davies, C. H., and Collingridge, G. L. (1994). A molecular switch activated by metabotropic glutamate receptors regulates induction of long-term potentiation. Nature *368*, 740-3.

Bradley, S. R., Levey, A. I., Hersch, S. M., and Conn, P. J. (1996).

Immunocytochemical localization of group III metabotropic glutamate receptors in the hippocampus with subtype specific antibodies. J. Neurosci 16, 2044-2056.

Brennan, P. A., and Keverne, E. B. (1989). Impairment of olfactory memory by local infusions of non-selective excitatory amino acid receptor antagonists into the accessory olfactory bulb. Neuroscience *33*, 463-8.

Brennan, P., Kaba, H., and Keverne, E. (1990). Olfactory recognition: a simple memory system. Science *250*, 1223-1226.

Brown, E. M., Gamba, G., Riccardi, D., Lombardi, M., Butters, R., Kifor, O., Sun, A., Hediger, M. A., Lytton, J., and Hebert, S. C. (1993). Cloning and characterization of an extracellular Ca(2+)-sensing receptor from bovine parathyroid. Nature *366*, 575-80.

Bruce, H. M. (1959). An exteroceptive block to pregnancy in the mouse. Nature *184*.

Brunjes, P. C., and Frazier, L. L. (1986). Maturation and plasticity in the olfactory system of vertebrates. Brain Research *396*, 1-45.

Calabresi, P., Pisani, A., Mercuri, N. B., and Bernardi, G. (1993). Heterogeneity of metabotropic glutamate receptors in the striatum: electrophysiological evidence. Eur J Neurosci *5*, 1370-7.

Chen, W. R., Midtgaard, J., and Shepherd, G. M. (1997). Forward and backward propagation of dendritic impulses and their synaptic control in mitral cells. Science *278*, 463-7.

Chess, A., Simon, I., Cedar, H., and Axel, R. (1994). Allelic inactivation regulates olfactory receptor gene expression. Cell *78*, 823-34.

Cho, J. Y., Min, N., Franzen, L., and Baker, H. (1996). Rapid down-regulation of tyrosine hydroxylase expression in the olfactory bulb of naris-occluded adult rats. J Comp Neurol *369*, 264-76.

Clements, J. D., Lester, R. A., Tong, G., Jahr, C. E., and Westbrook, G. L. (1992). The time course of glutamate in the synaptic cleft. Science *258*, 1498-501.

Collins, G. G. (1982). Some effects of excitatory amino acid receptor antagonists on synaptic transmission in the rat olfactory cortex slice. Brain Research *244*, 311-8.

Collins, G. G., and Howlett, S. J. (1988). The pharmacology of excitatory transmission in the rat olfactory cortex slice. Neuropharmacology 27, 697-705.

Conquet, F., Bashir, Z. I., Davies, C. H., Daniel, H., Ferraguti, F., Bordi, F., Franz-Bacon, K., Reggiani, A., Matarese, V., Conde, F., Collingridge, G. L., and Crepel, F. (1994). Motor deficit and impairment of synaptic plasticity in mice lacking mGluR1. Nature *372*, 237-243.

Cotman, C. W., Flatman, J. A., Ganong, A. H., and Perkins, M. N. (1986). Effects of excitatory amino acid antagonists on evoked and spontaneous excitatory potentials in guinea-pig hippocampus. J. Physiol. Lond. *378*, 403-415.

Craig, A. M., Blackstone, C. D., Huganir, R. L., and Banker, G. (1993). The distribution of glutamate receptors in cultured rat hippocampal neurons: postsynaptic clustering of

AMPA-selective subunits. Neuron 10, 1055-68.

Dale, N., and Roberts, A. (1985). Dual-component amino-acid-mediated synaptic potentials: excitatory drive for swimming in Xenopus embryos. Journal of Physiology *363*, 35-59.

Davies, J., and Watkins, J. C. (1982). Actions of D and L forms of 2-amino-5-phosphonovalerate and 2-amino-4-phosphonobutyrate in the cat spinal cord. Brain Res. *235*, 378-386.

Dickenson, A. H., and Sullivan, A. F. (1990). Differential effects of excitatory amino acid antagonists on dorsal horn nociceptive neurones in the rat. Brain Research *506*, 31-9.

Durand, G. M., Kovalchuk, Y., and Konnerth, A. (1996). Long-term potentiation and functional synapse induction in developing hippocampus. Nature *381*, 71-5.

Duvoisin, R. M., Zhang, C., and Ramonell, K. (1995). A novel metabotropic glutamate receptor expressed in the retina and olfactory bulb. J Neurosci 15, 3075-83.

Eccles, J., and McGeer, P. (1979). Ionotropic and metabotropic neurotransmission. TINS *2*, 39-40.

Evans, R. H. (1986). Pharmacology of amino acid receptors on vertebrate primary afferent nerve fibres. Gen. Pharmacol. *17*, 5-11.

Evans, R. H., Francis, A. A., Hunt, K., Oakes, D. J., and Watkins, J. C. (1979). Antagonism of excitatory amino acid-induced responses and of synaptic excitation in the

isolated spinal cord of the frog. Br. J. Pharmacol. *67*, 591-603.

Fields, R. D., Eshete, F., Stevens, B., and Itoh, K. (1997). Action potential-dependent regulation of gene expression: temporal specificity in ca2+, cAMP-responsive element binding proteins, and mitogen-activated protein kinase signaling. Journal of Neuroscience *17*, 7252-66.

Forsythe, I. D., and Westbrook, G. L. (1988). Slow excitatory postsynaptic currents mediated by N-methyl-D-aspartate receptors on cultured mouse central neurones. J Physiol Lond *396*, 515-33.

Fotuhi, M., Sharp, A. H., Glatt, C. E., Hwang, P. M., von-Krosigk, M., Snyder, S. H., and Dawson, T. M. (1993). Differential localization of phosphoinositide-linked metabotropic glutamate receptor (mGluR1) and the inositol 1,4,5-trisphosphate receptor in rat brain. J Neurosci 13, 2001-12.

Friedman, B., and Price, J. L. (1986). Plasticity in the olfactory cortex: age-dependent effects on deafferentation. J. Comp. Neurol. 246, 1-19.

Ganong, A. H., and Cotman, C. W. (1982). Acidic amino acid antagonists of lateral perforant path synaptic transmission: agonist-antagonist interactions in the dentate gyrus. Neurosci. Lett. *34*, 195-200.

Ginty, D. D. (1997). Calcium regulation of gene expression: isn't that spatial? Neuron *18*, 183-6.

Graybiel, A. M. (1990). Neurotransmitters and neuromodulators in the basal ganglia.

Trends Neurosci. *13*, 244-254.

Guthrie, K. M., and Gall, C. M. (1995). Functional mapping of odor-activated neurons in the olfactory bulb. Chem Senses *20*, 271-82.

Guthrie, K. M., Anderson, A. J., Leon, M., and Gall, C. (1993). Odor-induced increases in c-fos mRNA expression reveal an anatomical "unit" for odor processing in olfactory bulb. Proc Natl Acad Sci U S A *90*, 3329-33.

Haberly, L. B., and Bower, J. M. (1989). Olfactory cortex: model circuit for study of associative memory? Trends Neurosci. *12*, 258-264.

Hamilton, K., and Kauer, J. (1989). Patterns of intracellular potentials in salamander mitral/tufted cells in response to odor stimulation. J Neurophysiol *62*, 609-625.

Hampson, D. R., Theriault, E., Huang, X. P., Kristensen, P., Pickering, D. S., Franck, J. E., and Mulvihill, E. R. (1994). Characterization of two alternatively spliced forms of a metabotropic glutamate receptor in the central nervous system of the rat. Neuroscience 60, 325-36.

Harris, E. W., and Cotman, C. W. (1983). Effects of acidic amino acid antagonists on paired-pulse potentiation at the lateral perforant path. Exp. Brain. Res. *52*, 455-460.

Harris, E. W., Ganong, A. H., Monaghan, D. T., Watkins, J. C., and Cotman, C. W. (1986). Action of 3-((+/-)-2-carboxypiperazin-4-yl)-propyl-1-phosphonic acid (CPP): a new and highly potent antagonist of N-methyl-D-aspartate receptors in the hippocampus. Brain Res *382*, 174-7.

Harrison, T. A., and Scott, J. W. (1986). Olfactory bulb responses to odor stimulation: analysis of response pattern and intensity relationships. J. Neurophysiol. *56*, 1571-89.

Hasselmo, M. E., and Bower, J. M. (1991). Selective suppression of afferent but not intrinsic fiber synaptic transmission by 2-amino-4-phosphonobutyric acid (AP4) in piriform cortex. Brain Res 548, 248-55.

Hayashi, Y., Momiyama, A., Takahashi, T., Ohishi, H., Ogawa-Meguro, R., Shigemoto, R., Mizuno, N., and Nakanishi, S. (1993). Role of a metabotropic glutamate receptor in synaptic modulation in the accessory olfactory bulb. Nature 366, 687-90.

Hearn, T. J., Ganong, A. H., and Cotman, C. W. (1986). Antagonism of lateral olfactory tract synaptic potentials in rat prepyriform cortex slices. Brain Res. *379*, 372-376.

Heimer, L., and Kalil, R. (1978). Rapid transneuronal degeneration and death of cortical neurons following removal of the olfactory bulb in adult rats. Journal of Comparative Neurology 178, 559-609.

Helton, D. R., Tizzano, J. P., Monn, J. A., Schoepp, D. D., and Kallman, M. J. (1998). Anxiolytic and side-effect profile of LY354740: a potent, highly selective, orally active agonist for group II metabotropic glutamate receptors. Journal of Pharmacology & Experimental Therapeutics *284*, 651-60.

Hestrin, S., Nicoll, R. A., Perkel, D. J., and Sah, P. (1990). Analysis of excitatory synaptic action in pyramidal cells using whole-cell recording from rat hippocampal slices. Journal of Physiology *422*, 203-25.

Hollman, M., and Heinemann, S. (1994). Cloned glutamate receptors. Ann Rev Neurosci *17*, 31-108.

Hori, N., Auker, C. R., Braitman, D. J., and Carpenter, D. O. (1982). Pharmacologic sensitivity of amino acid responses and synaptic activation of in vitro prepyriform neurons. J. Neurophysiol. *48*, 1289-1301.

Houamed, K. M., Kuijper, J. L., Gilbert, T. L., Haldeman, B. A., O'Hara, P. J., Mulvihill, E. R., Almers, W., and Hagen, F. S. (1991). Cloning, expression, and gene structure of a G protein-coupled glutamate receptor from rat brain. Science *252*, 1318-1321.

Hummler, E., Cole, T. J., Blendy, J. A., Ganss, R., Aguzzi, A., Schmid, W., Beermann, F., and Schutz, G. (1994). Targeted mutation of the CREB gene: compensation within the CREB/ATF family of transcription factors. Proceedings of the National Academy of Sciences of the United States of America *91*, 5647-51.

Iversen, L., Mulvihill, E., Haldeman, B., Diemer, N. H., Kaiser, F., Sheardown, M., and Kristensen, P. (1994). Changes in metabotropic glutamate receptor mRNA levels following global ischemia: increase of a putative presynaptic subtype (mGluR4) in highly vulnerable rat brain areas. J. Neurochem. *63*, 625-633.

Jahr, C., and Nicoll, R. (1982). An intracellular analysis of dendrodendritic inhibition in the turtle *in vitro* olfactory bulb. J Physiol *326*, 213-134.

Jardemark, K., Nilsson, M., Muyderman, H., and Jacobson, I. (1997). Ca2+ ion

permeability properties of (R,S) alpha-amino-3-hydroxy-5-methyl-4-isoxazolepropionate (AMPA) receptors in isolated interneurons from the olfactory bulb of the rat. Journal of Neurophysiology *77*, 702-8.

Joly, C., Gomeza, J., Brabet, I., Curry, K., Bockaert, J., and Pin, J. P. (1995). Molecular, functional, and pharmacological characterization of the metabotropic glutamate receptor type 5 splice variants: comparison with mGluR1. J Neurosci 15, 3970-81.

Jonas, P., Major, G., and Sakmann, B. (1993). Quantal components of unitary EPSCs at the mossy fibre synapse on CA3 pyramidal cells of rat hippocampus. Journal of Physiology *472*, 615-63.

Kaba, H., and Keverne, E. B. (1988). The effect of microinfusions of drugs into the accessory olfactory bulb on the olfactory block to pregnancy. Neuroscience *25*, 1007-1011.

Kaba, H., and Nakanishi, S. (1995). Synaptic mechanisms of olfactory recognition memory. Rev Neurosci 6, 125-41.

Kaba, H., Hayashi, Y., Higuchi, T., and Nakanishi, S. (1994). Induction of an olfactory memory by the activation of a metabotropic glutamate receptor. Science *265*, 262-4.

Kano, M., Hashimoto, K., Kurihara, H., Watanabe, M., Inoue, Y., Aiba, A., and Tonegawa, S. (1997). Persistent multiple climbing fiber innervation of cerebellar Purkinje cells in mice lacking mGluR1. Neuron *18*, 71-9.

Kaupmann, K., Huggel, K., Heid, J., Flor, P. J., Bischoff, S., Mickel, S. J., McMaster,

G., Angst, C., Bittiger, H., Froestl, W., and Bettler, B. (1997). Expression cloning of GABA(B) receptors uncovers similarity to metabotropic glutamate receptors. Nature *386*, 239-46.

Keinanen, K., Wisden, W., Sommer, B., Werner, P., Herb, A., Verdoorn, T., Sakmann, B., and Seeburg, P. (1990). A family of AMPA-selective glutamate receptors. Science *249*, 556-560.

Kinoshita, A., Ohishi, H., Neki, A., Nomura, S., Shigemoto, R., Takada, M., Nakanishi, S., and Mizuno, M. (1996). Presynaptic localization of a metabotropic glutamate receptor, mGluR8, in the rhinencephalic areas - a light and electron microscope study in the rat. Neurosci Lett *207*, 61-64.

Kinzie, J. M., Saugstad, J. A., Westbrook, G. L., and Segerson, T. P. (1995). Distribution of metabotropic glutamate receptor 7 messenger RNA in the developing and adult rat brain. Neuroscience 69, 167-76.

Kinzie, J. M., Shinohara, M. M., van den Pol, A. N., Westbrook, G. L., and Segerson, T. P. (1997). Immunolocalization of metabotropic glutamate receptor 7 in the rat olfactory bulb. Journal of Comparative Neurology *385*, 372-84.

Kinzie, J. M., Westbrook, G. L., and Segerson, T. P. (In Press). Metabotropic Glutamate Receptors in the Olfactory Bulb. In Metabotropic Glutamate Receptors and Brain Function, F. Moroni, F. Nicoletti and D. E. Pellegrini-Giampietro, eds. (London: Portland Press).

Knopfel, T., Kuhn, R., and Allgeier, H. (1995). Metabotropic glutamate receptors: novel targets for drug development. J Med Chem 38, 1417-26.

Koerner, J. F., and Cotman, C. W. (1981). L-2-amino-phosphonobutyric acid selectively inhibits perforant path synapses from lateral entorhinal cortex. Brain Res. *216*, 192-198.

Konieczny, J., Ossowska, K., Wolfarth, S., and Pilc, A. (1998). LY354740, a group II metabotropic glutamate receptor agonist with potential antiparkinsonian properties in rats. Naunyn-Schmiedebergs Archives of Pharmacology *358*, 500-2.

Lanthorn, T. H., Ganong, A. H., and Cotman, C. W. (1984). 2-Amino-4-phosphonobutyrate selectively blocks mossy fiber-CA3 responses in guinea pig but not rat hippocampus. Brain Res. *290*, 174-178.

Lefkowitz, R., Hausdorff, W., and Caron, M. (1990). Role of phophorylation in desensitization of the beta-adrenoreceptor. Trends Pharmacol Sci *11*, 190-194.

Leon, M. (1987). Plasticity of olfactory output circuits related to early olfactory learning. Trends Neurosci. *10*, 434-438.

Lester, R. A., Quarum, M. L., Parker, J. D., Weber, E., and Jahr, C. E. (1989). Interaction of 6-cyano-7-nitroquinoxaline-2,3-dione with the N-methyl-D-aspartate receptor-associated glycine binding site. Molecular Pharmacology *35*, 565-70.

Liao, D., Hessler, N. A., and Malinow, R. (1995). Activation of postsynaptically silent synapses during pairing-induced LTP in CA1 region of hippocampal slice. Nature *375*, 400-4.

Llinas, R., Sugimori, M., and Silver, R. B. (1992). Microdomains of high calcium

concentration in a presynaptic terminal. Science *256*, 677-9.

Lorenzon, N. M., and Foehring, R. C. (1995). Characterization of pharmacologically identified voltage-gated calcium channel currents in acutely isolated rat neocortical neurons. I. Adult neurons. Journal of Neurophysiology *73*, 1430-42.

Luskin, M. B., and Price, J. L. (1983). The topographic organization of associational fibers of the olfactory system in the rat, including centrifugal fibers to the olfactory bulb. J. Comp. Neurol. 216, 264-291.

Martin, L. J., Blackstone, C. D., Huganir, R. L., and Price, D. L. (1992). Cellular localization of a metabotropic glutamate receptor in rat brain. Neuron 9, 259-70.

Masu, M., Tanabe, Y., Tsuchida, K., Shigemoto, R., and Nakanishi, S. (1991). Sequence and expression of a metabotropic glutamate receptor. Nature *349*, 760-765.

Mayer, M. L., and Westbrook, G. L. (1987). Permeation and block of N-methyl-D-aspartic acid receptor channels by divalent cations in mouse cultured central neurones. Journal of Physiology *394*, 501-27.

Mayer, M. L., Vyklicky, L., Jr., and Westbrook, G. L. (1989). Modulation of excitatory amino acid receptors by group IIB metal cations in cultured mouse hippocampal neurones. J Physiol Lond *415*, 329-50.

Mayer, M. L., Westbrook, G. L., and Guthrie, P. B. (1984). Voltage-dependent block by Mg2+ of NMDA responses in spinal cord neurones. Nature *309*, 261-3.

Mayer, M., and Westbrook, G. (1987). The physiology of excitatory amino acids in the vertebrate central nervous system. Prog. Neurobiol. *28*, 197-276.

McBain, C. J., and Mayer, M. L. (1994). N-methyl-D-aspartic acid receptor structure and function. Physiological Reviews *74*, 723-60.

McLellan, R. A., Wilkinson, M., and Brown, R. E. (1998). MK-801 and male odours induce c-fos expression in the AOB of juvenile female mice. Neuroreport *9*, 3919-24.

Minakami, R., Katsuki, F., Yamamoto, T., Nakamura, K., and Sugiyama, H. (1994). Molecular cloning and the functional expression of two isoforms of human metabotropic glutamate receptor subtype 5. Biochem Biophys Res Commun 199, 1136-43.

Moghaddam, B., and Adams, B. W. (1998). Reversal of phencyclidine effects by a group II metabotropic glutamate receptor agonist in rats. Science *281*, 1349-52.

Monyer, H., Burnashev, N., Laurie, D. J., Sakmann, B., and Seeburg, P. H. (1994). Developmental and regional expression in the rat brain and functional properties of four NMDA receptors. Neuron *12*, 529-40.

Morgan, J. I., and Curran, T. (1991). Stimulus-transcription coupling in the nervous system: involvement of the inducible proto-oncogenes fos and jun. Annual Review of Neuroscience *14*, 421-51.

Mu, X., Silos-Santiago, I., Carroll, S. L., and Snider, W. D. (1993). Neurotrophin receptor genes are expressed in distinct patterns in developing dorsal root ganglia. J. Neurosci. *13*, 4029-4041.

Musgrave, M. A., Ballyk, B. A., and Goh, J. W. (1993). Coactivation of metabotropic and NMDA receptors is required for LTP induction. Neuroreport *4*, 171-4.

Nakajima, Y., Iwakabe, H., Akazawa, C., Nawa, H., Shigemoto, R., Mizuno, N., and Nakanishi, S. (1993). Molecular characterization of a novel retinal metabotropic glutamate receptor mGluR6 with a high agonist selectivity for L-2-amino-4-phosphonobutyrate. J. Biol. Chem. *268*, 11868-11873.

Nakanishi, S. (1994). Metabotropic glutamate receptors: synaptic transmission, modulation, and plasticity. Neuron *13*, 1031-1037.

Nawy, S., and Jahr, C. (1990). Suppression by glutamate of cGMP-activated conductance in retinal bipolar cells. Nature 346, 269-271.

Nicoll, R. A. (1971). Pharmacological evidence for GABA as the transmitter in granule cell inhibition in the olfactory bulb. Brain Research *35*, 137-49.

Nicoll, R. A., and Jahr, C. E. (1982). Self-excitation of olfactory bulb neurones. Nature *296*, 441-4.

Nomura, A., Shigemoto, R., Nakamura, Y., Okamoto, N., Mizuno, N., and Nakanishi, S. (1994). Developmentally regulated postsynaptic localization of a metabotropic glutamate receptor in rat rod bipolar cells. Cell *77*, 361-9.

Nowak, L., Bregestovski, P., Ascher, P., Herbet, A., and Prochiantz, A. (1984). Magnesium gates glutamate-activated channels in mouse central neurones. Nature *307*,

462-5.

Nowycky, M. C., Mori, K., and Shepherd, G. M. (1981). GABAergic mechanisms of dendrodendritic synapses in isolated turtle olfactory bulb. Journal of Neurophysiology *46*, 639-48.

O'Brien, J. A., Isaacson, J. S., and Berger, A. J. (1997). NMDA and non-NMDA receptors are co-localized at excitatory synapses of rat hypoglossal motoneurons. Neuroscience Letters *227*, 5-8.

Ohishi, H., Akazawa, C., Shigemoto, R., Nakanishi, S., and Mizuno, N. (1995). Distributions of the mRNAs for L-2-amino-4-phosphonobutyrate-sensitive metabotropic glutamate receptors, mGluR4 and mGluR7, in the rat brain. J Comp Neurol 360, 555-70.

Ohishi, H., Nomura, S., Ding, Y., Shigemoto, R., Wada, E., Kinoshita, A., Li, J., Neki, A., Nakanishi, S., and Mizuno, N. (1995). Presynaptic localization of a metabotropic glutamate receptor, mGluR7, in the primary affecent neurons: an immunohistochemical study in the rat. Neurosci L 202, 85-8.

Ohishi, H., Shigemoto, R., Nakanishi, S., and Mizuno, N. (1993). Distribution of the messenger RNA for a metabotropic glutamate receptor, mGluR2, in the central nervous system of the rat. Neuroscience 53, 1009-18.

Ohishi, H., Shigemoto, R., Nakanishi, S., and Mizuno, N. (1993). Distribution of the mRNA for a metabotropic glutamate receptor (mGluR3) in the rat brain: an in situ hybridization study. J Comp Neurol 335, 252-66.

Okamoto, N., Hori, S., Akazawa, C., Hayashi, Y., Shigemoto, R., Mizuno, N., and Nakanishi, S. (1994). Molecular characterization of a new metabotropic glutamate receptor mGluR7 coupled to inhibitory cyclic AMP signal transduction. J. Biol. Chem. *269*, 1231-1236.

Petralia, R. S., and Wenthold, R. J. (1992). Light and electron immunocytochemical localization of AMPA-selective glutamate receptors in the rat brain. J Comp Neurol *318*, 329-54.

Petralia, R. S., Wang, Y. X., and Wenthold, R. J. (1994). The NMDA receptor subunits NR2A and NR2B show histological and ultrastructural localization patterns similar to those of NR1. J Neurosci *14*, 6102-20.

Pin, J. P., and Duvoisin, R. (1995). The metabotropic glutamate receptors: structure and functions. Neuropharmacology 34, 1-26.

Pin, J. P., Waeber, C., Prezeau, L., Bockaert, J., and Heinemann, S. F. (1992). Alternative splicing generates metabotropic glutamate receptors inducing different patterns of calcium release in Xenopus oocytes. Proc Natl Acad Sci U S A 89, 10331-5.

Price, J. L. (1973). An autoradiographic study of complementary laminar patterns of termination of afferent fibers to the olfactory cortex. J Comp Neurol 150, 87-108.

Price, J., and Powell, T. (1970). The morphology of granule cells within the olfactory bulb. J Cell Sci *7*, 91-123.

Rall, W., Shepherd, G. M., Reese, T. S., and Brightman, M. W. (1966). Dendrodendritic

synaptic pathway for inhibition in the olfactory bulb. Experimental Neurology *14*, 44-56.

Ressler, K. J., Sullivan, S. L., and Buck, L. B. (1994). Information coding in the olfactory system: evidence for a stereotyped and highly organized epitope map in the olfactory bulb. Cell *79*, 1245-1255.

Romano, C., Sesma, M. A., McDonald, C. T., O'Malley, K., Van-den-Pol, A. N., and Olney, J. W. (1995). Distribution of metabotropic glutamate receptor mGluR5 immunoreactivity in rat brain. J Comp Neurol 355, 455-69.

Rosenmund, C., Clements, J. D., and Westbrook, G. L. (1993). Nonuniform probability of glutamate release at a hippocampal synapse. Science *262*, 754-7.

Rosselli-Austin, L., and Altman, J. (1979). The postnatal development of the main olfactory bulb of the rat. Journal of Developmental Physiology *1*, 295-313.

Ruat, M., Molliver, M. E., Snowman, A. M., and Snyder, S. H. (1995). Calcium sensing receptor: molecular cloning in rat and localization to nerve terminals. Proc Natl Acad Sci U S A *92*, 3161-5.

Rusznak, Z., Forsythe, I. D., Brew, H. M., and Stanfield, P. R. (1997). Membrane currents influencing action potential latency in granule neurons of the rat cochlear nucleus. European Journal of Neuroscience *9*, 2348-58.

Sallaz, M., and Jourdan, F. (1993). C-fos expression and 2-deoxyglucose uptake in the olfactory bulb of odour-stimulated awake rats. Neuroreport *4*, 55-8.

Sallaz, M., and Jourdan, F. (1993). C-fos expression and 2-deoxyglucose uptake in the olfactory bulb of odour-stimulated awake rats. Neuroreport *4*, 55-8.

Saugstad, J. A., Kinzie, J. M., Mulvihill, E. R., Segerson, T. P., and Westbrook, G. L. (1994). Cloning and expression of a new member of the L-2-amino-4-phosphonobutyric acid-sensitive class of metabotropic glutamate receptors. Mol Pharmacol 45, 367-72.

Saugstad, J. A., Kinzie, J. M., Shinohara, M. M., Segerson, T. P., and Westbrook, G. L. (1997). Cloning and expression of rat metabotropic glutamate receptor 8 reveals a distinct pharmacological profile. Mol Pharmacol 51, 119-25.

Saugstad, J. A., Segerson, T. P., and Westbrook, G. L. (1995). L-2-amino-3-phosphonopropionic acid competitively antagonizes metabotropic glutamate receptors 1 alpha and 5 in Xenopus oocytes. Eur J Pharmacol *289*, 395-7.

Saugstad, J., Segerson, T., and Westbrook, G. (1995). Modulation of ion channels and synaptic transmission by metabotropic glutamate receptors. In Excitatory amino acids and synaptic transmission, H. Wheal and A. Thomson, eds. (San Diego, Ca.: Academic Press, Inc.), pp. 77-88.

Schoepp, D. D., and Conn, P. J. (1993). Metabotropic glutamate receptors in brain function and pathology. Trends Pharmacol. Sci. 14, 13-20.

Schoepp, D., Bockaert, and Sladeczek, F. (1990). Pharmacological and functional characteristics of metabotropic excitatory amino acid receptors. Trends Pharmocol Sci *11*, 508-515.

Schwob, J. E., and Price, J. L. (1984). The development of lamination of afferent fibers to the olfactory cortex in rats, with additional observations in the adult. J Comp Neurol 223, 203-22.

Scott, J. W., Wellis, D. P., Riggott, M. J., and Buonviso, N. (1993). Functional organization of the main olfactory bulb. Microsc. Res. Tech. *24*, 142-156.

Sheng, M., McFadden, G., and Greenberg, M. E. (1990). Membrane depolarization and calcium induce c-fos transcription via phosphorylation of transcription factor CREB. Neuron *4*, 571-82.

Shepherd, G. M. (1972). Synaptic organization of the mammalian olfactory bulb. Physiol. Rev. *52*, 864-917.

Shepherd, G. M. and Price, J.L. (1990). Olfactory bulb. In G.M. Shepherd (ed.) The Synaptic Organization Of The Brain. New York, Oxford: Oxford University Press, pp. 133-169.

Shigemoto, R., Kulik, A., Roberts, J. D., Ohishi, H., Nusser, Z., Kaneko, T., and Somogyi, P. (1996). Target-cell-specific concentration of a metabotropic glutamate receptor in the presynaptic active zone. Nature *381*, 523-5.

Shigemoto, R., Nakanishi, S., and Mizuno, N. (1992). Distribution of the mRNA for a metabotropic glutamate receptor (mGluR1) in the central nervous system: an in situ hybridization study in adult and developing rat. J. Comp. Neurol. *322*, 121-135.

Shipley, M. T., Halloran, F. J., and de-la-Torre, J. (1985). Surprisingly rich projection

from locus coeruleus to the olfactory bulb in the rat. Brain Res. *329*, 294-299.

Silver, R. A., Traynelis, S. F., and Cull-Candy, S. G. (1992). Rapid-time-course miniature and evoked excitatory currents at cerebellar synapses in situ. Nature *355*, 163-6.

Sladeczek, F., Pin, J.-P., Recasens, M., Bockaert, J., and Weiss, S. (1985). Glutamate stimulates inositol phosphate formation in striatal neurones. Nature *317*, 717-719.

Slaughter, M. M., and Miller, R. F. (1985). Characterization of an extended glutamate receptor of the on bipolar neuron in the vertebrate retina. J Neurosci 5, 224-33.

Slotnick, B. M., Graham, S., Laing, D. G., and Bell, G. A. (1987). Detection of propionic acid vapor by rats with lesions of olfactory bulb areas associated with high 2-DG uptake. Brain Res *417*, 343-6.

Stopfer, M., Bhagavan, S., Smith, B. H., and Laurent, G. (1997). Impaired odour discrimination on desynchronization of odour-encoding neural assemblies. Nature *390*, 70-4.

Storm, J. F. (1988). Temporal integration by a slowly inactivating K+ current in hippocampal neurons. Nature *336*, 379-81.

Stuart, G. J., Dodt, H. U., and Sakmann, B. (1993). Patch-clamp recordings from the soma and dendrites of neurons in brain slices using infrared video microscopy. Pflugers Archiv - European Journal of Physiology *423*, 511-8.

Sugiyama, H., Ito, I., and Hirono, C. (1987). A new type of glutamate receptor linked to inositol phospholipid metabolism. Nature *325*, 531-533.

Tanabe, Y., Masu, M., Ishii, T., Shigemoto, R., and Nakanishi, S. (1992). A family of metabotropic glutamate receptors. Neuron *8*, 169-179.

Tanabe, Y., Nomura, A., Masu, M., Shigemoto, R., Mizuno, N., and Nakanishi, S. (1993). Signal transduction, pharmacological properties, and expression patterns of two rat metabotropic glutamate receptors, mGluR3 and mGluR4. J Neurosci *13*, 1372-8.

Tank, D., Gelperin, A., and Kleinfeld, D. (1994). Odors, oscillations, and waves: does it all compute? Science *265*, 1819-20.

Testa, C. M., Standaert, D. G., Young, A. B., and Penney, J. B., Jr. (1994). Metabotropic glutamate receptor mRNA expression in the basal ganglia of the rat. J. Neurosci. *14*, 3005-3018.

Thomsen, C., Kristensen, P., Mulvihill, E., Haldeman, B., and Suzdak, P. D. (1992). L-2-amino-4-phosphonobutyrate (L-AP4) is an agonist at the type IV metabotropic glutamate receptor which is negatively coupled to adenylate cyclase [published erratum appears in Eur J Pharmacol 1993 Jan 15;244(2):187]. Eur J Pharmacol 227, 361-2.

Trombley, P. Q., and Shepherd, G. M. (1992). Noradrenergic inhibition of synaptic transmission between mitral and granule cells in mammalian olfactory bulb cultures. J Neurosci *12*, 3985-91.

Trombley, P. Q., and Shepherd, G. M. (1993). Synaptic transmission and modulation in the olfactory bulb. Curr Opin Neurobiol *3*, 540-7.

Trombley, P. Q., and Westbrook, G. L. (1992). L-AP4 inhibits calcium currents and synaptic transmission via a G-protein-coupled glutamate receptor. J Neurosci *12*, 2043-50.

Valverde, F., Santacana, M., and Heredia, M. (1992). Formation of an olfactory glomerulus: morphological aspects of development and organization. Neuroscience *49*, 255-275.

van den Pol, A. N. (1995). Presynaptic metabotropic glutamate receptors in adult and developing neurons: autoexcitation in the olfactory bulb. Journal of Comparative Neurology *359*, 253-71.

van den Pol, A. N. (1995). Presynaptic metabotropic glutamate receptors in adult and developing neurons: autoexcitation in the olfactory bulb. Journal of Comparative Neurology 359, 253-71.

van den Pol, A. N., Waurin, J. P., and Dudek, F. E. (1990). Glutamate, the dominant excitatory neurotransmitter in neuroendocrine regulation. Science *250*, 1276-1278.

Vassar, R., Chao, S. K., Sitcheran, R., Nunez, J. M., Vosshall, L. B., and Axel, R. (1994). Topographic organization of sensory projections to the olfactory bulb. Cell *79*, 981-991.

Watanabe, M., Inoue, Y., Sakimura, K., and Mishina, M. (1993). Distinct distributions of five N-methyl-D-aspartate receptor channel subunit mRNAs in the forebrain. Journal of Comparative Neurology *338*, 377-90.

Wellis, D. P., and Kauer, J. S. (1993). GABAA and glutamate receptor involvement in

dendrodendritic synaptic interactions from salamander olfactory bulb. J Physiol Lond *469*, 315-39.

Wellis, D. P., and Kauer, J. S. (1994). GABAergic and glutamatergic synaptic input to identified granule cells in salamander olfactory bulb. J Physiol Lond *475*, 419-30.

Wellis, D. P., and Scott, J. W. (1990). Intracellular responses of identified rat olfactory bulb interneurons to electrical and odor stimulation. Journal of Neurophysiology *64*, 932-47.

Wellis, D. P., Scott, J. W., and Harrison, T. A. (1989). Discrimination among odorants by single neurons of the rat olfactory bulb. J. Neurophysiol. *61*, 1161-1177.

Westbrook, G. L. (1994). Glutamate receptor update. Curr. Opin. Neurobiol. *4*, 337-346.

Westrum, L. E., and Bakay, R. A. (1986). Plasticity in the rat olfactory cortex. Journal of Comparative Neurology 243, 195-206.

White, W. F., Nadler, J. V., Hamberger, A., Cotman, C. W., and Cummins, J. T. (1977). Glutamate as transmitter of hippocampal perforant path. Nature *270*, 356-357.

Woolf, T. B., Shepherd, G. M., and Greer, C. A. (1991). Local information processing in dendritic trees: subsets of spines in granule cells of the mammalian olfactory bulb. Journal of Neuroscience *11*, 1837-54.

Wouterlood, F. G., Mugnaini, E., and Nederlof, J. (1985). Projection of olfactory bulb efferents to layer I GABAergic neurons in the entorhinal area. Combination of anterograde

degeneration and immunoelectron microscopy in rat. Brain Res 343, 283-96.

Wu, G., Malinow, R., and Cline, H. T. (1996). Maturation of a central glutamatergic synapse. Science *274*, 972-6.

Zucker, R. S. (1993). Calcium and transmitter release at nerve terminals. Biochemical Society Transactions *21*, 395-401.